

Determination of Soil Based Upland Field Irrigation Plan for
Afghanistan

A Thesis

Submitted to the Division of Environmental Science and Technology

For the Degree of Master of Science

In the Graduate School of Bioresources

University of Mie, Japan

February, 2015

Abdul Saboor Rahmany

513M202

Determination of Soil Based Upland Field Irrigation Plan for
Afghanistan

Abdul Saboor Rahmany

Abstract

Demand for food and raw materials are increasing with world population growth. To ensure food security for world's increasing population, a great concern should be put on sustainable use of natural resources, especially fresh water resources, which is even more important for arid and semi-arid climates like Afghanistan.

Low water use efficiency and bad irrigation practices are reported as main reasons, in field level, for low self-sufficiency ratio of food production in Afghanistan.

Many models have been proposed and practices so far for planning and scheduling of irrigation. Some of these models rely on metrological data by calculating ET_o with minimal consideration to soil properties, while some models more emphasized on soil water status and availability to plants, but not much research and emphasis have been done on detailed soil physical properties for irrigation planning and scheduling. This study focuses and deals with detailed and fundamental study of soil physical properties for irrigation planning and scheduling. The model is developed on case study of three upland fields in Mie prefecture of Japan.

Characteristic of Afghanistan agriculture has been organized. In particular, the importance of upland agriculture is commentary. Current problems and challenges for upland field irrigation are described. Furthermore, the needs to focus on the soil of farmland were discussed.

Discussion on the behavior of irrigation water in the soil is presented and it was noted for the mutual relationship of macropores (for drainage) and soil matrix (for soil water retention). In addition, fundamental perspectives of irrigation planning were discussed. Detailed field investigation methods (for farmland irrigation), laboratory analysis methods (for formulate upland irrigation plan), and results for both field and lab investigation is presented.

Understanding of the results was discussed among three study sites (as case study) for comparing the suitability, problems and challenges of each site for upland irrigation planning. General comprehensive discussion has been taken.

The author conducted a comprehensive proposal for new approaches to the upland irrigation plan in Afghanistan.

Same model detailed investigation is required to be implemented in Afghanistan and current irrigation practices have to be improved to increase food production toward food self-sufficiency.

Table of contents

Abstract	i
Table of contents	iii
List of Tables	v
List of Figures	vii
List of Photos	xi
1. Introduction	1
1.1 Background of Afghanistan Agriculture	1
1.2 Research background	6
1.3 Outline of the thesis.....	10
2. Irrigation planning concepts.....	13
2.1 Irrigation.....	13
2.2 Macropores and Water flow in Soils (Keith Beven and Peter Germann, 1982)	24
2.3 Soil pores quantification.....	34
2.4 pF – θ characteristics	46
3. Methodology	57
3.1 Study area as case study	57
3.2 Laboratory experiments.....	67
3.3 Results (Case Study)	102
4. Understanding of results.....	161
4.1 Soil condition and basic physical properties	161
4.2 Soil pores structure.....	166
4.3 pF – θ (Readily Available Soil moisture).....	176
4.4 Water flow in soil	178
5. New approaches to be added to upland agriculture in Afghanistan	181

6. General discussion.....	183
Acknowledgement.....	187
References	189
Appendixes	

List of Tables

- Table 2.1 Different units that can be used to define potential of the soil water
- Table 3.1 Collected samples from different layers of Ureshino Tengejicho Broccoli Field
- Table 3.2 Collected samples from different layers of Ureshino Tengejicho Beans Field
- Table 3.3 Collected samples from different layers of Tomato field in Yokkaichi Agriculture Center
- Table 3.4 Broccoli Field on-site soil profile cross section investigation results
- Table 3.5 Beans Field on-site soil profile cross section investigation results
- Table 3.6 Yokkaichi Agriculture Center on-site soil profile cross section investigation results
- Table 3.7 Basic soil physical properties results, “Broccoli Field” Matsusaka
- Table 3.8 Basic soil physical properties results, “Beans Field” Matsusaka
- Table 3.9 Basic soil physical properties results, “Yokkaichi Agriculture Center”
- Table 3.10 Particle size distribution, “Broccoli Field” Matsusaka
- Table 3.11 Particle size distribution, “Beans Field” Matsusaka
- Table 3.12 Particle size distribution, “Yokkaichi Agriculture Center”
- Table 3.13 Liquid – plastic limit and Plasticity index, “Broccoli Field” Matsusaka
- Table 3.14 Liquid – plastic limit and Plasticity index, “Yokkaichi Agriculture Center”
- Table 3.15 Broccoli Field water holding capacity and volumetric water content θ (cm³cm⁻³)
- Table 3.16 Beans Field water holding capacity and volumetric water content θ (cm³cm⁻³)
- Table 3.17 Yokkaichi Agriculture Center water holding capacity and volumetric water content θ (cm³cm⁻³)
- Table 3.18 Saturated hydraulic conductivity k_{sat} for all sites
- Table 4.1 Basic physical soil properties of each layer for all sites

Table 4.2 Soil phase relation and plasticity data of all sites

Table 4.3 Pore size distribution (capillary and non-capillary pores) for all sites

Table 4.4 Significant minimum equivalent pore size diameter and groups for drainage

List of Figures

- Fig. 1.1 Agricultural land use (1000 ha) (FAO, 2014; CSO, 2013~14)
- Fig. 1.2 Land use by most reported crops (1000 ha) (FAO, 2014; CSO, 2013~14)
- Fig. 2.1 Schematic view of water balance in soil, source; (JICA, leaflet, edited Rahmany 2014)
- Fig. 2.2 Macropores structure and water flow in soil (K. Beven and P. Germman, 1982)
- Fig. 2.3 Schematic view of mass and volume fraction of soil phases
- Fig. 2.4 Classification of Soil Pores (Narioka, 1989; edited Rahmany, 2014)
- Fig. 2.5 Schematic drawing of Inter-aggregates pores (Rahmany, 2015)
- Fig. 2.6 Schematic classification of air-entry macropores (H. Narioka, 1992; edited Rahmany)
- Fig. 2.7 PK drainage curve (H. Narioka, 1992; edited Rahmany)
- Fig. 2.8 Classification of drainage curve based on slope (H.Narioka, 1992; edited Rahmany)
- Fig. 2.9 Water in unsaturated soil is subjected to capillary and adsorption, (Source; D. Hillel, Environmental Soil Physics, 2003, Academic press)
- Fig. 2.10 Osmometer with a permeable membrane to water and impermeable to solution, (Source; M.B. Khirkham, Principles of Soil and plant water relationship, 2004)
- Fig. 2.11 pF- θ characteristics curve
- Fig. 2.12 Schematic view of soil water status in soil
- Fig. 3.1 Aerial view of Study Area, Ureshino Tengejicho (Source: Google map)
- Fig. 3.2 Close up view of Ureshino Tengejicho (Source: Google map)
- Fig. 3.3 Detailed view of study area in Ureshino Tengejicho (Source: Google

map)

- Fig. 3.4 Detailed and close view of Beans Field (Source: Google map)
- Fig. 3.5 Yokkaichi Agriculture Center Aerial view (Source: Google Map)
- Fig. 3.6 Close view of Yokkaichi Agriculture center (Source: Google Map)
- Fig. 3.7 Detailed view of study area Yokkaichi Agriculture Center
- Fig. 3.8 Soil texture triangle (Source: USDA, NRCS, Field book for handling and describing soil, 2002)
- Fig. 3.9 Schematic view of constant hydraulic conductivity test (Frutani, 2013; revised Rahmany)
- Fig. 3.10 Soil hardness distribution in (mm), Broccoli Field Matsusaka
- Fig. 3.11 Soil hardness distribution in (kg cm⁻²), Broccoli Field Matsusaka
- Fig. 3.12 Soil hardness distribution (mm), Beans Field Matsusaka
- Fig. 3.13 Soil hardness distribution (kg cm⁻²), Beans Field Matsusaka
- Fig. 3.14 Soil hardness distribution (mm) Yokkaichi Agriculture Center
- Fig. 3.15 Soil hardness distribution (kg cm⁻²) Yokkaichi Agriculture Center
- Fig. 3.16 Three phase distribution, “Broccoli Field” Matsusaka, (Unit: %)
- Fig. 3.17 Three phase distribution, “Beans Field” Matsusaka, (Unit: %)
- Fig. 3.18 Three phase distribution, “Yokkaichi Agriculture Center”, (Unit: %)
- Fig. 3.19 Particle size distribution, “Broccoli Field” Matsusaka
- Fig. 3.20 Particle size distribution, “Beans Field” Matsusaka
- Fig. 3.21 Particle size distribution, “Yokkaichi Agriculture Center”
- Fig. 3.22 Textural class (USDA), “Broccoli Field” Matsusaka
- Fig. 3.23 Textural class (USDA), “Beans Field” Matsusaka
- Fig. 3.24 Textural class (USDA), “Yokkaichi Agriculture Center”
- Fig. 3.25 Standard description of plasticity chart
- Fig. 3.26 Plasticity index, “Broccoli Field” Matsusaka

- Fig. 3.27 Plasticity index, “Yokkaichi Agriculture Center”
- Fig. 3.28 pF-moisture characteristics curve Broccoli Field, Matsusaka
- Fig. 3.29 pF-moisture characteristics curve Beans Field, Matsusaka
- Fig. 3.30 pF-moisture characteristics curve Yokkaichi Agriculture Center
- Fig. 3.31 pF – θ distribution, “Broccoli Field ridge”
- Fig. 3.32 pF – θ distribution, “Broccoli Field layer I ”
- Fig. 3.33 pF – θ distribution, “Broccoli Field layer II”
- Fig. 3.34 pF – θ distribution, “Beans Field ridge”
- Fig. 3.35 pF – θ distribution, “Beans Field layer I ”
- Fig. 3.36 pF – θ distribution, “Beans Field layer II”
- Fig. 3.37 pF – θ distribution, “Beans Field layer III”
- Fig. 3.38 pF – θ distribution, “Yokkaichi Agriculture Center layer A1”
- Fig. 3.39 pF – θ distribution, “Yokkaichi Agriculture Center layer A2”
- Fig. 3.40 pF – θ distribution, “Yokkaichi Agriculture Center layer B”
- Fig. 3.41 Saturated hydraulic conductivity k_{sat} , “Broccoli Field” Matsusaka
- Fig. 3.42 Saturated hydraulic conductivity k_{sat} , “Broccoli Field” Matsusaka
- Fig. 3.43 Saturated hydraulic conductivity k_{sat} , “Beans Field” Matsusaka
- Fig. 3.44 Saturated hydraulic conductivity k_{sat} , “Beans Field” Matsusaka
- Fig. 3.45 Saturated hydraulic conductivity k_{sat} , “Yokkaichi Agriculture Center”
- Fig. 3.46 Saturated hydraulic conductivity k_{sat} , “Yokkaichi Agriculture Center”
- Fig. 3.47 Drainability, negative pressure, “Broccoli Field ridge, Matsusaka”
- Fig. 3.48 Drainability, negative pressure, “Broccoli Field layer I , Matsusaka”
- Fig. 3.49 Drainability, negative pressure, “Broccoli Field layer II , Matsusaka”
- Fig. 3.50 Drainability, negative pressure, “Beans Field ridge, Matsusaka”
- Fig. 3.51 Drainability, negative pressure, “Beans Field layer I , Matsusaka”
- Fig. 3.52 Drainability, negative pressure, “Beans Field layer II , Matsusaka”

Fig. 3.53 Drainability, negative pressure, “Broccoli Field layer III, Matsusaka”

Fig. 3.54 Drainability, negative pressure, “layer A1Yokkaichi Agriculture Center”

Fig. 3.55 Drainability, negative pressure, “layer A2 (H)Yokkaichi Agriculture Center”

Fig. 3.56 Drainability, negative pressure, “layer A2 Yokkaichi Agriculture Center”

Fig. 6.1 Brief importance of the model and its suitability.

List of Photos

- Photo 3.1 Trimming soil profile cross section
- Photo 3.2 Determining soil layers by hand-feeling
- Photo 3.3 Determining texture by hand-feeling
- Photo 3.4 Soil color determination
- Photo 3.5 Undisturbed soil sampling
- Photo 3.6 Soil hardness measurement by Yamanaka hardness meter
- Photo 3.7 Samples placed in pycnometer
- Photo 3.8 Heating the samples for air removal
- Photo 3.9 Beginning of reaction in the beaker
- Photo 3.10 Heating of samples for increasing reaction
- Photo 3.11 Placed beaker on stirrer
- Photo 3.12 Sedimentation time for each sample
- Photo 3.13 Sedimented particles for sieving
- Photo 3.14 Remaining particles in the different sieves sizes
- Photo 3.15 Transferred particles to evaporating dish
- Photo 3.16 Oven dried samples
- Photo 3.17 Liquid limit (L_L) device and sample prepared for measurement
- Photo 3.18 Constant head hydraulic conductivity system device and operation
- Photo 3.19 System setup and device for negative pressure test
- Photo 3.20 Pressure plate apparatus
- Photo 3.21 Capillary saturation
- Photo 3.22 Placing samples on the ceramic plate inside pressure plate apparatus
- Photo 3.23 Soft X-ray apparatus, DCTS-D003, SOFTEX, Japan
- Photo 3.24 Broccoli Field soil surface view and irrigation system condition

- Photo 3.25 Broccoli field soil profile cross section
- Photo 3.26 Soil profile cross section and ridge
- Photo 3.27 Ridge close view
- Photo 3.28 Macropores in II layer of soil profile
- Photo 3.29 Detailed view of macropores
- Photo 3.30 Bean Field soil profile cross section
- Photo 3.31 Beans Field soil profile cross section close view
- Photo 3.32 Soil profile cross section view of Yokkaichi Agriculture Center
- Photo 3.33 Close view of layer A1 Yokkaichi Agriculture Center
- Photo 3.34 Close view of subsoil layer A2 Yokkaichi Agriculture Center
- Photo 3.35 Soft X-ray image without application of heavy liquid, “layer II (H) of Broccoli Filed, Matsusaka”
- Photo 3.36 Soft X-ray image after application of heavy liquid, “layer II (H) of Broccoli Filed, Matsusaka”
- Photo 3.37 Soft X-ray image without application of heavy liquid, “ridge (V) of Beans Filed, Matsusaka”
- Photo 3.38 Soft X-ray image after application of heavy liquid. “ridge (V) of Beans Filed, Matsusaka”
- Photo 3.39 Soft X-ray image without application of heavy liquid, “layer II (V) of Beans Filed, Matsusaka”
- Photo 3.40 Soft X-ray image after application of heavy liquid, “layer II (V) of Beans Filed, Matsusaka”
- Photo 3.41 Soft X-ray image without application of heavy liquid, “Yokkaichi Agriculture Center layer B (H)”
- Photo 3.42 Soft X-ray image after application of heavy liquid, “Yokkaichi Agriculture Center layer B (H)”

- Photo 3.43 Stereoscopic view of Broccoli Field, “layer II (H) after application of heavy liquid, Matsusaka”
- Photo 3.44 Stereoscopic view of Yokkaichi Agriculture Center, “layer B (H) after application of heavy liquid”
- Photo 4.1 Soft X-ray image, visual view of vertical distribution and connectivity of pores in Broccoli Field layer II
- Photo 4.2 Soft X-ray image, visual view of horizontal distribution and connectivity of pores in Beans Field ridge layer
- Photo 4.3 Soft X-ray image, visual view of horizontal distribution and connectivity of pores in Beans Field layer I
- Photo 4.4 Soft X-ray image, visual view of vertical distribution and connectivity of pores in layer B of Yokkaichi Agriculture Center

1. Introduction

1.1 Background of Afghanistan Agriculture

Afghanistan is a land lock country located between 29° 35' – 38° 40' latitude and 60° 31' – 74° 55' of longitude, with high potential for agriculture and food production. Even though 75% (United States Agency for International Development - USAID, 2014) of the population is engaged to this sector and it has natural resources for food production, still it is depended to food to be imported from other countries.

According to data of World Bank (2014) for 6 years of 2003 to 2008 regarding main four cereal crops production and national demand, the self-sufficient ratio for cereals is fluctuating with highest 0.96 in 2003, lowest 0.53 in 2004. However, it was 0.88 in 2007 but dramatically dropped to 0.59 in 2008 and drought is reported as main causative of this sharp drop.

Afghanistan has diverse range of climates, however; mostly it is characterized as continental climate to semi-arid. The spatial annual precipitation ranges from maximum 992mm – 1169mm in North Salang Mountains, to minimum 50mm in Zaranj city, and most other cities rainfall lies between 150 – 300mm. The occurrence of precipitation is temporal which mostly happen between November to April (Climatemaps, 2014; International Center for Agricultural Research in the Dry Areas - ICARDA, 2002).

Agricultural land use data and cropping pattern for most important crops are presented in **Fig. 1.1 – 1.2** (FAO, 2014; Central Statistics Organization of Afghanistan - CSO, 2013~14). As shown by FAO data for 1993 in **Fig. 1.1**, 7.8 million hectares of land are suitable for agriculture which 3.3 million of that is classified irrigated lands and 4.5 million rain-fed, while forests and pastures makes respectively 1.33 and 29.1 million hectares. For 2013 the agricultural land use classified by Afghanistan Statistical Center described based on actual cultivated data in which irrigated land, rain-fed, fallow, forests, and pastures, respectively, occupies 2.09, 1.5, 4.2, 1.7 and 30 million hectares lands.

In Fig. 1.2 for 2013, out of 7.8 million hectares agricultural lands, 0.38% is paddy field and rest 99.62% is upland fields which most important crops are wheat, barley, maize, pulses, fruits and vegetables, however, there is no data presented about forage crops like alfalfa, clover, millet and etc.

National soil mapping has been done in small scale and there are no detailed characteristics of agricultural soil. The pH level is high in arable land, nitrogen and organic content are very low and lacking of phosphorous is among most important characteristics that is recorded (FAO, 2014).

The irrigation water is provided mostly through surface river-water which is fed by snow in mountains and rainfall in all watersheds of the rivers, while during summer some farmers use underground water, through wells, as supplemental irrigation water. Over 80% of water resources is originated from Hindu Kush mountains where it act as snow reservoir during winter and support potential flow to the major rivers during summer by snowmelt (ICARDA, 2002).

The consecutive droughts years and civil wars impacted the infrastructure of the all sectors; among the most suffered ones is Agriculture. The total irrigated area in Afghanistan has fluctuated wildly in the past 30 years due to war, drought, flood damage and a failure to operate and maintain irrigation systems at a community and national level. Irrigation infrastructure has seriously deteriorated and many farmers cannot secure a reliable water supply to resume farming (Future Direction International - FDI, 2011).

[Fig. 1.1 Agricultural land use]

[Fig. 1.2 Land use by most reported crops]

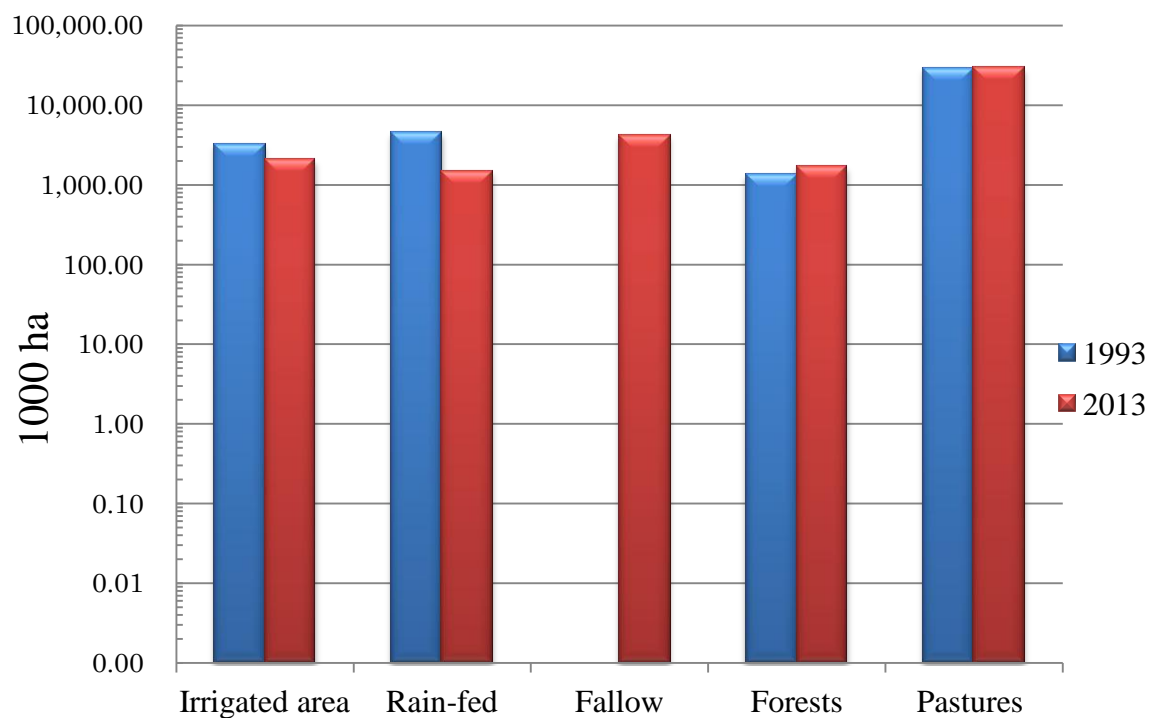


Fig. 1.1 Agricultural land use (1000 ha) (FAO, 2014; CSO, 2013~14)

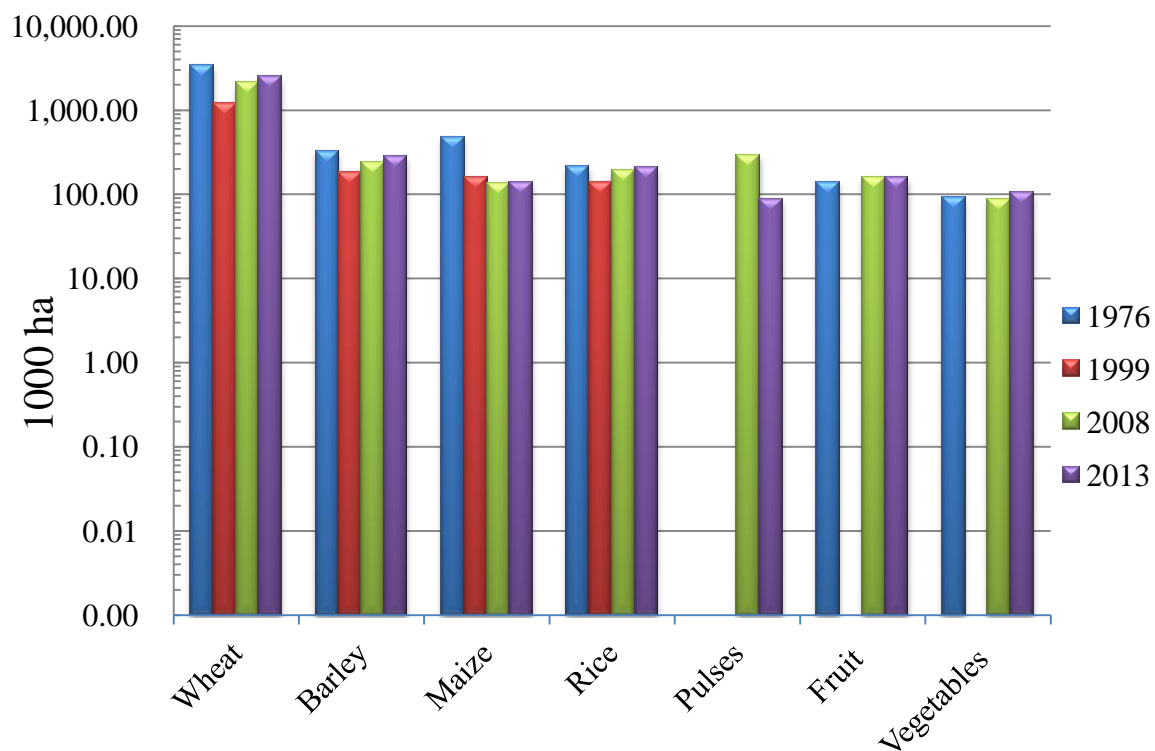


Fig. 1.2 Land use by most reported crops (1000 ha) (FAO, 2014; CSO, 2013~14)

According to ICARDA (2002), and CFC (Civil-Military Fusion Center,2012), the annual estimated potential of surface water and ground water in Afghanistan is respectively 57 billion cubic meter (bcm) and 18 (bcm), which presently it is used for irrigation 20 (bcm) respectively for surface water and ground water 17 (bcm) and 3 (bcm) annually, while rest of the surface water leaves the country due to lack of dams and reservoirs.

Irrigation systems are classified in two forms of formal and informal by the way of operations (CFC, 2012). Formal systems are the ones which is developed, financed, managed, operated and maintained by government support. These systems are mainly as, constructing reservoir dams, control structures, and improvement of canal structure through lining of canals for improvement of water distribution and water use efficiency. However, it is limited with covered area and total number. Recently some government projects and donors funded projects are working for improvement of informal systems to formal.

Informal systems are those which is run and managed by farmers group and Mirab system.

Mirab is a person selected by farmers in villages, for operation of irrigation related activities, as distribution, water right, arranging labor for canal maintenance in tertiary canals level. Mirabs of all villages select someone as Wakil of canal who will be implementing same task as Mirab, but in secondary canal level.

Water losses occur in all level of water supply from source to end user, farmers' farm. The structure of canals all, primary water ways as rivers, secondary canals and tertiary canals, which deliver water to the farms are all muddy with leakage, zigzag structures, and covered with weeds, which all increase the intensity of water loss up to 55% (On-farm Water Management Project - OFWMP, 2011).

Irrigation, water right and water allocation is based on turn and availability of water in the canal, and farmers irrigate their land mostly based on availability of water regardless of crop water need. Farmers try to provide supplemental irrigation water through well during

dry period when their water right is not sufficient, sometimes no supplemental water is provided. On the other hand, if there is water available during their turn they try to flood the plots, although when there is no need for irrigation. In this regard the farmers do not have knowledge of, “how much water to apply?”, “when to apply?”, “how soil depth is important?”, for each crops separately; however, they do have traditional knowledge of which crop need less or more water.

Water use efficiency by farmers practicing irrigation methods and agronomic practices is very low (ICARDA, 2002; CFC, 2012; Shinji Kawasaki et al., 2012). Lack of farmers’ knowledge regarding advanced agricultural systems, land leveling problems, and current irrigation practices are keys for mentioned problem.

Based on **Figure 1.2** which lacks data about forage crops, forage crops contribute a considerable land use because most farmers have the same time livestock, out of 7.8 million hectare around 700,000 hectare of lands are under those crops which their development, maturity and ripping stages are during summer, when there is no precipitation and water flow in canals decrease significantly.

Mentioned trends, issues, problems and challenges regarding temporal and spatial distribution of precipitation, lack of adequate dams and reservoirs, bad canal structures, current agronomic and irrigation practices, and importance of summer season for upland agriculture of Afghanistan, all combined together which made summer season land use around 10% of total agricultural land, or 35% of irrigated area. Even though there is water potential and land availability for increasing land use in summer season, but the current crop production is not satisfactory.

For a growing population in Afghanistan, food security is one of the most important issues and challenges for current and future of the country. As discussed about climate, water, and soil resources of Afghanistan, it indicate the importance of upland field for feeding of increasing population and how the water resources should be used efficiently. For ensuring

food security two important solutions are recommended (FAO, 2014; CFC, 2012; Shinji Kawasaki et al., 2012);

- (1) Construction of new irrigation facilities, as dams and canals.
- (2) Improving irrigation water use efficiency

Regarding water use efficiency all measures should be considered to improve water use efficiency, including prevention of conveyance water loss in secondary and tertiary canals through development of structures, and improving agronomic and irrigation practices, most important aspect in field level is introduction of an effective irrigation plan that can deal with water shortages and use water more efficiently (Shinji Kawasaki et al., 2012).

1.2 Research background

Demand for food and raw materials which are provided by agriculture sector for world population and industry are increasing with world population growth. To ensure food security for world's increasing population, a great concern should be put on sustainable use of natural resources, especially fresh water resources, which is even more important for arid and semi-arid climates like Afghanistan.

More than a third of the world's food now requiring irrigation for production (Goodwin and O'Connell, 2008), where in average in the world, irrigation demands more than 70% of consumptive allocated fresh water, while irrigated agriculture occupy approximately 17% of the cultivated regions (Jury and Vaux, 2007; H. Georgoussis et al., 2009).

Sustainable use of fresh water resources in agriculture is partially possible through improvement of water use efficiency (R. J. Smith, 2005; C. B. Hedley, 2013). Furthermore, high water use efficiency can be ensured when good irrigation planning, precise irrigation scheduling, good management and agronomic practices are practiced alongside extra technology (Terry A. Howell, 2001; Ali Morad Hassanli et al., 2009; Les Levidow et al.,

2014).

Lack of proper irrigation planning can create and increase water stress in crop and as the result economic yield loss; on the contrary it can cause water loss and fertilizer leaching due to excess application of irrigation water. In field level for better and scientific water use efficiency different models have been practiced and proposed for irrigation scheduling so far, in which each has their strength and weakness.

Weather-based crop models are good at estimating evapotranspiration (*ET*) and future irrigation needs over large areas (Thyssen and Detlefsen, 2006; Akyuz et al., 2008; Busch et al., 2009; H. Ganji et al., 2013), while these models are not precise in small scale for different soil to provide exact amount of water when needed based on soil physical properties.

Alminana et al., (2010) and N. M. Cid. Garcia et al., (2014) proposed mathematical multi-disciplinary models for irrigation planning and scheduling which cover broad range of variables of soil, water, irrigation network, technical conditions and logistics.

Computer application models are available for irrigation scheduling as FAO-CROPWAT and Irrigation Scheduling Model – ISM (B. A. Gorge et al., 2000). Both programs need many components for planning and calculation as weather data, soil information, and crop data to be inputted manually. For example; FAO-CROWAT is a good application for large scale water demand calculation and canal discharge design, while for small scale if detailed laboratory results for soil water holding capacity is not provided, the result is not accurate enough since the data for soil is set-up as general estimate.

Songhao Shang and Xiaomin (2006) proposed a simulation-optimization model of irrigation scheduling with limited water, which soil water balance is important component of the model; however, they did not point out other soil parameters which influence water balance in soil.

Some soil-based methods and models measure the soil state variables, soil water potential, that indicate water status of substrate by means of Tensiometers. These models

allow water saving and improve crop growth (Newman et al., 1991; Oki et al., 1996); however, irrigation control based on sensors like tensiometer can suffer from some technical problems, like their placement, establishment of good contact with soil particles and need for constant controls.

Based on mentioned models, for weather based models not much consideration is given for soil conditions, while some soil based water balance monitoring methods emphasized only on water content and the change in water status in soil.

Result for some researches and studies highlight the importance and need for detailed soil investigation for planning of irrigation and scheduling. For example, P. G. Home et al. (2002) studied effect of soil moisture depletion based on irrigation scheduling and method of irrigation. He found out that water loss through deep percolation is significantly influenced by irrigation method, timing and amount of applied water.

In another study, R. J. Smith (2006) showed in his study the dependency between deep drainage and irrigation management. He mentioned that magnitude of deep drainage is greater on light textured soils and where the depth of irrigation water applied is high. He suggested for maximum irrigation performance and minimal deep drainage, accurate measurement of soil moisture deficit should be applied.

Zengjiang Guo et al. (2014) optimized supplemental irrigation for winter wheat based on measured water content of various soil layers and the result showed that the increase in yield, yield component, and water use efficiency was related to soil water consumption. In other studies, Zuo et al. (2006) indicated how soil water distribution from soil surface to maximum rooting depth was significantly affected by irrigation method and quantity. J. Shi et al. (2015) in his research indicated that besides arithmetic average of soil water content, the relative distribution of water and roots were important factors affecting plant water status.

These researches address the fact that the soil resource is a dynamic freshwater reservoir and its ability to plant-available water varied temporally and spatially (Hedley and Yule,

2009; Zhu and Lin, 2011), and require detailed investigation of soil for soil-based irrigation planning.

Soil physical structure as a main attribute of soil quality is an important and unavoidable property of soil for agriculture, since each property of physical structure of soil directly and indirectly can effects, limits, and favors management practices, “soil-plant-water” relationship, plant growth, and yield. Irrigation planning and water use efficiency as management practices are quite dependent and interrelated to soil physical structural properties. For example some researchers pointed out the importance of those soil properties that has important role in irrigation, bellow some are reviewed.

Depth of soil profile plays significant role for root growth and extension in the soil, availability of nutrients for plant, total water holding capacity for a soil profile. The deeper the effective soil layer, the more nutrient available for plant and better growth, provided all other factors are available. J.W. Belcher (1995) founded that there is a great relation between soil depth and over soil biomass intensity in a grass *Trichostema brachiatum*. The study conducted on wild cherry showed that roots in deeper soil had much greater longevity than surface soil (John A. Baddeley, 2005).

Pore size distribution and pore shape are basic soil physical structure characteristics influencing hydraulic conductivity, aeration and plant root in soil. Aeration porosity, which is presenting the portion of macropores, is important for plant growth, after drainage of gravitational water for optimum growth of plants, it should not be less than 0.01 (P. Koorevaar, 1987). Macropores may take a small portion of the soil bulk, but they may dominate vertical flow during infiltration, and as well they increase the surface area for permeability of water into the soil matrix (Keith Beven and Peter Germann, 1982). Soil tubular macropores showed that the rain water that fall on surface plateau had rapid infiltration to groundwater level as the main route and further to micropores and soil matrix (H. Narioka and M. Komamura, 2003).

Soil water flow, availability and storage are influenced by soil structure and texture (Pachepsky and Rawls, 2003). Bypass flow that is increased by aggregation and interconnected pores, results in increasing infiltration, movement of water deeper in the soil profile, and reduce runoff and (Keith Beven and Peter Germann, 1982;A.J. Franzluebbers, 2002). Aggregates are important for aeration, infiltration and water retention in the soil.

Finally, this research is emphasizing on detailed study and research method on physical properties of soil for better understanding and planning irrigation for upland fields. Soil profile characteristics were investigated in three upland fields in Mie prefecture of Japan to determine effective soil layer, existence of hardpan depth, and physical drainage condition of the fields; furthermore, detailed laboratory experiments were conducted for characterizing of irrigation planning parameters.

Therefore the following objectives were set to be met by completion of the research.

- (1) Soil profile characterization and drainage condition both, on-site and in laboratory analysis.
- (2) Studying soil pores structure, especially macropores.
- (3) Determination of soil water holding capacity in term of readily available water.
- (4) Characterizing soil water flow, hydraulic conductivity and drainability.

Same model detailed investigation is required to be implemented in arid and semi-arid climates like Afghanistan and current irrigation practices have to be improved to increase food production toward food self-sufficiency.

1.3 Outline of the thesis

Chapter 1: Characteristic of Afghanistan agriculture has been organized. In particular, the importance of upland agriculture is commentary. Current problems and challenges for upland field irrigation are described. Furthermore, the needs to focus on the soil of farmland were discussed.

Chapter 2: Discussion on the behavior of irrigation water in the soil has been organized. It was noted for the mutual relationship of macropores (drainage) and soil matrix (soil water retention). Fundamental perspectives of irrigation planning were discussed.

Chapter 3: It has been organized for field research methods (farmland irrigation) laboratory analysis methods (formulate upland irrigation plan), and results of field investigation and laboratory are presented.

Chapter 4: Understanding of the results was discussed among three study sites for comparing the suitability, problems and challenges of each site for upland irrigation planning.

Chapter 5: New proposal for the Afghan field agriculture. Comprehensive importance of research methods and experimental methods have been proposed.

Chapter 6: General comprehensive discussion has been taken. The author conducted a comprehensive proposal for a new approach to the upland irrigation plan in Afghanistan.

2. Irrigation planning concepts

In this chapter, the basic and important concepts behind soil based irrigation planning and scheduling are discussed.

2.1 Irrigation

As a general rule, irrigation is the artificial application of water to the root zone of plant in proper time and proper way to protect them from water scarcity, support them for better growth and yield, helping the plants for normal growth, cooling the root environment of the plants, leaching of salts and softening the root environment.

In most cases the water that is applied in irrigation in a field is more than required water, this excess water is as harmful for the plant as lack of water in critical stages of growth. In lands which have natural drainage condition, this excess water can be easily controlled, while in lands with no natural drainage condition, this amount of water should be removed artificially.

Irrigation is one of the most important factors for intensification of agricultural production, while important problems in irrigation practices are “when to irrigate?” and “how much water to apply?”.

It is very critical to know the goal for irrigation, since a definition for it can be derived based on its goals. In case of protecting the crops against water scarcity and better growth, irrigation can be defined as; providing adequate amount of water to root zone of plants, by addition or removal of extra water through drainage.

To overcome such purposes by irrigation, different irrigation methods can be used and source of water can be any of rainfall, canal water or ground water.

Spatial and temporal variation of precipitation made the water a critical and concerning natural source. Agriculture uses around 70% of total earth fresh water and in a large scale threaten the quantity and quality of it; therefore, it is needed for improvement of water use

efficiency in crop production and sustainable use from water resources (Jury and Vaux, 2007; H. Georgoussis et al., 2009; M.A. Ali, 2010).

Water use efficiency is a broad and overall term; it can be defined according to E. Barton Worthington (1977); Overall (project) efficiency is the ratio between the quantity of water placed in the root zone (rain deficit) and the total quantity of water supplied to the irrigated areas; it represents the efficiency of the entire operation between diversion or source of flow and the root zone. Distribution efficiency is the ratio between the quantity of water applied to the fields and the total quantity of water supplied to the irrigated area. Farm efficiency is the ratio between the quantity of water under the farmer's control and the quantity effectively used by crops. Although, overall and distribution efficiencies are as important as farm efficiency, but in term of application efficiency more emphasis is on farm efficiency.

Efficient use of water for crop production requires knowledge of weather, soil, crop, water quality, and drainage situation and for better water use efficiency, it is important to know how much water to apply, when to irrigate and how to irrigate.

For planning a good irrigation system and irrigation scheduling climate and soil are main environmental factors to be considered (B. Yaron, E. Danfors, and Y. Vaadia, 1973; Neil Southorn, 1997).

Knowing the affecting characteristic of environmental factors as temperature, humidity, wind, solar radiation and precipitation; soil factors as topographic location of land, slope, texture, structure, soil water holding capacity, hydraulic conductivity of the soil, soil profile and depth; plant factors as plant growth stage, crop water requirement; furthermore, Jiro SUGI (edited, 1980) suggested prior to planning of irrigation understanding of other factors as water source, availability and limitation, are important. The water requirement of plants is different even in genotype level, to be fulfilled naturally or by irrigation.

In upland field, overall objectives of irrigation is improvement of land productivity and labor productivity in project area by supplying required water for upland crop and extending

employment of water usage through multipurpose application of facilities (Japanese Institute of Irrigation and Drainage - JIID, 1990).

2.1.1 Soil based Irrigation Scheduling

The purpose of irrigation scheduling is application of exact amount water in exact period of time to prevent water loss and provide adequate amount of water in root zone of plants.

Irrigation scheduling can answer the questions of “when to irrigate” and “how much to apply”. Irrigation scheduling is as important as crop water consumption or ET_c , to control water losses by irrigation and also prevent occurrence of stress in plant from water shortage.

There are different models of irrigation scheduling as Hand feel and appearances of soil, Gravimetric soil moisture (soil based), Tensiometers, Electrical resistance blocks, Water budget approach, and Modified approach.

Among mentioned methods, the soil based has high accuracy, but it needs intense laboratory and field work as well time consuming.

In natural condition the water balance in the soil through inputs and outputs as of schematic **Fig. 2.1** shows can be stated as **Equation 2.1**

$$SMB = P + I + C - ET_c - R - D \quad [2.1]$$

Where;

SMB : Soil moisture balance (mm)

P : Precipitations (mm)

I : Irrigation (mm)

C : Capillary rise (mm)

ET_c : Crop evapotranspiration (mm)

R : Runoff (mm)

D : Deep percolation (mm)

Effective irrigation planning and scheduling maintain water status of soil in field capacity without water loss through runoff and deep percolation.

It is critical to know the crop water requirement (CWR), which enables accurate scheduling and commercial production without water loss. Here we will explain step-by-step of irrigation scheduling.

Step 1: CWR can be calculated through **Equation 2.2**.

$$CWR (ET_c) = ET_0 \times k_c \quad [2.2]$$

Where;

CWR: Crop water requirement (mm)

ET₀: Reference evapotranspiration (mm)

k_c: Crop coefficient

The amount of water that crop consumes as daily bases in a field is through evaporation from soil surface that crop is cultivated in and through transpiration that is lost from leaf stomata and these two both are called evapotranspiration (*ET_c*) or crop water consumption to be provided for crop naturally or artificially by irrigation. The applied water by irrigation should always be equal to total water that the crop losses through *ET_c*. If the amount *ET_c* is more than the irrigated water, stress occur in plant and if this continues the plant will go to permanent wilting point and die; on the other hand, while the *ET_c* is less than applied water by irrigation and the soil is saturated for long time, the plant will face to lack of oxygen to the root zone and again stress happen.

ET₀ can be calculated through different equation, as Pan evaporation, Penman-Monteith and etc., *k_c* for most crops can be found from FAO provided tables online.

[Fig. 2.1 Schematic view of water balance in soil]

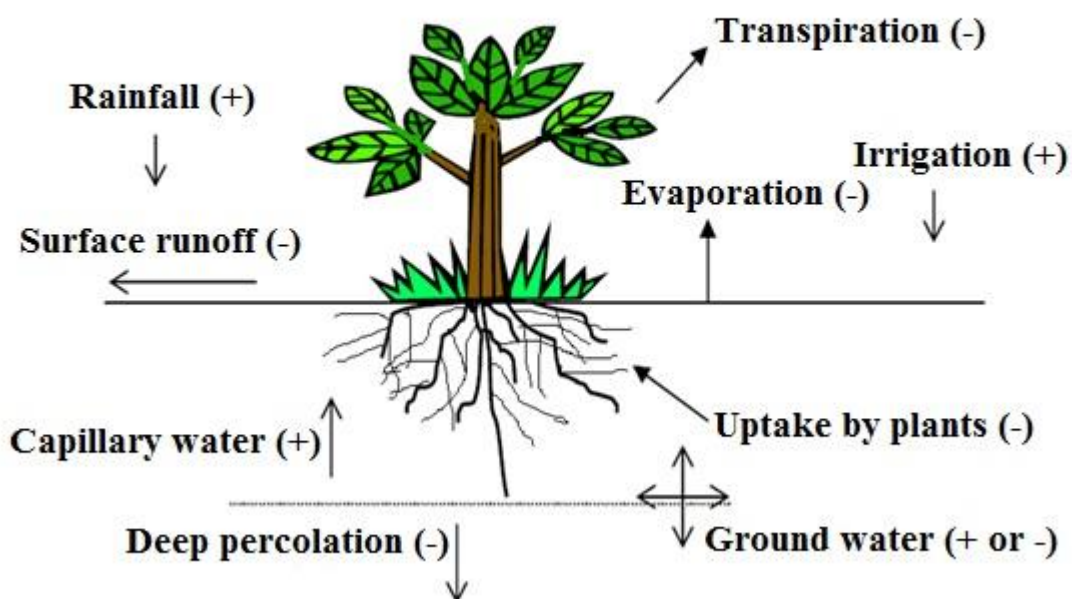


Fig. 2.1 Schematic view of water balance in soil, source; (JICA, leaflet, edited Rahmany 2014)

Step 2: In soil based irrigation scheduling detail of soil characteristics as water holding capacity, effective soil depth for targeted plant, soil texture and structure play significant role in determination of exact amount of irrigation water , because the amount of water applied in each irrigation interval should be sufficient for crop and also should not be lost from soil.

Upland irrigation is not for mere maintenance of the crops, but is understood positively to improve the crop quality and increase the yield (JIID, 1990).

Hence, under such circumstances the lower limit of available water is not permanent wilting point, but the point in which crop begin to be damaged. The moisture amount in this point which obstructs normal crop growth is called the depletion of moisture content for optimum growth.

According to JIID (1990), the lower limit moisture content in which optimum growth of crop is not affected is pF 3.0.

Soil water holding capacities should be determined in laboratory between ranges of pF 1.8 – pF 3.0. pF 0 – pF 1.8 is the gravitational water content which is not available for the plant in the soil and leaves the soil due to gravity force. The pF 1.8 – pF 3.0 is the portion amount of available moisture (AM) which is readily available for the plant.

Available moisture (AM) is the difference between field capacity (FC) pF 1.8, and permanent wilting point (PWP) pF 4.2. Since between pF 3.0 – 4.2 there is still water, but plant need to exert more energy force to uptake it and physiologically crop goes to stress and production decreases, therefore the term readily available moisture (RAM) which is the difference between pF 1.8 – pF 3.0 is used for planning.

Therefore, RAM for each layer of soil can be calculated through **Equation 2.3**.

$$RAM_{ln} = (WC_{pF1.8} - WC_{pF3.0})dn \quad [2.3]$$

Where;

RAM_{In} : Readily available moisture in layer n (mm)

$WC_{pF1.8}$: Water content of soil in pF 1.8 (mm mm^{-1})

$WC_{pF3.0}$: Water content in pF 3.0 (mm mm^{-1})

dn : Depth of n layer in (mm)

It is importance to notice that all parameters should be used same, if the water content is presented in cm cm^{-1} , the depth should be used in cm too.

Step 3: In this step, it is required to determine soil depth of each layer, effective soil depth and soil moisture extraction pattern (SMEP).

Effective soil depth indicates the depth of soil in which moisture is consumed by evapotranspiration. Another term is important soil layer (limiting layer), which dominates moisture consumption. In another word, moisture condition in this layer directly influences the growth of crops, yield and quality. Therefore it is the layer with smallest readily available moisture content. Important layer does not directly involve in calculation, but only is used for decision making regarding which layer should be selected in irrigation scheduling and net amount of water need in each interval. It can be calculated from RAM and SMEP as **Equation 2.4** (JIID, 1990).

$$LL = SMEP \times RAM \quad [2.4]$$

Where;

LL : Limiting layer (important layer with least amount of moisture content),

$SMEP$: Soil moisture extraction pattern (fraction)

RAM : Readily available water (mm)

Since moisture decrease in effective soil layer is not uniform, SMEP is the ratio of moisture decreases in each layer of whole effective soil layers and is an important element to

decide the required amount of irrigation water. SMEP can be calculated through field work by measuring root portion in each layer of effective soil depth and by recording of field Tensiometer, specific for each crop in different depths.

When practical research for determining SMEP and important layer is not possible, the upper 20cm – 30cm of soil depth can be used for planning (JIID, 1990).

Step 4: In this step, daily consumptive water use (CWU) in each layer should be calculated. It is the amount of water in the effective soil depth consumable for optimum growth of crops with high quality and commercial output.

Consumptive water use (CWU) for each layer can be calculated in different ways. One way is to have Tensiometers installed in each depth and record daily water use through differences in water pressure, in which the recorded data is measurement of water loss through Evapotranspiration in each layer. The second way is to follow this methodology and calculate it through **Equation 2.5** (JIID, 1990).

$$CWU = ET_C \times SMEP \quad [2.5]$$

Where;

CWU: Consumptive water use (mm day⁻¹)

ET_c: Actual crop evapotranspiration (mm day⁻¹)

SMEP: Soil moisture extraction pattern (fraction)

Since the irrigation scheduling is based on important layer (limiting layer), there is no need to calculate CWU for other layers.

Step 5: Now it is time for determination of irrigation interval (II) and net amount of water to be applied as total readily available moisture (TRAM) in each irrigation interval.

Irrigation interval (II) is the time differences between two intervals and it can be calculated by dividing RAM to CWU as **Equation 2.6** (Extended equation from JIID, 1990).

$$II = \frac{RAM}{CWU} = \frac{(WC_{pF1.8} - WC_{pF3.0})dn}{ET_C \times SMEP} \quad [2.6]$$

Where;

II : Irrigation intervals (day)

RAW : Readily available moisture (mm)

CWU : Consumptive water use (mm day^{-1})

$WC_{pF1.8}$: Water content in pF 1.8 (mm mm^{-1})

$WC_{pF3.0}$: Water content in pF3.0 (mm mm^{-1})

dn : Depth of n layer, here the limiting layer (mm)

ET_C : Crop evapotranspiration (mm day^{-1})

$SMEP$: Soil moisture extraction pattern

The net amount of water to be applied as total readily available moisture ($TRAM$) in each interval can be calculates as multiplying II with ET_C as **Equation 2.7** and **2.8**.

$$TRAM_{net} = ET_C \times II \quad [2.7]$$

$$TRAM_{gross} = ET_C \times II \times e \quad [2.8]$$

Where;

$TRAM_{net}$: Net total readily available moisture to be applied in each interval (mm)

$TRAM_{gross}$: Gross amount of water to be applied (mm)

e : Application efficiency

These equations were developed for situations where $SMEP$ is known for each crop and soil, while $SMEP$ is not clear **Equation 2.9** is recommended to be used. And **Equation 2.10** can be used for determining irrigation intervals.

$$TRAM_{net} = \sum_{i=1}^n (WC_{pF1.8} - WC_{pF3.0}) dn \quad [2.9]$$

$$\text{Irrigation interval} = \frac{TRAM_{net}}{ET_c} \quad [2.10]$$

Where:

x : Soil layer

n : Number of soil layer in effective soil depth

dn : Depth of n soil layer in effective soil depth (mm).

Mostly the upper 30cm depth of soil is recommended as effective soil depth if in-site investigation is not performed. This 30cm can be consists of 1 layer or more than one layer. If it is consists of more than one layer, the RAM for each layer should be calculated as **Equation 2.9** .

In case laboratory equipments are limited for determining RAM between ranges of pF 1.8 – pF3.0, an indirect method of measurement can be use by tensiometer.

- (1) Install tensiometer in soil in different depth as desired for irrigation and irrigate the land.
- (2) Take soil sample in a core sampler when the tensiometer reading is on 6.17kPa, or 6.1cbar (centibar), or pF 1.8 according to what is the reading system of tensiometer

Equation 2.11.

- (3) Put the sample in the oven for 24 hours in 105°C and measure mass different for before and after oven dry sample.
- (4) When tensiometer reading becomes 97kPa, or 97cbar, or pF 3.0, take sample again and do same procedure **Equation 2.12.**

- (5) Subtract mass different of pF 3.0 from mass different of pF 1.8 and multiply the outcome with soil bilk density to get volumetric water content in term of RAM between the ranges of pF 1.8 – pF3.0 **Equation 2.13.**

$$GW_{pF1.8} = \frac{m_w - m_d}{m_w} \quad [2.11]$$

$$GW_{pF3.0} = \frac{m_w - m_d}{m_w} \quad [2.12]$$

$$TRAM_{pF1.8-pF3.0}(\theta) = (GW_{pF1.8} - GW_{pF3.0})\rho_b \quad [2.13]$$

Where:

$GW_{pF1.8}$: Gravimetric water content at pF 1.8 (g g^{-1})

$GW_{pF3.0}$: Gravimetric water content at pF 3.0 (g g^{-1})

m_w : Mass of soil sample before putting in oven (g)

m_d : Mass of sample after oven dry (g)

ρ_b : Bulk density of sample (g cm^{-3})

After all these steps, then the system or method of irrigation should be selected, which this also need critical thinking and decision making based on water availability and limitation, environmental condition and soil situation.

In conclusion it can be said that from planning till implementing of any irrigation system for any crop, the characteristics of soil, crop, and environment is strongly related to be considered.

2.2 Macropores and Water flow in Soils (Keith Beven and Peter Germann, 1982)

2.2.1 Introduction

From the long past time, it was guessed that large continuous opening (macropores) may be very important for the movement of water, at least under certain conditions. Such voids are readily visible, and it was known that they may be continuous for distances of several meters both vertically and laterally.

In microscopic scale, storage and movement of water in any void depends to the size and irregular shape of that void.

In particular, flow rates will be controlled by the void of smallest size in any single continuous flow path. Thus it is expected a complex relationship between void geometry and flow characteristics at some macroscopic of interest. This has led to a number of indirect ways of classifying pore space.

The method most commonly has been used to interpret the soil moisture retention curve in terms of pores size classes, where a measure of effective pore size is related to capillary potential through Laplace equation for capillary pressure. This involves an analogy between the macroscopic retention characteristics of the soil and the microscopic concept of the behavior of a bundle of capillary tubes. This technique cannot provide an unequivocal definition of a macropore. The choice of an effective size to delimit macropores is necessarily arbitrary and is often related more to details of experimental techniques than to considerations of flow processes.

Porosity may also be classified with respect to hydraulic conductivity of the soil, where data on the change of conductivity with soil moisture are available.

Based on morphological aspects, the macropores are divided in below groups.

2.2.1.1 Pores that are made by soil fauna

These pores are tubular and their sizes range from 1mm to over 50mm that have been made by animals like gopher. These kinds of pores are mostly located to soil surface. The moisture condition and pH of soil influence the population and variety of fauna, as in acidic soils the insects are more adopted while the earthworms prefer less acidic to neutral soils.

2.2.1.2 Pores that are formed by plant roots

These voids are also tubular and are associated with decay or live roots. Distinguishing these pores are difficult due to tendency of newly roots to follow the cannel of previous roots.

The geometry of these pores is different and is related to variety of plant and growth condition and they may be effective in channeling through the soil, even under unsaturated condition. The hallows that formed due to decay of tree stumps and windblown trees may act as funneling system that channel water to the network of macropores formed by decaying roots. The roots of grass case to more a system of equally sized macropores.

2.2.1.3 Cracks and fissures

These macropores are formed either by shrinkage resulting from clay dryness or by chemical weathering of bedrock materials.

Thawing and freezing cycle and cultivation techniques like drainage can produce cracks. Depending on soil moisture condition, shrinkage and swelling of clay soils is subjected to seasonal variation.

Once a crack is formed, it may reoccur at the same location through a series of wetting and drying cycle. In heavy drained clay soils, cracks between structural peds may not close even after prolong wetting.

2.2.1.4 Natural soil pipes

These pipes may form due to subsurface erosive flow, where the applied pressure by water flow on soil particles is more than structural competence of the soil. Such conditions generally occur only in highly permeable, relatively non-cohesive materials that are subjected to high hydraulic gradients.

2.2.2 Experimental determination of macroporosity

Any experiment that is used to determine macroporosity should distinguish between two types of voids, the voids that hydrologically are effective in channeling of water flow in soil and the voids that are not. The concept of hydrologically effectiveness is nebulous, because it has been shown that different number and sizes of macropores are effective under different condition. However, channeling implies a degree of continuity and/or connectivity to other macropores, which this concept is not true for all macropores.

Some techniques that are used to determine the total macroporosity like impregnation and sectioning is not necessarily closely related to channeling macroporosity.

Dye water is used in some experiments as tracer to make the preferential pathways of infiltrating water visible. Ehlers (1975) used mentioned technique in describing the macropores that are formed by earthworms.

Kissel et al (1973), Omoti and Wild (1979), by using florescent dye and ultra-violet photography demonstrated effective macropores at profile scale.

Bouma and Dekker (1978), Bouma and Woster (1979), and Bouna et al (1977-1979) with preparing a thin section of undisturbed soil after application of different amount of dye water, made a further improvement and a new method for describing quantity, size, shape, volume and connectivity of macropores.

Hydrologists are interested in hydrologically effective macropores in channeling of

water flow in a plot, hill slopes and catchment areas. The existing data of small scale experiment can be used for analogy of big scale; however, the evidences have shown that these analogies will neglect big variances.

2.2.3 Macropores Dynamics

Almost all soils possess macropores that the volume and structure of macropores present the dynamic balance between constructive and destructive processes. Any change in community of “soil-plant-animal” and their external condition, such as weather pattern, will affect the balance.

Weather has a great effect on macropores system, for example, dryness case cracking of clay soils and freezing decrease the population of soil animal.

Long term ecological changes also affect the macropores. The most important change in soil macroporosity is the land use. Plowing one - two of soil in a year case in formation of cracks and also cut the natural soil macropores and disconnects vertical connectivity of macropores network.

Ehlers (1975) found that the number of earthworm in surface layer of a tilled soil was less than untilled soil. Use of heavy machinery compact the soil and destroy the macropores. Surface macropores can be destroyed by grazing animal as well.

Several observation and estimates of the age of macropores are reported. Green and Askew (1965) considered the age of ant-developed macropores system to be several hundreds of years. Mellanby (1971) suggest that where food is available, mole runs may be hundreds of years old and may not be apparent from soil surface. Macropores formed by root of a tree may last at least 50-100 years in a soil with 30% of clay. The effective age of macropores may assumed to increase with stability of soil structure, which is a function of soil texture and composition of organic matter.

Thus it is possible that macropores are forms under favorable condition at least in 1-2

years and may last for considerable period of time. On the other hand the effectiveness of macropores can be destroyed within one rainstorm, by washing of material detached by rain splash. We may assume that under comparable condition, the most effective macropores may occur at relatively undisturbed soil, forest sites, and lowest macroporosity in land use area.

2.2.4 Macropores and Infiltration

The presence of macropores near to soil surface is important particularly for infiltration of rainfall and solutes into the soil. **Fig. 2.2** shows simplified view.

Accordingly, three stages of flow may be expected.

$$P(t) < I_1(t) \quad [2.14]$$

All water arriving at the surface is absorbed by micropores connected to the surface.

$$I_1(t) < P(t) < I_1(t) + S_1(t) \quad [2.15]$$

During this period, surface runoff on small scale may occur. Both macropores and micropores open to soil surface take up water simultaneously. As soon as there is enough flow into the macropores, flow down the walls will start $\{S_2(t) > 0\}$. These lateral losses will temporarily reduce the macropores flow S_2 and the depth of infiltration of water along the walls of the macropores. The flow of the water in the macropores can greatly increase the surface area available for infiltration into the matrix in this way.

$$P(t) > I_1(t) + S_1(t) \quad [2.16]$$

Significant amount of water will begin to store at soil surface, and overland flow will start on a large scale $\{O(t) > 0\}$. Note that all symbols represent volume flux densities.

Direct infiltration into the macropores can be neglected during the first stage, since they contribute very little to total surface area.

The second and third stages suggest a process that will not be adequately described by

approaches to infiltration based on Darcy's law, since assumption of homogeneity of hydraulic properties of the soil over some representative cross-sectional area will no longer be valid.

Macropores may make up only a small portion of total soil voids, but may dominate vertical flow rates during infiltration under some conditions. A theoretical relationship may be derived by assuming that macropore flow is analogous to laminar Poiseuille flow through vertical tubes (e.g, Childs 1969) such that:

$$Q_s \propto E_{ma}^2 \quad [2.17]$$

Where Q_s is the saturated flux density of the macropores and E_{ma} is the porosity of the macropore system.

Germann and Beven (1982) showed that the relationship will be of little predictive value.

In **Fig. 2.2** all the effects of macropores on infiltration are not included, where high input rates are applied over large areas of soil, air entrapment under ponding may exert a considerable influence on infiltration rates. Linden and Dixon (1976) found a drastic reduction in infiltration rates, from 1.1×10^{-4} to 8.3×10^{-6} , as a result of an internal air pressure of only 0.5kPa. In such cases, macropores may provide important pathways for escape of air.

One consequence of the concepts summarized in **Fig. 2.2** is that the same volume of water applied at higher intensity may run deeper into the profile along the macropores.

Some attempts have been made to relate soil hydrological properties to morphometric information on soil voids, macropores in particular, from soil thin section. Morphometric data was related with hydraulic conductivity/water content relationship by interpreting the size distribution of active pores under different flow conditions.

[**Fig. 2.2** Macropores structure and water flow in soil]

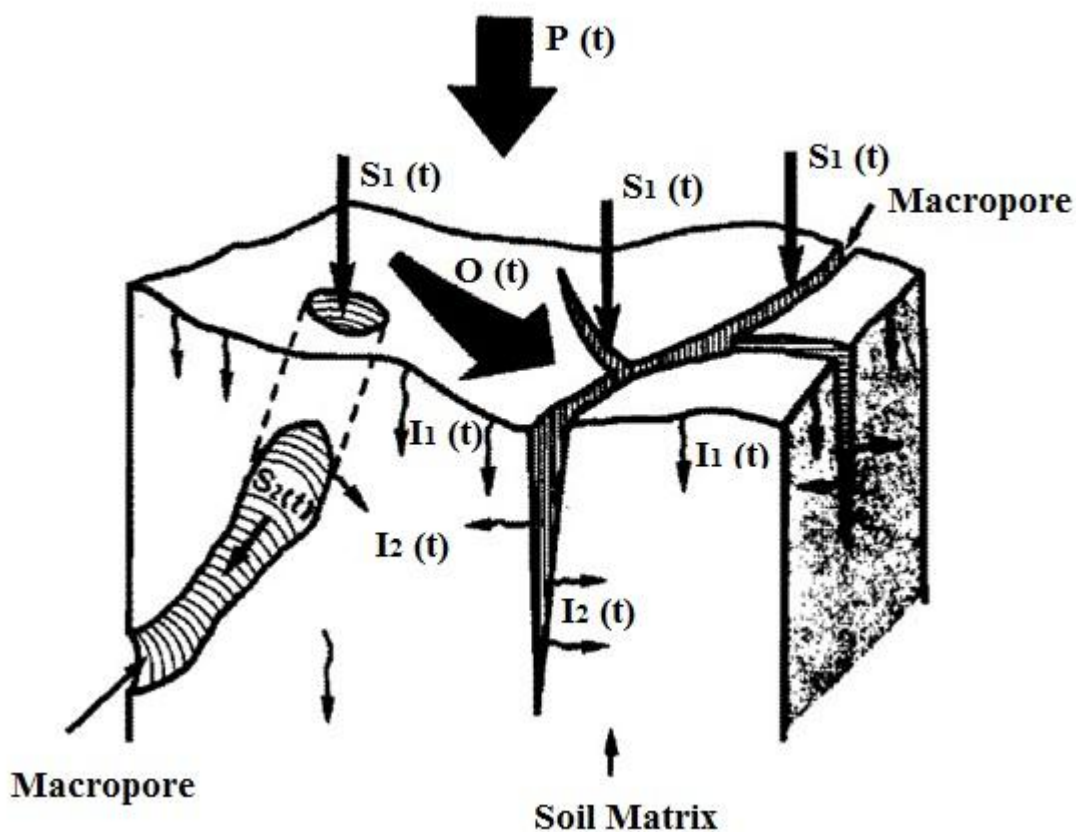


Fig. 2.2 Macropores structure and water flow in soil (K. Beven and P. Germman, 1982)

Figure definition: Definition of diagram for water flow during infiltration into a block of soil with micropores.

$P(t)$, overall input (precipitation, irrigation)

$I_1(t)$, infiltration into the matrix from the surface

$I_2(t)$, infiltration into the matrix from the walls of the macropores

$S_1(t)$, seepage into the macropores at the soil surface

$S_2(t)$, flow within the macropores; $O(t)$, overland flow.

2.2.5 Theoretical studies

According to experimental evidence mentioned, the theories of soil water flow that treat the soil as a relatively homogeneous porous medium confirming to Darcian principles may not adequately describe the infiltration and redistribution of water where the soil contains macropores.

Thus we may expect that prediction based on Darcy law may be significantly in error when the macropores conduct significant amount of water. Since the model based on Darcy law has well proved, any theoretical structure cannot reject traditional approaches.

This suggests the introduction of a domain concept to model combined macropore/matrix system, with the matrix as one domain that can be described by hydraulic principles based on Darcy's law and macropores as second domain.

There are a number of important components to be specified in a complete model.

- (1) The nature of flow in the matrix domain.
- (2) The nature of flow in the macropore system.
- (3) The spatial and temporal characteristics of the macropore system.
- (4) Interaction between the domains.
- (5) Initiation of flow in the macropores.

According to model simulation, the presence of macropores at the soil surface always serves to increase infiltration rates, because additional surfaces are made available for infiltration into the matrix at depth. The effect of macropores is dependent on spacing between large pores, the pattern of rainfall intensities and hydraulic characteristics of the matrix. The effect will be greatest when the hydraulic conductivity of matrix is lower than average rainfall, because in such case little water infiltrate into macropores and their main effect is to increase volume of storage before surface runoff is initiated.

2.2.6 Macropores and subsurface storm-flow

It is now commonly accepted that in many catchments the magnitude and shape of the storm hydrograph is dominantly controlled by subsurface flows. Evidence for this comes from areas where little or no overland flow is observed and by hydrograph separation techniques based on the chemical characteristics of rain, soil and ground water that suggest that pre-storm water may make up a significant proportion of the hydrograph peak.

If macropores are effective in transmitting flow to the stream channel, they may do so at velocities of the same order as overland flow. Hewlett and Hibbert (1967) suggested the term “translatory flow” to describe a new mechanism in which new water entering the saturated zone on a hill slope causes a displacement of old water at the base of the slope.

The response of the subsurface flow system as a whole will also depend on the lag in the unsaturated zone. If the saturated flow is close to the surface, this lag will be short. If macropores are effective in transmitting water rapidly to depth, this lag will be short. The lag may be short in some soils because where a significant capillary fringe has developed over a water table prior to the onset of rainfall, only very small additions of water are required to convert the capillary fringe to a zone of positive pressure, with consequent rapid changes in the boundary conditions of the saturated zone. In this case the velocity of the leading edge of the wetting front, or the flow of small quantities of water in macropores, may assume particular importance.

There are two important ways in which the presence of macropores may give rise to responses that differ from predictions based on “Darcian principles”. The first is when they conduct water rapidly through unsaturated soil ahead of the wetting front in the soil matrix. The second is when flow in the macropores is quasi- or fully turbulent in either the saturated or unsaturated zones.

According to evidence, the macropores may conduct water laterally downslope through

unsaturated soils. In this case, to be an important mechanism in the supply of water to streams and consequently in the generation of subsurface stormflow, there must be excess supply of water to macropores in excess of lateral losses to surrounding soil. In addition, the macropore system must have a sufficient degree of connectivity to transmit water for some distance downslope or at least to a saturated zone that contribute to streamflow.

In summary, it is likely that a variable zone of saturation at the base of the soil profile, or above a relatively impermeable horizon, will dominate lateral macropore flows through unsaturated soil in generating subsurface stormflow.

In saturated zone, fast response will depend on steep slopes and high hydraulic conductivity caused by macropores. The lateral connectivity of the macropores network is less important in the saturated zone, due to there is sufficient large pores to maintain a high saturated permeability.

2.3 Soil pores quantification

2.3.1 Soil porosity

Pore size distribution and pore shape are basic soil physical structure characteristics influencing hydraulic conductivity, aeration, permeability, drainability, and plant rooting in soil. Storage, availability and conductivity of water and aeration are depended not on pores sizes and shapes, but on pore size distribution.

Porosity is the functional entity of soil structure (Rattan Lal & Manoj K.Shukla; 2004), which is a general term refers to the total portion volume of soil that is occupied by pore spaces or voids containing water and/or air. Porosity is a moving target, that essence of biological processes which support life and biochemical and physical which determine environmental quality are governed by it.

Pores of all sizes and shapes combine to make up the total porosity of a soil. Porosity, however, does not tell us anything about the size of pores. It is inversely related to bulk density.

Porosity is calculated as a percentage of the soil volume: **Equations 2.18 – 2.19.**

$$\frac{\rho_b}{\rho_s} \times 100 = \text{solid phase (\%)} \quad [2.18]$$

$$100\% \text{ (soil bulk volume)} - \% \text{ solid phase} = \text{pore phase (\%)} \quad [2.19]$$

Loose, porous soils have lower bulk densities and greater porosities than tightly packed soils. Porosity varies depending on particle size and aggregation. It is greater in clayey and organic soils than in sandy soils. Compaction decreases porosity as bulk density increases. If compaction increases the bulk density from 1.3 g cm^{-3} to 1.5 g cm^{-3} , porosity decreases from 50 to 43%.

Porosity can be presented in different ways based of **Fig. 2.3**:

Total porosity (n): Is the ratio of total pores to total volume of bulk.

$$n = \frac{V_v}{V_t} = \frac{V_v}{V_s + V_v} = \frac{V_v/V_s}{1 + V_v/V_s} = \frac{e}{1 + e} \quad [2.20]$$

Air filled porosity (na): Refers to proportion of air filled pores.

$$na = \frac{V_a}{V_t} \quad [2.21]$$

According to Robert E. White (2005), knowledge of air filled porosity is important for assessment of aeration, soil structural quality and designing soil drainage system.

Void ratio (e): the relative proportion of voids to that of solids is expressed as void ratio, being a ratio; it is also a dimensionless quantity.

$$e = \frac{V_v}{V_s} = \frac{V_v}{V_t - V_v} = \frac{V_v/V_t}{1 - V_v/V_t} = \frac{n}{1 - n} \quad [2.22]$$

Air ratio (a): is the ratios of the air volume to solid volume.

$$a = \frac{V_a}{V_s} \quad [2.23]$$

[**Fig. 2.3** Schematic view of mass and volume fraction of soil phases]

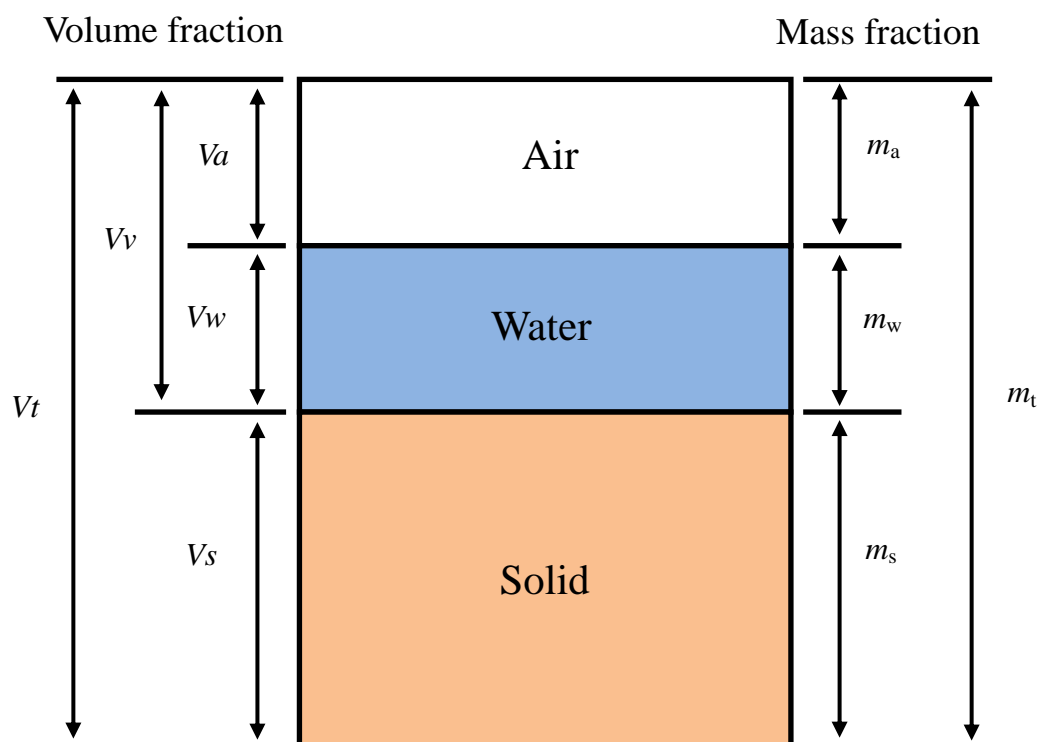


Fig. 2.3 Schematic view of mass and volume fraction of soil phases

2.3.2 Soil pores classification

Soil pores are classified based on their sizes, functionality, and even origin of formation in different groups; Narioka (1989), classified soil pores as **Fig. 2.4**.

Here we will briefly explain each pores group.

[**Fig. 2.4** Classification of Soil Pores (Narioka, 1989; edited Rahmany, 2014)]

2.3.2.1 Inter-aggregate

The primary soil particles bind together and form secondary particles, aggregates. In well developed structure soils, the binding force between particles is stronger than between aggregates, which permits void spaces become among the aggregates.

Aggregates defines structural porosity, inter-aggregates (Derdour et al., 1993), which in this form of porosity total volume of pores, pores size distribution and continuity are extremely important (Rattan Lal & Manoj K.Shukla; 2004). Besides endogenous factor that qualify aggregates and these kind of pores, on the other hand exogenous factors as climatic like wet-dry and freeze-thaw cycles, cropping system, soil management system and returning of crop residue to the soil, plays important role in characterizing quantity and sizes of structural pores. Inter-aggregate pores are very important in hydraulic conductivity of soil, soil aeration, and drainability, while the second group is important in water holding capacity and capillary rise of water which determine the amount of water that can be readily available for plants. Having adequate information about field inter-aggregates can lead to convenient irrigation plan.

We will describe macropores of this group here; capillary pores will be discussed in same group of intraaggregate pores.

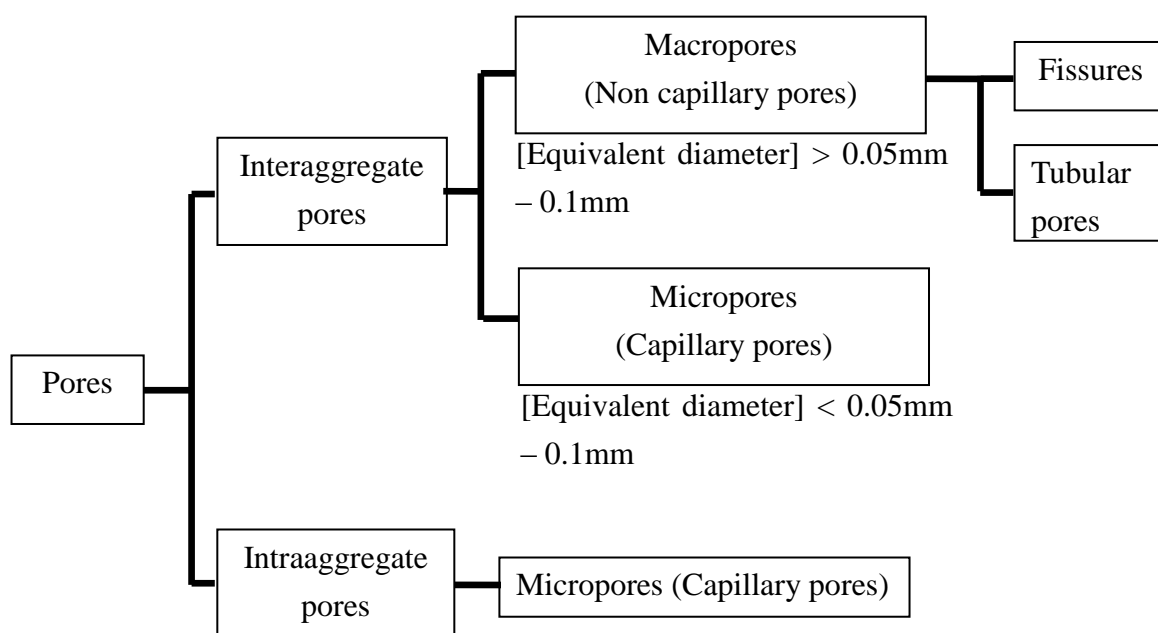


Fig. 2.4 Classification of Soil Pores (Narioka, 1989; edited Rahmany, 2014)

Fissures (cracks)

Fissures or cracks are may formed either by shrinkage resulting from clay soil desiccation, chemical weathering of bed rock material, freeze and thaw cycle, as well as cultivation techniques (cited by: P. Beven and P. Germann, 1982; from: Blake et. al., 1973 and; Lewis, D. T., 1977).

Fissures are larger in diameter than the tubular macropores, but their density is lesser than that of macropores. They look like curved shape from soil surface continuing to the vertical direction. These pores play important role in hydraulic conductivity of soil during high rainfall and irrigation and decrease the chance of run-off, vertical direction fissures lead the roots downward, but if the horizontal fissures present in soil profile, they ban root development since roots do not develop in completely void space. As cited by Rattan Lal & Manoj K.Shukla (2004) from Greenland (1977), the sizes of fissures are more than 500 μm ; while Reeves (1980) categorized fissures in two sub groups of enlarged macrofissures and fissures, the former has equivalent diameter of 2000 μm – 10,000 μm and the later 200 μm – 20,000 μm . **Fig. 2.5** shows a schematic view of macropores.

Tubular pores

Tubular macropores refers to continuous pores with circular diameter or close to it (H. Narioka, 1989). As origin of these porese can be small organism and plant roots. These pores are important in substance mass transport in the soil, water movement, aeration and air and water permeability.

Macropores may take a small portion of the soil bulk, but they may dominate vertical flow during infiltration, and as well they increase the surface area for permeability of water into the soil matrix (K. Beven and P. Germann, 1982). Soil tubular macropores showed that the rain water that fall on surface plateau had rapid infiltration to groundwater level as the main route and further to microspores and soil matrix (H. Narioka, M. Komamura, 2003).

Aeration porosity, which is presenting the portion of macropores, is important for the diffusion of oxygen into the soil and diffusion of carbon dioxide from soil into the atmosphere. After drainage of gravitational water for optimum growth of plants, it should not be less than 10% (P. Koorevaar, 1999). Susceptibility to oxygen deficiency is varying among the plant, for example; tomato is very susceptible to oxygen deficiency and water saturated environment, in case of prolonged saturated field tomato can go to oxygen stress and even die (Henry D. Foth, 1990).

By pass flow that is increased by aggregation and interconnected pores, results in increasing infiltration and reduce runoff and movement of water deeper in the soil profile (K. Beven and P. Germann, 1982; A.J. Franzluebbers, 2002).

[Fig. 2.5 Schematic drawing of Inter-aggregates pores]

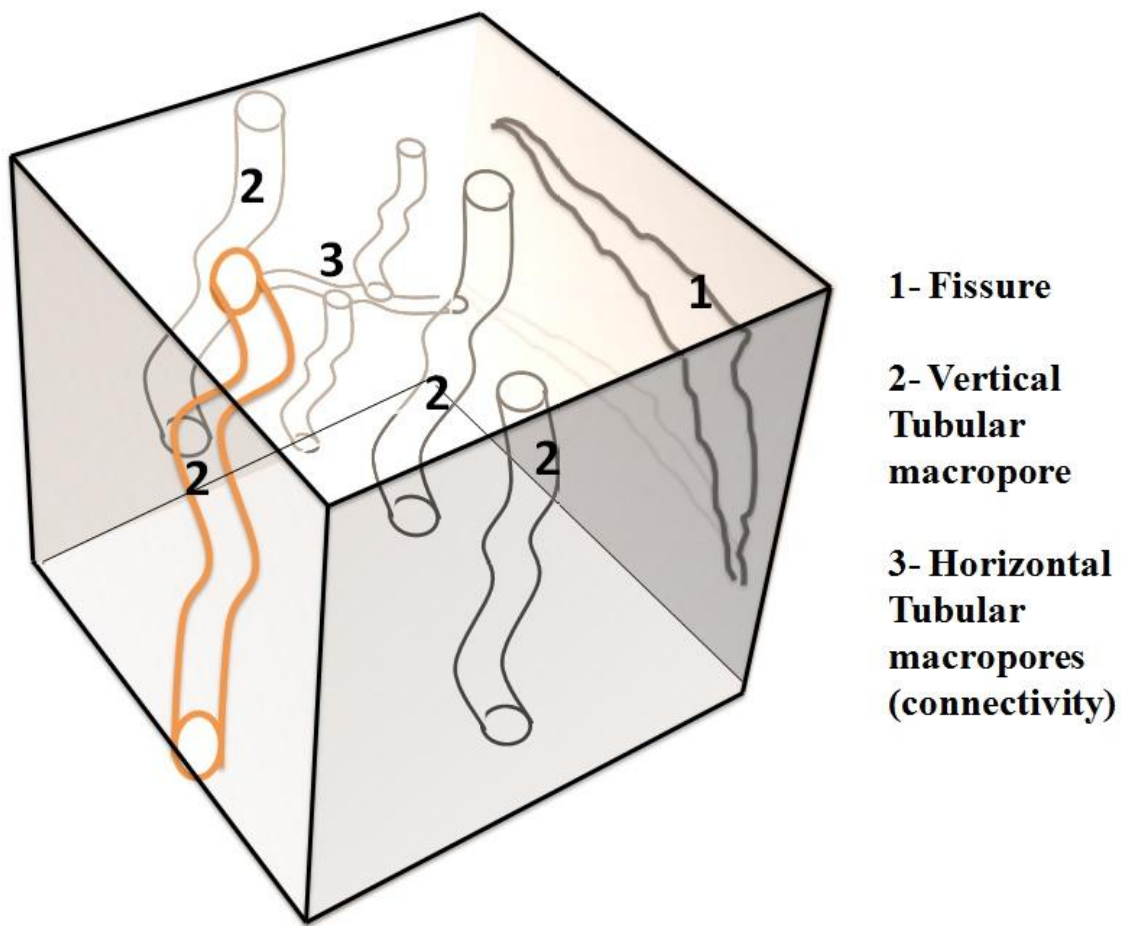


Fig. 2.5 Schematic drawing of Inter-aggregates pores (Rahmany, 2015)

2.3.2.2 Intraaggregate

Intraaggregates which are called textural porosity refers to pores and their size distribution in relation to particle size distribution. The sizes of these pores are related to particle sizes and arrangement of primary particles, for instance, in coarse texture soils this pores have bigger size comparing to fine texture soils. The total volume of textural pores may change during wetting especially in swelling soils.

Microspores retain water which plant can use and conductivity of water in these pores is very slow. These pores which are critical for available-plant-water, characterize water holding capacity of the soil, and capillary rise in soil, their sizes are smaller than 0.05mm in diameter. In another way, we can say the pF 1.8 is the boundary between micropores of this group and macropores of former group.

2.3.3 Air-entry pressure

The importance of pores in water and salute transportation in soil was already discussed. And air-entry value or air entry pressure is explained in section 2.4.2. Macropores based on air-entry pressure was classified by Narioka (1989, 1992), The **Fig. 2.6** shows schematic classification of “air-entry pressure macropores”.

The **Fig. 2.6** shows the groups of macropores based on stages of the air-entry pressure from 0 stage – 5th stage, while 0 stage is the lowest negative pressure and 5th stage is highest negative pressure.

Pores of group A are perfect-open macropores which play significant role in saturated hydraulic conductivity. Group B macropores are imperfect macropores, those which are connected to group A are also as important as group A even they are not perfect-open. Group C are perfect closed macropores which even till highest negative load pressure they do not drain.

The classification system of air-entry macropores of **Fig. 2.6** is shown in **Fig. 2.7** as

“ P_K -drainage curve”.

In **Fig. 2.6**, group A before reaching negative pressure H_u (ultimate pressure) drain completely. The reason why these pores drain completely before ultimate negative pressure, is that their meniscus tip is bigger than equal pores size of the ultimate negative pressure.

From **Fig. 2.7**, slope of curve can be classified in two group of steep slope, (a, b, c) and gentle slope (d, e, f) as **Fig. 2.8**. It represents different pore sizes, in another word, the steep slopes represent coarser macropores and gentle slopes represent finer macropores.

In both curves, slopes (a, d) has similar convex curve, (b, e) has uniform straight gradient, and (c, f) has concave curve. This relations show how the macropores are open in each stages of negative pressure. Convex curve shows much drainage in initial negative load stages, while concave curve shows much drainage in periodic negative load pressure, in the other word, drainage is high with ultimate negative load pressure of concave curve group, and finally the uniform gradient is a special case which with increase in load pressure, the drainage gradually and uniform increase.

Narioka (1992) defined curves with steep slopes (a, b, c) as “conical shape macropores” those which have cone type open front. They response in small change of load pressure and drain soon. Narioka (1992) defined curves with gentle slopes (d, e, f) as “cylindrical macropores”, which their open front and end has similar cylinder shape. These pores drain gradually with change in load pressure.

[**Fig. 2.6** Schematic classification of air-entry macropores]

[**Fig. 2.7** P_K drainage curve]

[**Fig. 2.8** Classification of drainage curve based on slope]

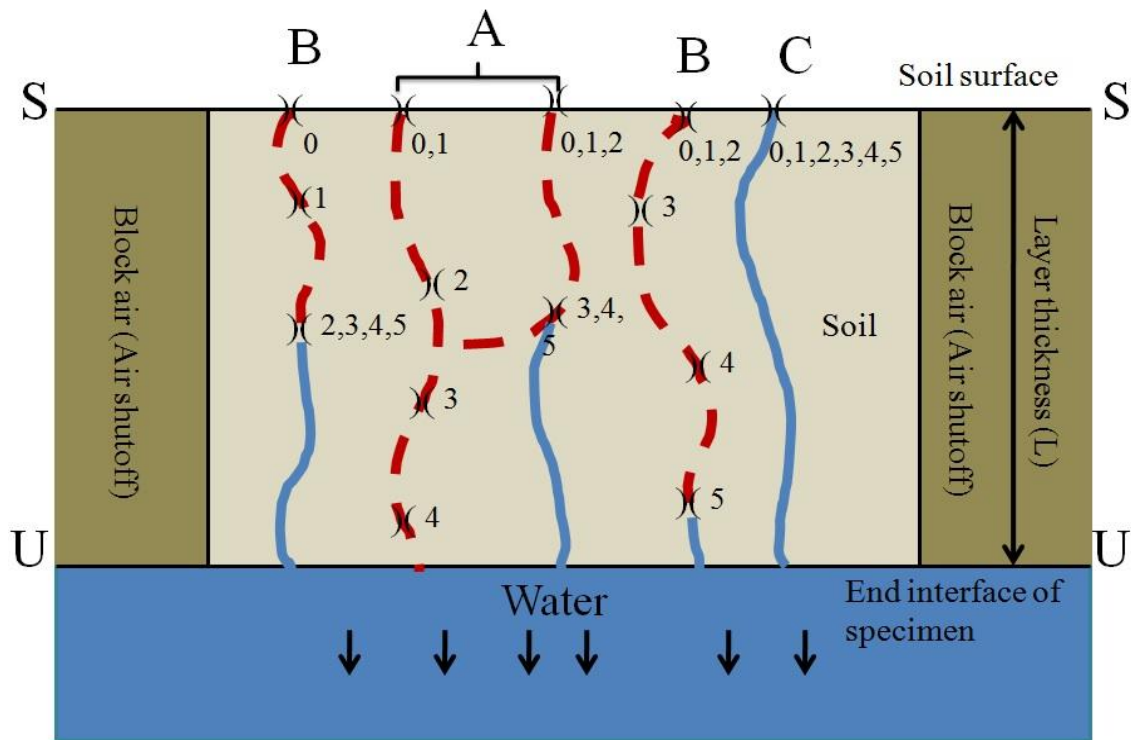


Fig. 2.6 Schematic classification of air-entry macropores (H. Narioka, 1992; edited Rahmany)

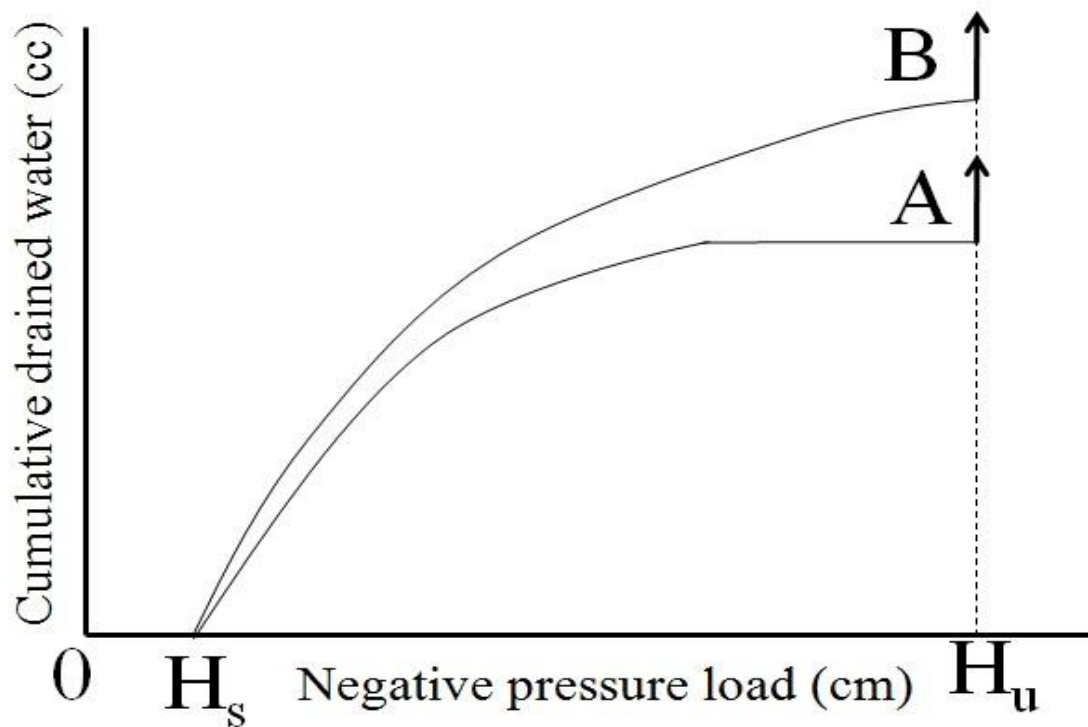


Fig. 2.7 P_K drainage curve (H. Narioka, 1992; edited Rahmany)

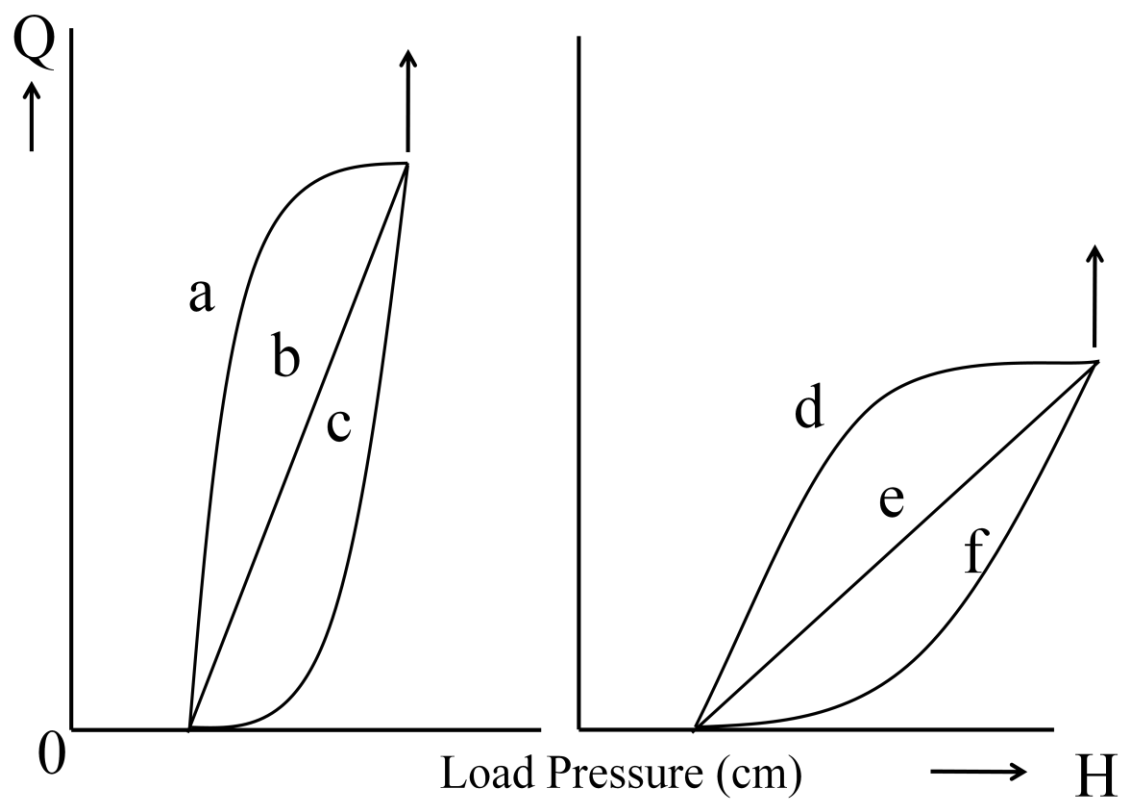


Fig. 2.8 Classification of drainage curve based on slope (H.Narioka, 1992; edited Rahmany)

2.4 pF – θ characteristics

2.4.1 Soil Moisture

The soil-water can be expressed in two ways of soil water content, which represent the amount of water in the soil, and soil water potential, which relates the energy level of water in the soil, indicating how much water is readily available for plants uptake and water movement in the soil.

2.4.1.1 Soil Water Content

Soil water content is the amount of water in a soil based on volumetric or gravimetric that is calculated through weight loss by 105C° in 24 hours from the soil. Soil water content can be presented by weigh as (kg kg^{-1}), or as volume as ($\theta \text{ m}^3 \text{m}^{-3}$) or by degree of saturation as (θ/S) where S is the saturated percent of soil pores.

Gravimetric water content as **Equation 2.24** (D. Hillel, 2003):

$$GW = \frac{m_{\text{wet}} - m_{\text{dry}}}{m_{\text{wet}}} \times 100 \quad [2.24]$$

Volumetric water content as **Equation 2.25** (D. Hillel, 2003):

$$\theta = GW \times \left\{ \frac{\rho_b}{\rho_s} \right\} \quad [2.25]$$

Degree of saturation as **Equation 2.26** (D. Hillel, 2003):

$$S = \left(\frac{V_w}{V_v} \right) \times 100 \quad [2.26]$$

Where:

G_w : Gravimetric water content (%)

m_{wet} : Mass of soil with water (g)

m_{dry} : Mass of soil after oven dry (g)

θ : Volumetric water content ($\text{cm}^3 \text{cm}^{-3}$)

ρ_b : Bulk density of soil (g cm^{-3})

ρ_s : Particle density (g cm^{-3})

S: Degree of saturation (%)

V_w : Volume of water ($\text{cm}^3 \text{cm}^{-3}$)

V_v : Volume of voids ($\text{cm}^3 \text{cm}^{-3}$)

2.4.1.2 Soil Water Potential

Soil water is influenced by variable origin and intensity of forces. The primary two forms of water energy is kinetic and potential, the first one is the virtue of motion which is proportional to velocity squared, since the movement of water in the soil is less than 0.1m/h, its kinetic energy is negligible (Freddie R. Lamm, et al, 2007; D. Hillel, 2003).

This state of soil water is the state of energy potential of small amount of water, or soil water potential is the energy potential of soil water per volume comparing to pure water in reference position (G.S. Campbell, 1985).

Soil water potential is determining the movement of water from one point to another that is under influence of variable origin and intensity as gravitational potential , matric potential, osmotic potential, and other potential, thus water in soil can move laterally, vertically downward or vertically upward for wetting the upper layer of soil. Soil water potential is important for understanding of water movement in soil and in plant and it is presented in Latin letter of ψ .

The total of all pressure that influences the movement of water in soil is called soil water potential. The reference point for this potential is taken as pure water in a certain position.

Since the soil water is under forces of surface adsorption, cohesion and solubility, thus,

comparing to pure water it has less energy and this is why the potential of soil water is negative.

Gravitational potential (ψ_g): Gravitational potential is the result of body forces applied to the water as a consequence of the water being in a gravitational field. When the soil is in saturation and water is standing on its surface or filled its entire pores, the gravity exerts a pulling force on it downward. This force is a positive force on soil water, because it help water move downward, but when the lower layer of the soil is wet and upper layer is dry, for water movement upward, this force is negative, because if the water should move upward then it should overcome this force.

The gravitational potential of soil water is determined by its high comparing to high of a reference point. Mostly for this potential the reference point is taken as soil surface that all the time this potential is zero or positive.

Gravitational potential can be measured as **Equation 2.25** (G.S. Campbell, 1985; D. Hillel, 2003)

$$\psi_g = gh \quad [2.27]$$

Where:

ψ_g : Gravitational potential (kPa)

g : gravitational acceleration (9.8 m s^{-2})

h : height (m)

Matric Potential or Matric pressure (ψ_m): Matric potential is the amount of work per unit mass of water, required to transport an infinitesimal quantity of soil solution from soil matrix to a reference pool of the same soil solution at the same elevation, pressure and temperature.

When the soil particles become in contact with water, they exert a pressure on water which is called adhesion and is calculated as matric potential of the soil. In another word,

from mutual action of capillary force and adsorptive force between water and soil matrix this potential is created and bridge the water with soil and decrease its potential energy comparing to bulk of free water.

It results from the interactive capillary and adsorptive forces between water and the soil matrix, which bind water in the soil and lower its potential energy below that of bulk water (**Figure 2.9**). This force decreases the energy of water and limits the movement of water in the soil pores. This potential in any soil lower from saturation, is a negative number, it means that the potential energy of water that is influenced by matric force is a negative energy.

If the water is required to move in the soil, there should be a positive pulling or pushing force exerted to overcome matric potential.

With drying of the soil and losing its wetness, the matric potential change to a bigger negative number.

Matric potential can be measured through **Equation 2.28** (G.S. Campbell, 1985).

$$\psi_m = -2\sigma/r\rho_w \quad [2.28]$$

Where:

ψ_m : Matric potential (J/kg or kPa)

σ : Surface tension ($7.27 \times 10^{-2} \text{ J m}^{-2}$ at 20°C)

r : Radius of curvature of the interface (μm)

ρ_w : Water density (g cm^{-3})

In the range of matric potential between $-10^4 \text{ J kg}^{-1} < \psi_m < -10^3 \text{ J kg}^{-1}$, the capillary analogy breaks down because most of the water is absorbed in surface layer of particles rather than inside pores.

Osmotic potential (ψ_o): Osmotic potential is the measurement of amount of ions (dissolved salts) that exert a positive adsorptive force on water, which is a negative potential (M. B. Khirkham, 2004).

The solute potential energy or solute potential is the portion of the water potential that

can be attributed to the attraction of solutes for water. If pure water and solution are separated by a membrane, pressure will build up on the solution side of the membrane that is equivalent to the energy difference in the water on the two sides of the membrane (**Fig. 2.10**).

According to D. Hillel (2003), there is a principal difference between osmotic potential and other potential, since other potentials (gravitational and matric) influence water solution in soil, while osmotic potential influence substance alone. Therefore, he suggested that osmotic potential should not be added in total potential.

With increasing the amount of the dissolved salts, the amount of free ions in solution of soil water increase and the osmotic potential become a greater negative number. This potential does not influence the movement of water in the soil significantly, but it is very important when the presence of a selectively permeable membrane or a diffusion barrier which transmit water more readily than salts like root system of plants. Soil osmotic potential can be measured through **Equation 2.29** (A.W. Warrick, 2002).

$$\psi_o = -RTC_s \quad [2.29]$$

Where;

ψ_o : Osmotic potential (kPa)

R : Universal gas constant ($8.314 \times 10^{-3} \text{ kPa m}^3 \text{ mol}^{-1} \text{ K}^{-1}$)

T : Absolute temperature (Kelvin temperature)

C_s : Solute concentration (mol m^{-3}).

A useful approximation which might be used to estimate ψ_o in kPa from electrical conductivity of the soil solution at saturation (EC_s) in dS m^{-1} as **Equation 2.30** (A.W. Warrick, 2002; G. S. Campbell, 1985)

$$\psi_o \approx -36 EC_s \quad [2.30]$$

There are other potentials as overburden potential and pressure and pneumatic potentials, but as far as concerning agriculture, especially irrigation most focus is on matric potential.

The total soil water potential is as **Equation 2.31**.

$$\psi_t = \psi_g + \psi_m + \psi_o \quad [2.31]$$

Accordingly the total potential will be a negative number, unless in saturation situation. When the number is a small negative number, the water content of the soil is higher amount, whereas the number is a greater negative number, the water content of the soil is lower amount.

In agricultural and engineering purposes for determining of this potential the indirect measurement of potential is used which is water height in cm.

The energy state of soil water is called in different terms as suction, tension, capillary pressure head, water head or matric head.

[**Fig. 2.9** Water in unsaturated soil is subjected to capillary and adsorption]

[**Fig. 2.10** Osmometer with a permeable membrane to water and impermeable to solution]

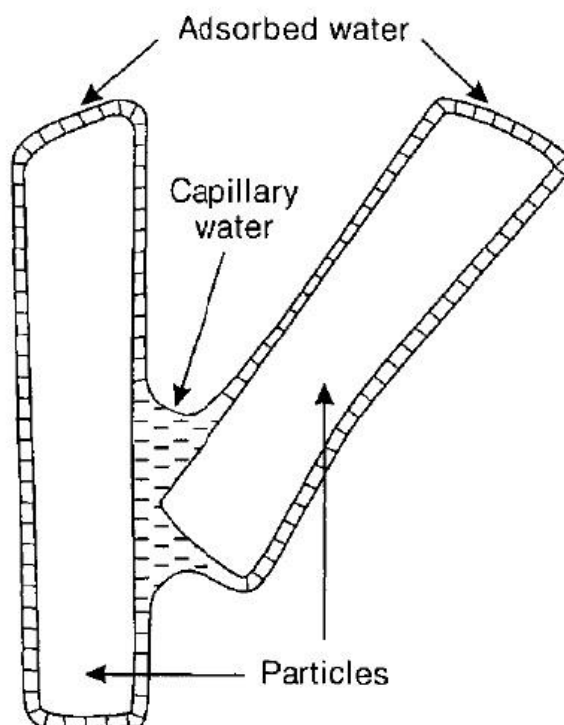


Fig. 2.9 Water in unsaturated soil is subjected to capillary and adsorption, (Source; D. Hillel, Environmental Soil Physics, 2003, Academic press)

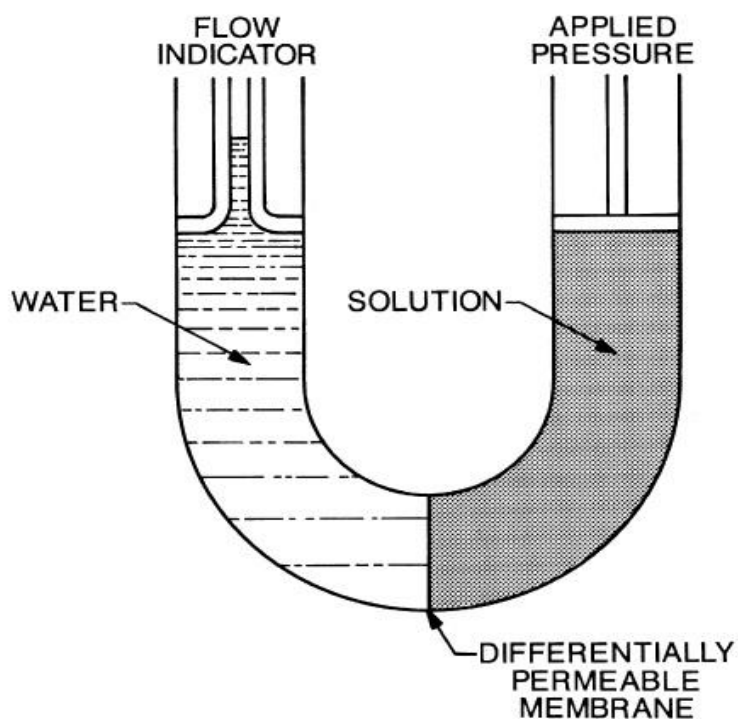


Fig. 2.10 Osmometer with a permeable membrane to water and impermeable to solution, (Source; M.B. Khirkham, Principles of Soil and plant water relationship, 2004)

2.4.2 pF – θ characteristics

The relation between soil water content and matric potential is an important factor for defining soil hydrological characteristics. This relation is called with different names as soil water retention curve, soil water characteristic curve, soil water release curve, pF curve (Potential of free water) and others.

This relation is relating the factor of capacity, water content, to factor of intensity, energy state of soil water.

The need for this relationship is from different aspects, because through this curve the soil characteristics can be defined as its porosity, water retention capacity, and also for calculation of Richard (1931) equation for water flow in unsaturated soil, this relationship is important to be known.

When using the potential per unit weight, the range of water retention of soil start from 0cm – (–1500)cm of water column in the soil, where 0cm stands for saturation and –1500cm for permanent wilting point. To avoid from an irregular diagram, this height of water is shown in \log_{10} of water column in cm, which the –1500cm water column is pF 4.2 that is permanent wilting point.

The pF curve has relation to soil particle density which is defining soil texture and their arrangement, soil structure, that an indication of pore size distribution. Therefore any changes in soil structure and pore size distribution, changes the soil moisture characteristics.

The pressure in which soil largest water filled pores start to drain from saturation is called air-entry value or air entry potential. Air entry suction, potential, is generally small in coarse textures and well-aggregate soil, a higher suction, higher negative pressure, in dense and fine texture soil. **Fig. 2.11** demonstrate the air-entry pressure and pF curve for the ranges of pF 0 – pF 3.0.

Organic matter plays important role in lower suctions especially in field capacity level,

pF 1.8 – pF 3.0, in this level the soil water content increase with the increase to soil organic matter and the diagram on the curve in this range will be more linear.

Under certain suction degree, the water retention is also subjected to change with change in ambient temperature, with increase in temperature the water holding capacity decrease (Rattan Lal and Manoj K. Shukla, 2004).

The soil potential can be measured by different equipment. Tensiometers can only measure from 0 – (-98kpa) which is around -0.98 bar equal to -980 cm height of water. Its limitation is due to air entry through the porous ceramic when the pressure is more than this range.

Other equipment that is used for determining the soil potential is Electric Resistance Blocks that can measure up to -15 of pressure. Gypsum blocks, fiber glass blocks, thermocouple Psychrometer, pressure chamber, pressure plate, and Buchner funnels are other equipment for measuring the soil potential pressure.

For irrigation scheduling and planning, as discussed in section 2.1.1 the best ranges to be considered is between pF 1.8 – pF 3.0; however, some authors suggested pF 3.5 as maximum limit for planning in dry land areas. The **Fig. 2.12** shows Schematic view of water status and intensity in soil.

[**Table 2.1** Different units that can be used to define potential of the soil water]

[**Fig. 2.11** pF- θ characteristics curve]

[**Fig. 2.12** Schematic view of soil water status in soil]

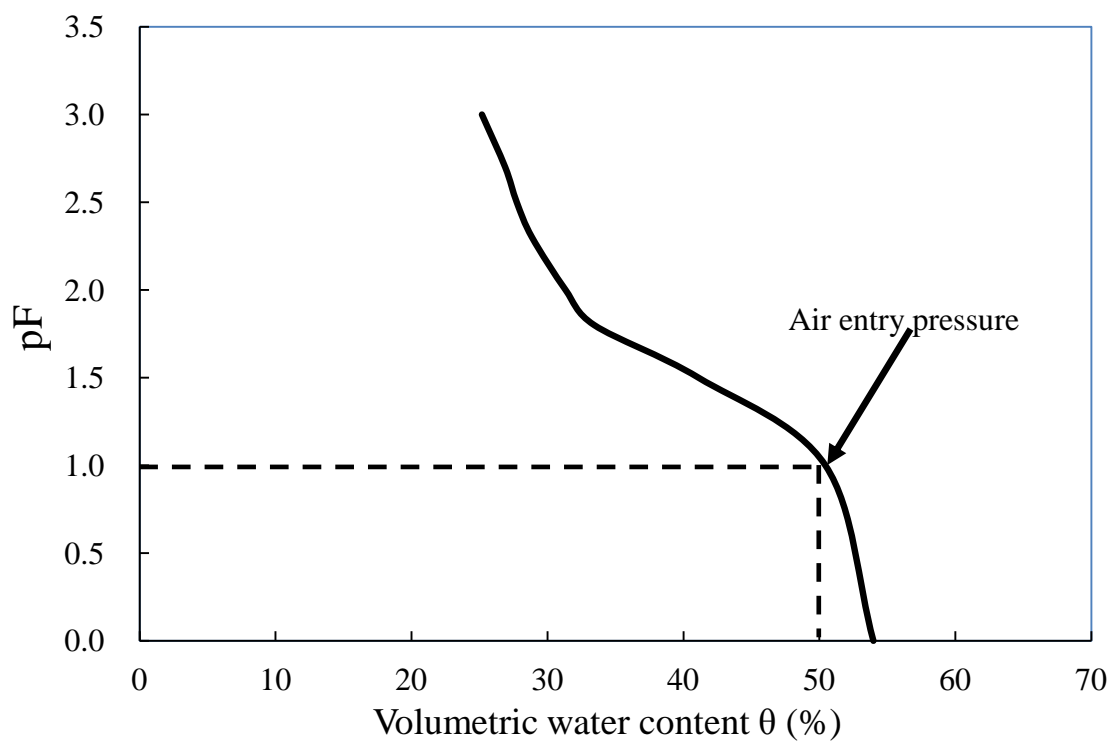


Fig. 2.11 pF- θ characteristics curve

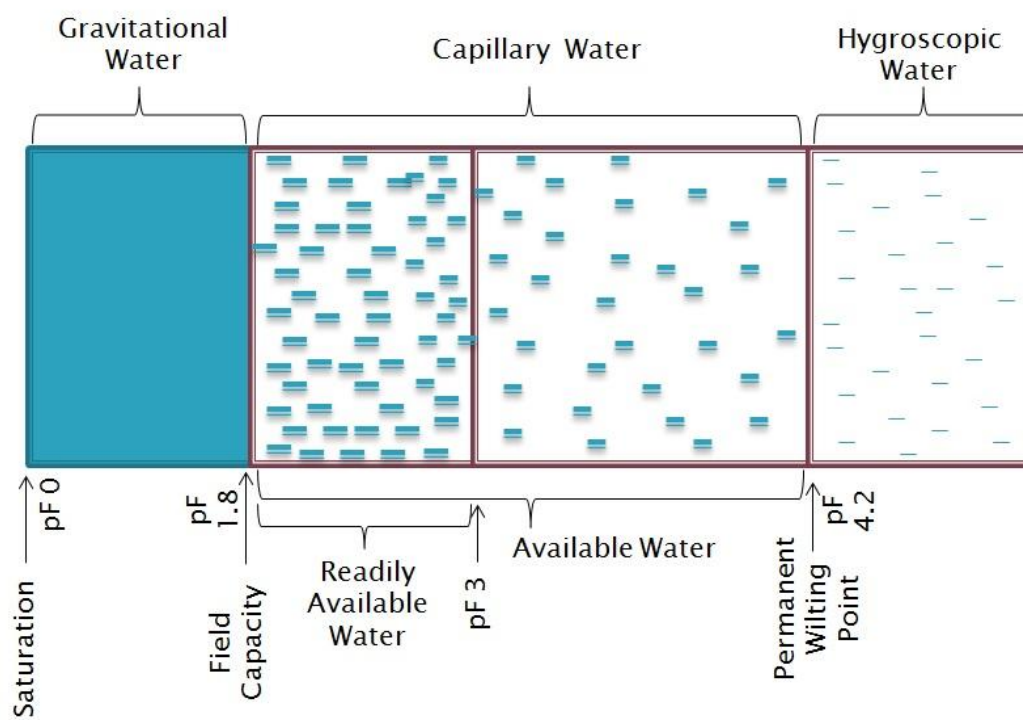


Fig. 2.12 Schematic view of soil water status in soil

Table 2.1 Different units that can be used to define potential of the soil water

Bar	height (cm)	pF	kPa
-0	-0	0	-0
-0.01	-10	1	-1
-0.1	-100	2	-10
-0.33	-330	2.52	-330
-1	-1000	3	-100
-10	-10000	4	-1000
-15	-15000	4.18	-1500*

Due to suction is negative, in front of column 1, 2 and 4 is a negative sign.

* Permanent wilting point

3. Methodology

3.1 Study area as case study

Investigation took place in three sites as case study, since the field were cultivated and was not applicable for probability sampling, judgment sampling was applied (M.R. Carter & E.G. Gregorich, 2007). Prior to lab analysis of soil for planning irrigation, determination of plow layer thickness and other physical parameters are important (JIID, 1990).

Each sites' soil profile were investigated for physical site parameters, disturbed and undisturbed soil samples were collected for laboratory analysis. On-site soil properties were determined by palpation and soil color book was used for color characteristic diagnosis and Yamanaka Hardness meter was used to measure the horizons harness **Photos 3.1 – 3.6** show some of onsite investigation practices.

For future operation and sampling, it is recommended to take GPS coordinates of the investigated field (Alfred R.Conklin, JR. 2005), therefore coordinates of the each investigated area was taken by GPS receiver.

[Photo 3.1 Trimming soil profile cross section]

[Photo 3.2 Determining soil layers by hand-feeling]

[Photo 3.3 Determining texture by hand-feeling]

[Photo 3.4 Soil color determination]

[Photo 3.5 Undisturbed soil sampling]

[Photo 3.6 Soil hardness measurement by Yamanaka hardness meter]



Photo 3.1 Trimming soil profile cross section



Photo 3.2 Determining soil layers by hand-feeling



Photo 3.3 Determining texture by hand-feeling



Photo 3.4 Soil color determination



Photo 3.5 Undisturbed soil sampling



Photo 3.6 Soil hardness measurement by Yamanaka hardness meter

3.1.1 Matsusaka Ureshino Tengejicho Broccoli Field

This area is located in 34°38'00.5"N 136°27'52.2"E and 10m altitude in Ureshino Tengejicho of Matsusaka city, Mie prefecture, Japan. The field is used for the first time for broccoli cultivation. Drainage condition of the field especially in after 20cm of soil depth is poor and water ponding on ridges easily could be distinguished. The center parts of ridges were not leveled, lower than the ridge sides, which increase the condition of ponding in the center part of ridges.

The investigation and sampling took place after 2 days after rain stopped. The study area is surrounded from east, north and west by upland fields and from south by residential houses. **Fig. 3.1** is an aerial view of study area with its surrounding geography, **Fig. 3.2** is a close up view of Ureshino Tengechino village and pointing the study area, and **Fig. 3.3** is the close view of study area in mentioned village.

Disturbed and undisturbed collected samples are shown in **Table 3.1**.

The horizontal direction collected samples are for study of macropores Soft X-ray imaging and horizontal hydraulic conductivity. Vertical direction collected samples are for study of soil undisturbed structure by image analysis, hydraulic conductivity, pF-moisture characteristic, and soil bulk density. Disturbed soil will be used for soil particle size distribution, particle density, and soil three phase liquid-plastic relationship.

[**Table 3.1** Collected samples from different layers of Ureshino Tengejicho Broccoli Field]

[**Fig. 3.1** Aerial view of Study Area, Ureshino Tengejicho]

[**Fig. 3.2** Close up view of Ureshino Tengejicho]

[**Fig. 3.3** Detailed view of study area in Ureshino Tengejicho]

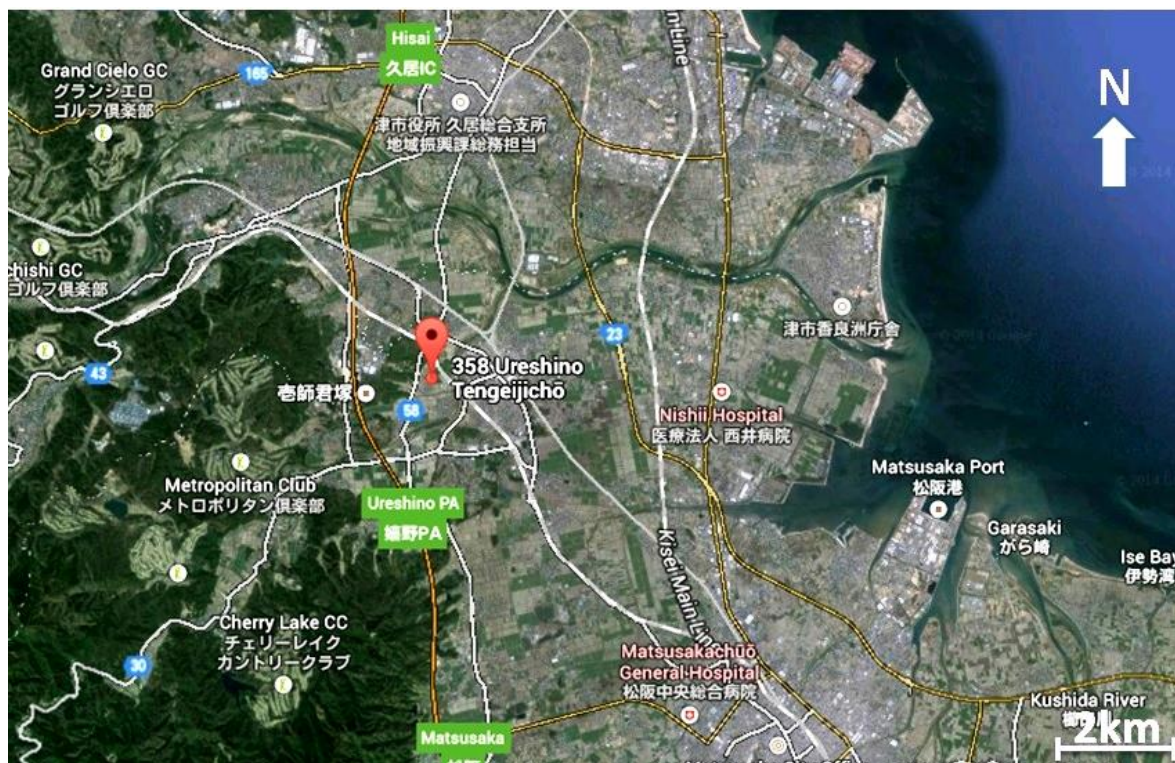


Fig. 3.1 Aerial view of Study Area, Ureshino Tengejicho (Source: Google map)



Fig. 3.2 Close up view of Ureshino Tengejicho (Source: Google map)



Fig. 3.3 Detailed view of study area in Ureshino Tengejicho (Source: Google map)

Table 3.1 Collected samples from different layers of Ureshino Tengejicho Broccoli Field

Layer	100cc cylinder Horizontal (H)			100cc cylinder Vertical (V)			50cc cylinder vertical (V)					Disturbed samples
Ridge				S8	F9	S57						A4 size plastic bag
I	UK13	K8	J10	P8	UK 15	UK 16						A4 size plastic bag
II	F10	UK 11	UK 14	J6	B12	B21	UK 1	UK 2	UK 5	UK 7	UK 8	A4 size plastic bag
III												A4 size plastic bag
IV												A4 size plastic bag

3.1.2 Matsusaka Ureshino Tengejicho Beans Field

This field is also located in same geographical location in Ureshino Tengejicho in 34°38'07.00"N 136°28'01.90"E and 8m altitude. The field is located in plain where it is connected to lower part of hill. The Beans Field is surrounded from North, East and South by Upland fields and from west by road. The aerial view of the village in **Fig. 3.1** and a close view of village, Ureshino Tengejicho, in **Fig. 3.2** are shown. The **Fig. 3.4** shows the detailed close view of the beans field. Disturbed and undisturbed token samples are shown in **Table 3.2**.

[**Table 3.2** Collected samples from different layers of Ureshino Tengejicho Beans Field]

[**Fig. 3.4** Detailed and close view of Beans Field]



Fig. 3.4 Detailed and close view of Beans Field (Source; Google map)

Table 3.2 Collected samples from different layers of Ureshino Tengejicho Beans Field

Layer	100cc cylinder vertical (V)			Disturbed samples
Ridge	S8	F9	S57	A4 size plastic bag
I	P8	UK15	UK16	A4 size plastic bag
II	J6	B12	B21	A4 size plastic bag
III	N14	UK21	A27	A4 size plastic bag

3.1.3 Yokkaichi Agriculture Center Tomato field

The tomato field is located in Yokkaichi Agriculture Center in Yokkaichi city of Mie prefecture between 35° 0'31.51"N 136° 33'24.36"E with 45m altitude. The plot under investigation is used for greenhouse tomato production and is surrounded from North, East and South by farm road and from west by another greenhouse plot. Investigation was done on the south end of ridge to do not disturb farm condition and the same time has good view of physical and biological, roots density, and properties of soil. **Fig. 3.5, 3.6** and **3.7** show respectively the aerial view of the area, close view of the Agriculture Center of Yokkaichi and detailed view of study area. Disturbed and undisturbed samples are shown in **Tables 3.3**.

[**Table 3.3** Collected samples from different layers of Yokkaichi Agriculture Center]

[**Fig. 3.5** Yokkaichi Agriculture Center Aerial view]

[**Fig. 3.6** Close view of Yokkaichi Agriculture center]

[**Fig. 3.7** Detailed view of study area Yokkaichi Agriculture Center]



Fig. 3.5 Yokkaichi Agriculture Center Aerial view (Source: Google Map)



Fig. 3.6 Close view of Yokkaichi Agriculture center (Source: Google Map)



Fig. 3.7 Detailed view of study area Yokkaichi Agriculture Center

Table 3.3 Collected samples from different layers of Tomato field in Yokkaichi Agriculture Center

Layer	100cc cylinder Horizontal (H)			100cc cylinder Vertical (V)			Disturbed samples
A0							A4 size plastic bag
A1	S56	R2	S12	K10	P16	P2	A4 size plastic bag
A2	S1	X4	K28	P28	K2		A4 size plastic bag
B	S5	R28	S4	S39	S3	S22	A4 size plastic bag

3.2 Laboratory experiments

3.2.1 Bulk density

Bulk density is defined as the dry weight of soil per unit volume of soil. Bulk density considers both the solids and the pore space. Soil bulk density can be shown in two ways of dry bulk density (ρ_b) which is without the mass or weight of water and wet bulk density (ρ'_b) which is including solids and water mass or weight.

In a dry soil water volume V_w is zero. Wet soil bulk density is an ever changing entity because of soil evaporation at all times under natural conditions. Therefore, soil bulk density is preferably reported as a dry soil bulk density.

Root growth, in general, starts to be restricted when the bulk density reaches 1.55 to 1.6 g cm^{-3} and is prohibited at about 1.8 g cm^{-3} (Rattan Lal & Manoj K. Shukla, 2004). Tillage can increase bulk density if it breaks down aggregates and allows soil separates to pack more tightly. Adding organic material decreases bulk density because organic material has a lower bulk density. However, additions are typically so small in proportion to the weight of soil that they do not markedly influence bulk density except at the soil-atmosphere interface. Bulk density is also important because it tells us about the porosity of a soil.

3.2.1.1 Wet-Bulk density(ρ'_b); (JIS A 1202, JGS 0111)

Procedure:

- (1) Samples were taken by core samplers and it was protected by zero-tape to prevent water loss.
- (2) The **Equation 3.1** was used to determine wet-bulk density.

$$\rho'_b = \frac{m_t(m_s+m_w)}{V} \quad [3.1]$$

Where;

ρ'_b : Wet bulk density (g cm^{-3})

m_t : Total mass of sample (g)

m_s : Mass of solid (g)

m_w : Mass of water (g)

V : Volume of core (cm^3)

3.2.1.2 Dry-bulk density(ρ_b); (JIS A 1202, JGS 0111)

Procedure:

- (1) After determining wet-bulk density, samples were placed in electric furnace and were oven dried for 24 hours in 105°C .
- (2) After cooling to room temperature, soil mass was measured.
- (3) Dry bulk density was calculated through **Equation 3.2**.

$$\rho_b = \frac{m_s}{V} \quad [3.2]$$

Where;

ρ_b : Dry bulk density (g cm^{-3})

m_s : mass of solid (g)

V : volume of core (cm^3)

3.2.2 Particle density (ρ_s); (JIS A 1202, JGS 0111)

Particle density which is also called true density or specific gravity (G_s) is the ratio of the mass (weight) of soil divided by volume of solid. Particle density is presented as g cm^{-3} .

Particle density of inorganic soils ranges from 2.6 g cm^{-3} to 2.8 g cm^{-3} , and those of minerals commonly found in soils. The density of organic matter is about half of that of the inorganic mineral. In comparison, the density of water is about 1.0 g cm^{-3} and that of the air about 1.0 kg m^{-3} .

Procedure:

- (1) Measured the mass of pycnometer (m_f).
- (2) Pycnometer was filled with distilled water and its mass with water (m_a') and temperature (T') was taken.
- (3) By using **Equation 3.3** (m_a) was measured from above data.
- (4) Half of distilled water was removed and around 10g sample were placed in each pycnometer (**Photo 3.7**).
- (5) The pycnometers were placed on an electric heater and samples were boiled for around 10 minutes. Then the samples were allowed to cool down to room temperature (**Photo 3.8**).
- (6) Again distilled water was added to pycnometer till the mouth of small whole filled with water, after that measured the mass (m_b) and temperature T .
- (7) The samples were placed in determined evaporative dish and put for 24 hours in 105°C in electric furnace.
- (8) The particle density (ρ_s) in water temperature T was calculated through **Equation 3.4** and was converted for value to temperature 15°C by **Equation 3.5**.

$$m_a = \frac{\rho_{w,(T)}}{\rho_{w,(T')}} \times (m_a' - m_f) + m_f \quad [3.3]$$

$$\rho_{s,T} = \frac{m_s}{m_s + (m_a - m_b)} \quad [3.4]$$

$$\rho_{s,15^\circ\text{C}} = \frac{\rho_{w,T}}{\rho_{w,15^\circ\text{C}}} \times \rho_{s,T} \quad [3.5]$$

Where;

m_f : Mass of pycnometer (g)

m_a : Mass of pycnometer filled with distilled water (g)

m_a : Actual mass of pycnometer at temperature (T) filled with distilled water (g)

m_b : Mass of pycnometer with degassed sample and distilled water (g)

$\rho_{w,T}$: Density of water at time temperature T g cm⁻³

$\rho_{w,15^\circ\text{C}}$: density of water in 15°C g cm⁻³

[Photo 3.7 Samples placed in pycnometer]

[Photo 3.8 Heating the samples for air removal]



Photo 3.7 Samples placed in pycnometer



Photo 3.8 Heating the samples for air removal

3.2.3 Particle size distribution; (JIS A 1204, JGS 0131)

Soil texture which is the relative proportion of clay, silt and sand, is one of important physical soil characteristics that has direct influence on water movement in soil, water holding capacity, infiltration, porosity, permeability, erodibility, and influence other physical and chemical process and characteristics.

Determination of soil texture in a detailed oriented of particle size distribution, which separates the inorganic mineral portion of the soil into classified grades according to particle size and determines their relative proportion by weight (Dipak Sarkar & Abhijit Halder, 2005), can be done in different ways as hydrometer and international pipette system through sedimentation (M.R. Carter & E.G. Gregorich; 2007, Alfred R.Conklin, JR.; 2005, Marc Pansu; 2006).

Analysis of soil particle distribution through sedimentation needs some pre-treatment steps for removal of organic matter and cementing agents as calcium and magnesium.

Since the Japanese soils characteristic is high organic matter content, the removal of organic matter through addition of oxygen peroxide as bellow.

3.2.3.1 Organic matter Removal procedure

- (1) About 10g (m_i) of soil was put in a 500mL tall beaker.
- (2) 50 mL of distilled water was added.
- (3) After 10mL of hydrogen peroxide 30% was added.
- (4) By monitoring the time, it was allowed for 30-60 minutes to start reaction (**Photo 3.9**).
- (5) When the reaction increase by arising white smoke, the beaker was placed on a heater providing 80°C (**Photo 3.10**).
- (6) When the liquid looked clear, the removal of organic matter finished.

3.2.3.2 Pipette method in sedimentation

- (1) Same tall beaker which was used for removal of organic matter was used and 5cm depth from the top line of 500mL was marked.
- (2) For each sample a set of evaporative dishes were provided and their weight were recorded.
- (3) The sedimentation time for each of particle sizes 0.02mm, 0.01mm, 0.005mm, 0.002mm, and 0.001mm to depth of 5cm was calculated through **Equation 3.6**.

$$t = \frac{1800 \times \zeta \times L}{(\rho_s - \rho_w) \times d^2 \times g} \quad [3.6]$$

where;

t : Sedimentation time (sec)

ζ : Viscosity coefficient of water (Pa sec)

L : Depth (cm)

ρ_s : Soil particle density (g cm^{-3})

ρ_w : Water density (g cm^{-3})

d : maximum particle diameter (mm)

g : acceleration due to gravity (cm sec^{-2})

- (4) The removed organic matter soil particle was sieved by 2mm sieve, the residual of sieve 2mm (m_1) was transferred in evaporative dish.
- (5) 10mL of sodium exametaphosphate was added to the beaker and after that distilled water was added to the beaker till 500mL, and then it was placed to stirrer for some minutes **(Photo 3.11)**.
- (6) For each beaker a stopwatch was allocated to control time elapse of each particle size classes 0.02mm – 0.001mm **(Photo 3.12)**.
- (7) After elapse of determined time for each particle size for sedimentation to depth of 5cm,

by a micropipette 10mL of suspension was taken from depth of 5cm and was transferred to separate evaporative dishes. From particle size 0.02mm – 0.001mm, respectively it was (m8) (m9) (m10) (m11) (m12).

(8) Samples were placed in electric furnace for 24 hours in 105°C.

[Photo 3.9 Beginning of reaction in the beaker]

[Photo 3.10 Heating of samples for increasing reaction]

[Photo 3.11 Placed beaker on stirrer]

[Photo 3.12 Sedimentation time for each sample]



Photo 3.9 Beginning of reaction in the beaker



Photo 3.10 Heating of samples for increasing reaction



Photo 3.11 Placed beaker on stirrer



Photo 3.12 Sedimentation time for each sample

3.2.3.3 Sieving method

- (1) Remaining sample from pipette method was passed through a set of sieves sizes 0.850mm, 0.425mm, 0.250mm, 0.106mm, 0.075mm and 0.053mm (**Photo 3.13 – 3.14**).
- (2) Residual of each sieve was transferred to evaporative dish and was placed in eclectic furnace for 24 hours in 105°C (**Photo 3.15 – 3.16**).
- (3) Respectively by particle sizes from coarser to finer, they were measured as (m_2) (m_3) (m_4) (m_5) (m_6) (m_7).

To calculate weight ration of each particle size bellow **Equation 3.7 – 3.18** was used:

$$W_{2.000} = m_t - m_1 \quad [3.7]$$

$$W_{0.850} = W_{2.000} - m_2 \quad [3.8]$$

$$W_{0.425} = W_{0.850} - m_3 \quad [3.9]$$

$$W_{0.250} = W_{0.425} - m_4 \quad [3.10]$$

$$W_{0.106} = W_{0.250} - m_5 \quad [3.11]$$

$$W_{0.074} = W_{0.106} - m_6 \quad [3.12]$$

$$W_{0.053} = W_{0.074} - m_7 \quad [3.13]$$

$$W_{0.020} = m_8 \times 50 \quad [3.14]$$

$$W_{0.010} = m_9 \times 49 \quad [3.15]$$

$$W_{0.005} = m_{10} \times 48 \quad [3.16]$$

$$W_{0.002} = m_{11} \times 47 \quad [3.17]$$

$$W_{0.001} = m_{12} \times 46 \quad [3.18]$$

Where;

W_x : mass of particle X diameter x mm (g)

Then to determine percentage ratio of each particle size, the **Equation 3.19** was used:

$$S_x = \frac{W_x}{m_t} \times 100 \quad [3.19]$$

Where;

S_x : percent (%) of particle X diameter x mm.

According to International Society of Soil Science (ISSS), the particles diameter between 2.00mm – 0.02mm are “sand”, 0.02mm – 0.002mm “silt” and smaller than 0.002mm are “clay”, so the percentage of each size group from **Equation 3.20 – 3.22** respectively from $S_{2.00}$ to $S_{0.02}$ for sand, $S_{0.02}$ to $S_{0.002}$ for silt and 0.002 for clay were calculated.

$$[\text{Sand}] = S_{2.00} + S_{0.85} + S_{0.425} + S_{0.250} + S_{0.106} + S_{0.074} + S_{0.053} \quad [3.20]$$

$$[\text{Silt}] = S_{0.020} + S_{0.010} + S_{0.005} \quad [3.21]$$

$$[\text{Clay}] = < 0.002 \quad [3.22]$$

After determination of sand, silt and clay proportion, the outcome was plotted on soil texture triangle as **Fig. 3.8**.

[**Photo 3.13** Sedimented particles for sieving]

[**Photo 3.14** Remaining particles in the different sieves sizes]

[**Photo 3.15** Transferred particles to evaporating dish]

[**Photo 3.16** Oven dried samples]

[**Fig. 3.8** Soil texture triangle]



Photo 3.13 Sedimented particles for sieving



Photo 3.14 Remaining particles in the different sieves sizes

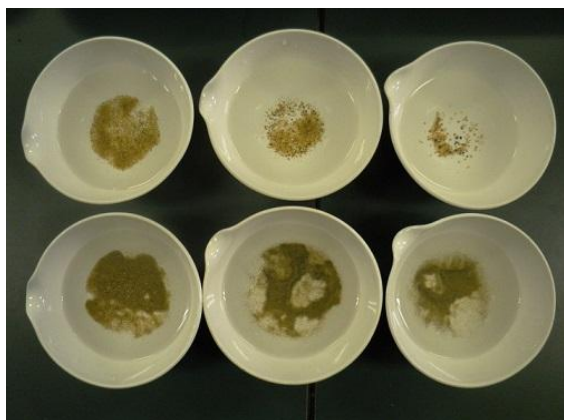


Photo 3.15 Transferred particles to evaporating dish



Photo 3.16 Oven dried samples

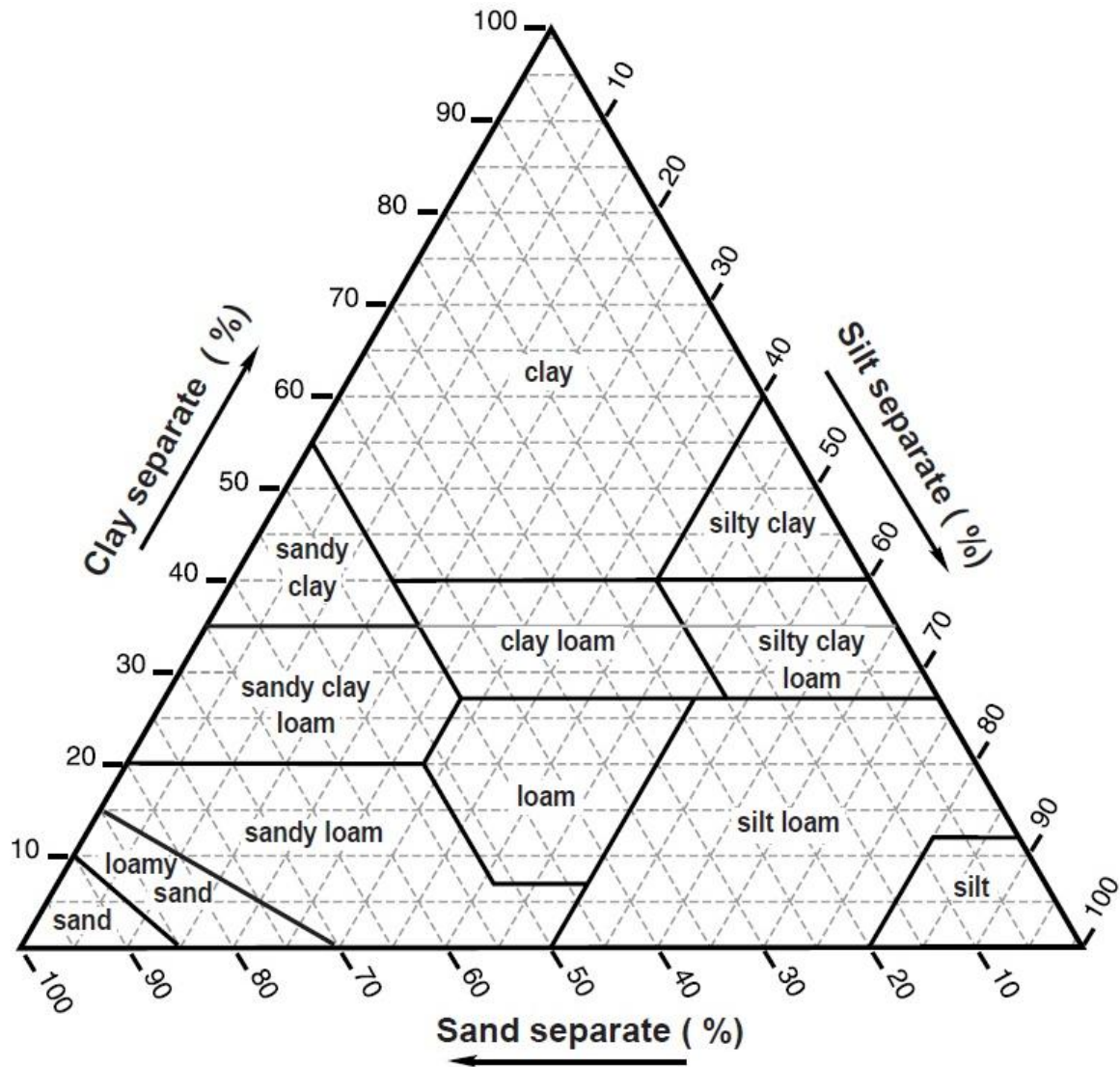


Fig. 3.8 Soil texture triangle (Source: USDA, NRCS, Field book for handling and describing soil, 2002)

3.2.4 Porosity (n); (JIS A 1202, JGS 0111)

Porosity or pore space refers to the volume of soil voids that can be filled by water and/or air. It is inversely related to bulk density. Porosity is calculated as a percentage of the soil volume as **Equation 3.23 – 3.24**.

$$\frac{\rho_b}{\rho_s} \times 100 = \text{solid phase (\%)} \quad [3.23]$$

$$100\% - \text{solid phase (\%)} = \% \text{ pore phase (n)} \quad [3.24]$$

Pores of all sizes and shapes combine to make up the total porosity of a soil. Porosity, however, does not tell us anything about the size of pores.

Porosity can be presented in different ways:

(1) **Total porosity (n)**: Is the ratio of total pores to total volume of bulk (**Equation 3.25**).

$$n = \frac{V_v}{V_t} = \frac{V_v}{V_s + V_v} = \frac{V_v/V_s}{1 + V_v/V_s} = \frac{e}{1 + e} \quad [3.25]$$

(2) **Air filled porosity (n_a)**: Refers to proportion of air filled pores (**Equation 3.26**).

$$n_a = \frac{V_a}{V_t} \quad [3.26]$$

(3) **Void ratio (e)**: the relative proportion of voids to that of solids is expressed as void ratio; it is also a dimensionless quantity (**Equation 3.27**).

$$e = \frac{V_v}{V_s} = \frac{V_v}{V_t - V_v} = \frac{V_v/V_t}{1 - V_v/V_t} = \frac{n}{1 - n} \quad [3.27]$$

(4) **Air ratio (a)**: is the ratios of the air volume to solid volume (**Equation 3.28**).

$$a = \frac{V_a}{V_s} \quad [3.28]$$

Where;

n ; porosity (%)

V_v ; volume of void

V_t ; total volume (solid+void)

V_s ; solid volume

V_a ; volume of air filled voids

e ; void ratio

3.2.5 Soil three-phase

Most soils are composed of four components, inorganic solid particles, organic solid particles, water and air, and three phases of solid, solution, and gas phase.

The solid phase which is composed of mineral and organic particles, the first is with different sizes, shapes and chemical components. Quarts, feldspar and colloidal silicates make the most part of this mineral part which their density ranges from 2600-2800 kg m⁻³. Other heavy mineral like magnetite and garnet also exist in the soil with very low amount. For scientific purposes the average solid particle density is taken as 2650 kg m⁻³. The organic matter of this phase is composed of debris of animal and plant parts which has the range density of 1200-1500 kg m⁻³.

Existing of organic matter decrease the density of solid particles, this is why the surface layer soils have lower density than the deeper layers.

The solid phase of the soil creates the skeleton or matrix of the soil.

3.2.5.1 Solid phase ratio

Solid phase ratio is the ratio of solid volume to the total volume and calculated through

Equation 3.29.

$$\text{Solid phase ratio (\%)} = \frac{V_s}{V_t} \times 100 = \frac{m_s}{\rho_s V_t} \times 100 \quad [3.29]$$

Where;

V_s ; Volume of solid (cm³)

V_t ; Total volume (cm³)

m_s ; Mass of solid (g)

ρ_s ; Particle density (g cm⁻³)

3.2.5.2 Liquid phase ratio

Liquid phase ratio is the ratio of liquid volume to total volume and calculated through

Equation 3.30. Since density of water is 1 g cm^{-3} , therefore direct volume ratio is used.

$$\text{Liquid phase ratio (\%)} = \frac{V_w}{V_t} \times 100 \quad [3.30]$$

3.2.5.3 Gas phase ratio

Gas phase ratio is the ratio of air volume to total volume and calculated through

Equation 3.31.

$$\text{Gas phase ratio (\%)} = \frac{V_a}{V_t} \times 100 = \frac{V_t - V_w - V_s}{V_t} \times 100 \quad [3.31]$$

Where:

V_a : Volume of air (cm^3)

V_w : Volume of water (cm^3)

3.2.6 Liquid Limit (L_L); (JIS A 1205)

Liquid limit test is used to determine the ratio of water that differentiates state of soil from plastic state change to liquid limit.

Procedure:

- (1) The brass plate was installed on the liquid limit measuring instrument; drop height on the hard rubber surface was adjusted to 1cm fall, which can be free fall at rate of 2 times per second.
- (2) Soil samples were passed through 0.425mm sieve.
- (3) To mixed and knead, distilled water added to the sample.
- (4) The sample is placed in a brass dish using a spatula, and 1 cm curve was made in the middle of the plate (**Photo 3.17**).
- (5) The handle was used to rotate in rate of 2rps (round per second).
- (6) Sample was taken for water content measurement from vicinity of the place which joined together after numbers of falling plate.
- (7) The experiment repeated as three times between 25 - 35 numbers of fallings and three times between 10 - 25 numbers of fallings.

3.2.7 Plastic limit (L_P)

Plastic limit is the moisture content ratio that soil state change to semi-solid state.

Procedure:

- (1) The sample water content was adjusted so that the sample can take the form of a ball-shape structure.
- (2) The ball shaped sample was rolled on glass plate by fingers till it takes string-like form. The rolling continued till the thickness of the string-shape sample became 3mm.

- (3) The 3mm diameter string-shaped sample was rolled on the glass plate till it bring apart and in this time sample was collected for measurement of water content ratio.
- (4) The step 1 – 3 repeated 3 times to measure water content ratio.
- (5) Collected samples were placed in electric furnace for 24 hours in 105°C.

3.2.8 Plasticity index (I_p)

Plasticity index is the difference between water content ratio of liquid limit (L_L) and that of plastic limit (L_P) as **Equation 3.32**.

$$I_p = L_L - L_P \quad [3.32]$$

[Photo 3.17 Liquid limit device and sample prepared for measurement]

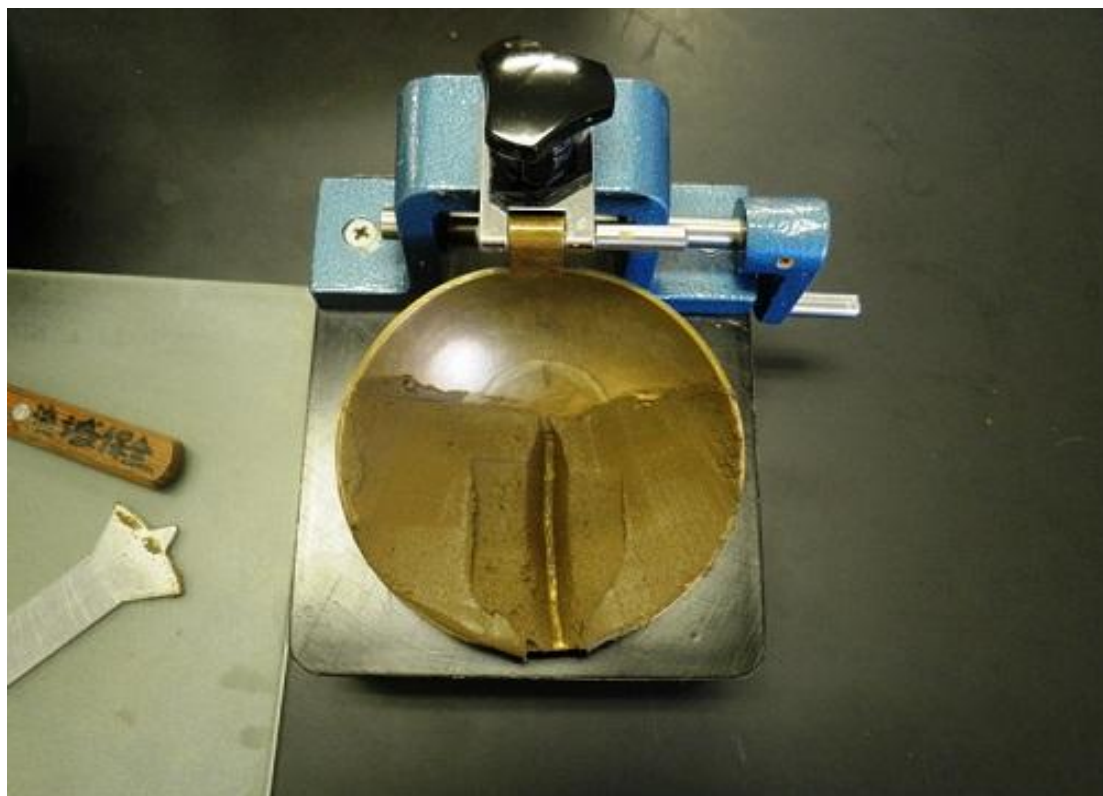


Photo 3.17 Liquid limit (L_L) device and sample prepared for measurement

3.2.9 Permeability – saturated hydraulic conductivity (k_{sat}); (JIS A 1218, JGS 0311)

- (1) After saturation of soil samples the mass of saturated sample was recorded and constant head hydraulic conductivity test was used.
- (2) The inner diameter of core, length (l), mass, and cross-section ($A\text{cm}^2$) was measured.
- (3) Sample was placed in pressure cap and through water supply the sample was saturated till water filled the top of pressure cap.
- (4) From the head difference of water supply (h), the water drainage discharge ($Q\text{cm}^3$) was measured.
- (5) The water temperature in the water supply bottle was measured.
- (6) The hydraulic conductivity coefficient was calculated through **Equation 3.33**.

Fig. 3.9 shows schematic view of testing device and **Photo 3.18** shows actually lab experiment device and operation.

$$k_{\text{sat}} = \frac{Q}{At} \frac{l}{h} \quad [3.33]$$

Where;

k_{sat} : saturated hydraulic conductivity (cm sec^{-1})

Q : drainage discharge volume (cm^3)

A : core cross section area (cm^2)

l : core length (cm)

t : drainage measurement time (sec)

h : difference of water height from drainage point to water level in bottle.

The saturated hydraulic conductivity can be converted in case of 20°C , Therefore, the **Equation 3.34** and **3.35** can be used in this regard.

$$C = \frac{\mu_T}{\mu_{20}} \quad [3.34]$$

$$k_{20} = k_{\text{sat}} \times C \quad [3.35]$$

Where:

C : Water temperature correction coefficient,

μ_T : Viscosity coefficient of water at T °C

μ_{20} : Viscosity coefficient of water in 20°C

k_{20} : The saturated hydraulic conductivity at 20°C (cm sec^{-1})

[**Fig. 3.9** Schematic view of constant hydraulic conductivity test]

[**Photo 3.18** Constant head hydraulic conductivity system device and operation]

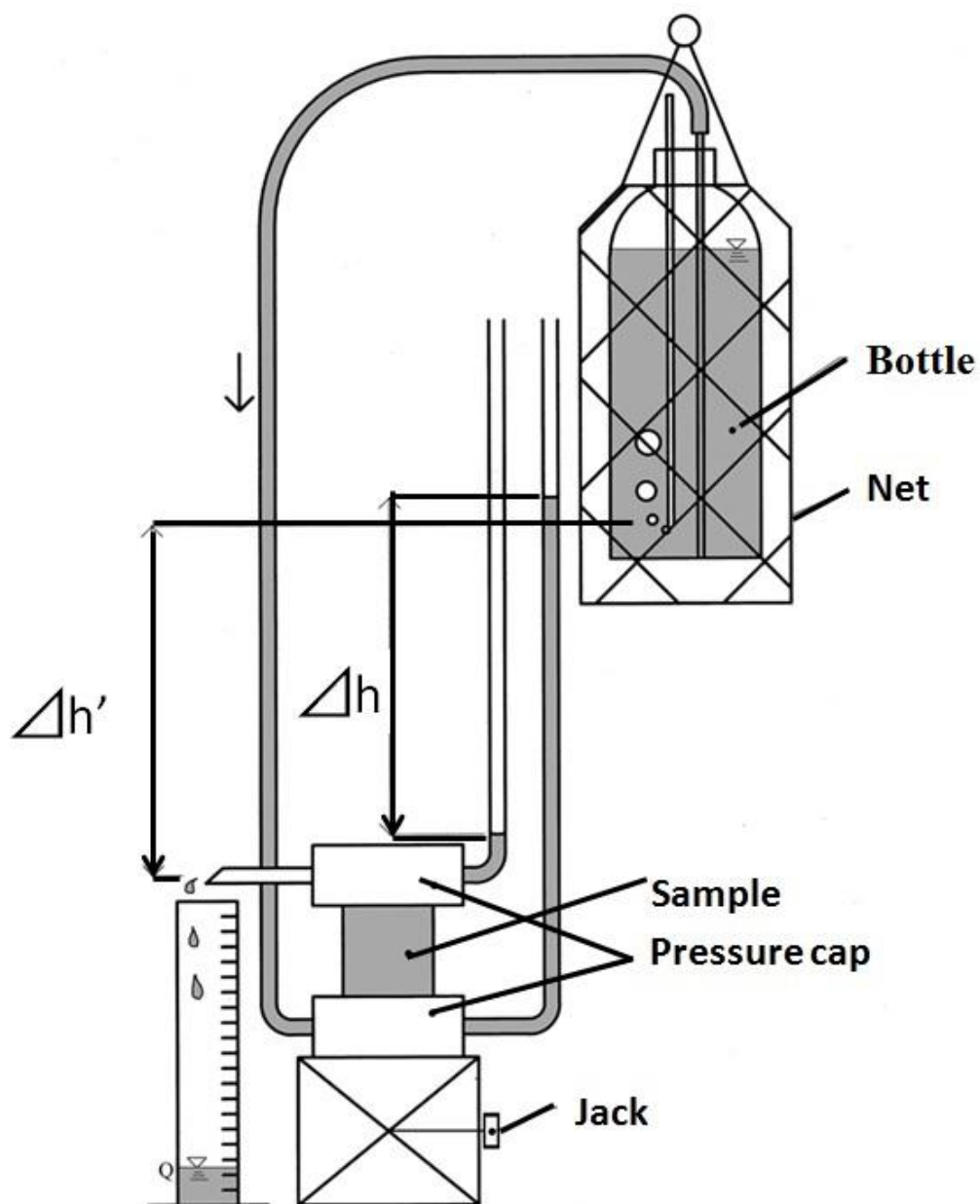


Fig. 3.9 Schematic view of constant hydraulic conductivity test (Frutani, 2013; revised Rahmany)



Photo 3.18 Constant head hydraulic conductivity system device and operation

3.2.10 Drainability (Limit negative P_K pressure)

Limit negative pressure test was measured through suction method. The entire apparatus can be seen in **Photo 3.19**.

Procedure:

- (1) The samples were placed for capillary saturation for 24 hours.
- (2) The pressure cap was equipped with O-ring rubbers to prevent air-entry.
- (3) Samples were placed in the pressure cap.
- (4) The pressure cap, which had sample inside, was saturated with degassed water to remove air inside it.
- (5) Sequentially the load of (2cm/30 min) was applied and the discharge drained water was measured.
- (6) In certain negative load that air bubble was produced at the end surface of the core sampler inside the pressure cap, the experiment was finished.

The obtained data from the mentioned procedure was used to draw drainage curve, where the horizontal axis load negative pressure H (kPa or cm head) and in the vertical axis the cumulative drained water Σq was placed.

[Photo 3.19 System setup and device for negative pressure test]

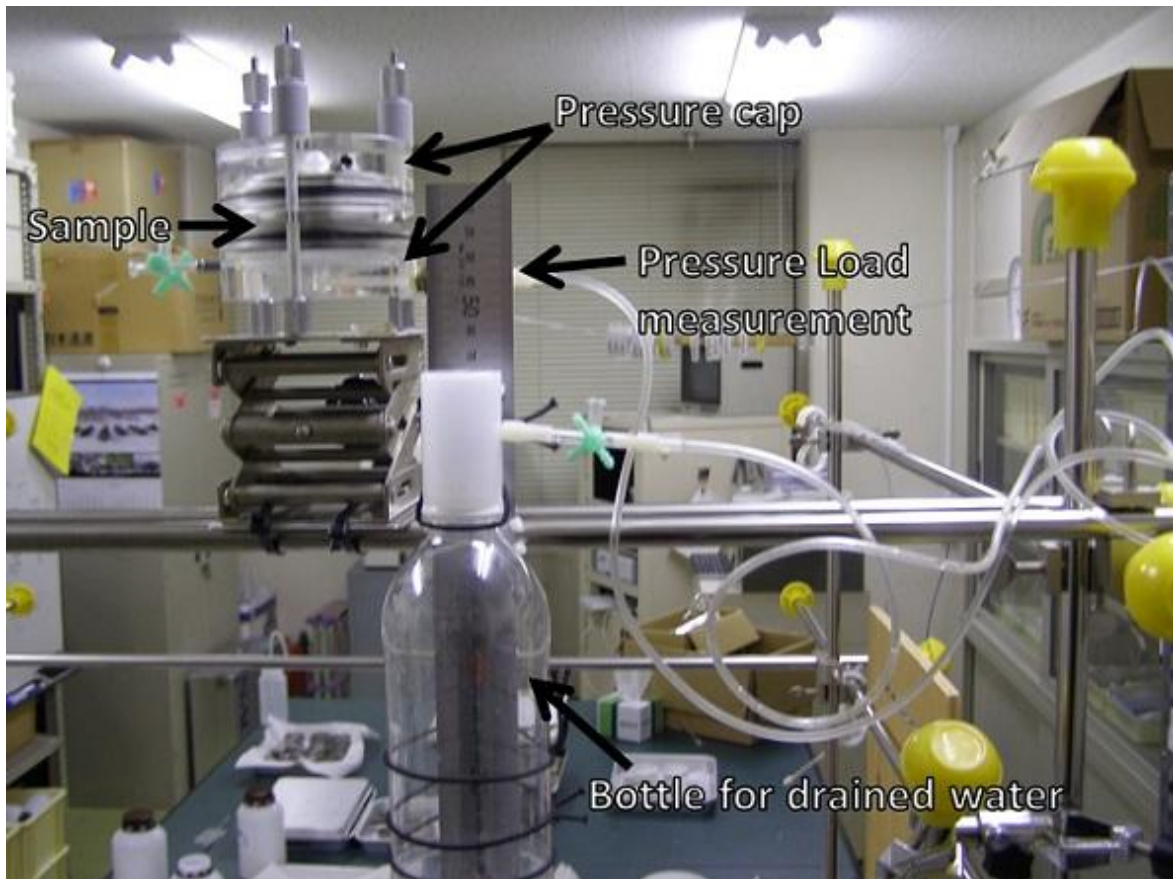


Photo 3.19 System setup and device for negative pressure test

3.2.11 Soil moisture characteristic experiment

The relation between soil water content and matric potential is an important factor for defining soil hydrological characteristics. This relation is called with different names as soil water retention curve, soil water characteristic curve, soil water release curve, pF curve and etc.

This relation is relating the factor of capacity, water content, to factor of intensity, energy state of soil water.

The pF curve has relation to soil particle density which is defining soil texture and their arrangement, soil structure, that an indication of pore size distribution. Therefore any changes in soil structure and pore size distribution, changes the soil moisture characteristics (Daniel Hillel; 2003, Freddie R. Lamm et. al.; 2007, and M.B. Khirkham; 2004).

Using pF curve implies how much suction is needed to retrieve certain amount of water soil holds in form of water column Hcm, p is the logarithmic symbol and F is the potential of free water.

$$pF = \log_{10} H \quad [3.36]$$

For this experiment the pressure plate apparatus was used. The undisturbed soil samples of 100cc were used. In **Photo 3.20** equipment is shown with descriptions. Desorption process was used for characterizing soil moisture characteristics.

Procedure:

- (1) The samples were attached with stocking and were placed in water for 24 hours to be saturated through capillary raise (**Photo 3.21**).
- (2) The exhaust valve and drainage valve was tightened.
- (3) The samples were placed carefully with filter paper on the ceramic filter. The filter paper was used to establish close contact between sample and ceramic filter (**Photo 3.22**).

- (4) The lid was closed; the automatic pressure regulator hose and air supply valve was connected.
- (5) For each targeted value of pF, the conversion input was added to the pressure device.
- (6) Switched the pressure on and opened the air-valve and ensured no leakage is occurring.
- (7) After the equilibrium occurred, the pressure regulator valve was closed and slowly the air supply valve was opened. The pressure regulating hose was unattached and carefully the lid was opened.
- (8) The samples were taken and weighted on a scale covered with aluminum foil.
- (9) After that same procedure was used for next steps, till pF 3.0.
- (10) The core samplers with samples were placed in the electric furnace for 24 hours for drying.

[Photo 3.20 Pressure plate apparatus]

[Photo 3.21 Soaked samples for capillary saturation]

[Photo 3.22 Placing samples on the ceramic plate inside pressure plate apparatus]

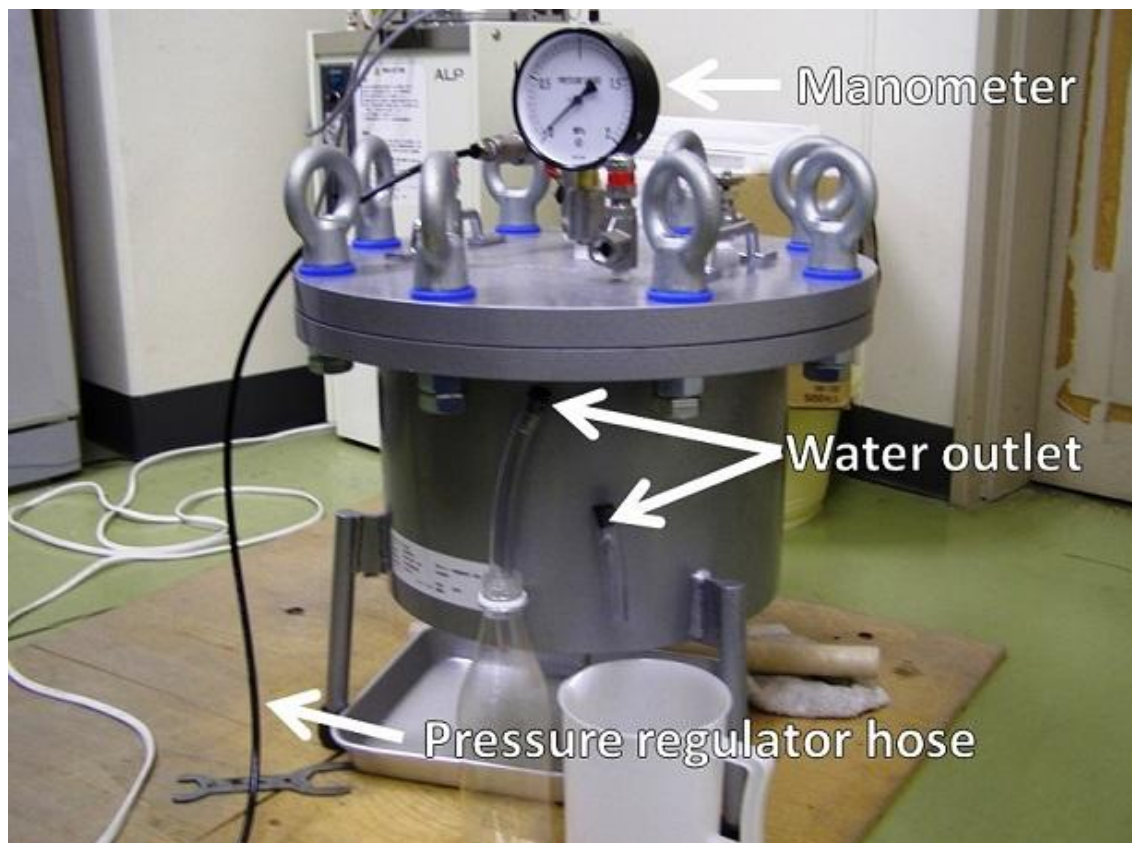


Photo 3.20 Pressure plate apparatus



Photo 3.21 Capillary saturation



Photo 3.22 Placing samples on the ceramic plate inside pressure plate apparatus

3.2.11.1 Volumetric water content (θ)

The total water weight of water was measured through **Equation 3.37**.

$$m_w = m_t - [m_c + m_{\text{dry}}] \quad [3.37]$$

Volumetric water content was measured through **Equation 3.38**.

$$\theta = \frac{m_w}{V_c} \quad [3.38]$$

Where;

m_w : Mass of water (g)

m_t : Total mass (g)

m_c : Mass of core (g)

m_{dry} : Mass of dried sample (g)

θ : Volumetric water content (g cm^{-3})

V_c : Volume of core (cm^3)

3.2.11.2 pF – θ curve

From obtained data, pF- θ curve and moisture distribution curves were drawn. The pF took place in vertical axis and volumetric water content $\theta\%$ in horizontal axis. The moisture distribution curve was drawn by putting $\Delta\theta / \Delta\text{pF}$ in the vertical axis and pores diameter $d(\text{mm})$ in horizontal axis, using Laplace Equation and derived Julin **Equation 3.45**.

As detailed described by Rattan Lal and Manoj K. Shukla (2004), at steady state when liquid stop rising, the net force acting on meniscus is zero. The downward force $F\downarrow$ is the gravitational pull (**Equation 3.39**).

$$F\downarrow = \pi r^2 h \rho_l g \quad [3.39]$$

Where;

r : Radius of capillary (cm)

h : Height of liquid rise (cm)

ρ_l : Density of liquid (g cm^{-3})

g : Acceleration due to gravity (980cm s^{-2})

The upward force $F \uparrow$ is due to surface tension (**Equation 3.40**).

$$F \uparrow = 2\pi r \gamma \cos \alpha \quad [3.40]$$

Where;

γ : Surface tension of liquid against the wetting surface

α : Contact angle for units of surface tension of H_2O and Hg at different temperatures and against a range of solid surfaces.

Thus at steady state, $F \downarrow = F \uparrow$

$$\pi r^2 h \rho_l g = 2\pi r \gamma \cos \alpha \quad [3.41]$$

$$h = \frac{2\gamma \cos \alpha}{r \rho_l g} \quad [3.42]$$

$$r = \frac{2\gamma \cos \alpha}{h \rho_l g} \quad [3.43]$$

Assuming that wetting liquid is H_2O at 20°C , then γ is $72.75 \text{ dynes cm}^{-1}$ or g s^{-2} , water density is 0.9982 g cm^{-3} , g is 980 cm s^{-2} , and α is 0 and $\cos 0$ is 1 . Substituting these values and rearranging Equation 3.43 to solve for r leads to:

$$r = \frac{0.15}{h} \quad [3.44]$$

Where;

r : Radius of pore (cm), change it to diameter in (mm)

Therefore, the result of **Equation 3.44** converted in **Equation 3.45** (Julin).

$$d = \frac{0.3}{h} \times 10 \quad [3.45]$$

Where;

d : Pore diameter (mm)

h : Head (cm)

3.2.12 Soft X-ray imaging method (DCTS-D003, SOFTEX, Japan)

Sample preparation:

Undisturbed samples of 50cc (thickness: 25mm) were used for Soft X-ray imaging. For macropores imaging, the surfaces of samples were lathed so that the macropores could be seen in bare eye and 1-2mL of contrast agent (heavy liquid, 1,1,2,2-Tetrabromoethane {Acetylene Tetrabromide}), solution was added on surface of the samples. We waited till the heavy liquid reached other side of core and the sample was ready for imaging.

Soft X-ray radiography:

Shooting was done in tube voltage of 60kV, tube current of 1.5mA, and 180sec of radiation. The film development machine liquid was set at 28°C and development time of 3 minutes. The Film Focus Distance (FFD) was 500mm.

The device parts and overview is shown in **Photo 3.23**.

Procedure:

- (1) A film was inserted in the imaging table.
- (2) A sample and a sample marker were placed on the imaging table.
- (3) The imaging table was horizontally adjusted to level gauge.
- (4) Shooting took place under above mentioned conditions.
- (5) The Soft X-ray image subjected to shot was developed in developer machine.

After ending the shooting with Soft X-ray, digital photography was done as well for comparison. During the digital shooting, camera was set on stand to ensure certain distance.

Digitization of the soft X-ray image:

Since the X-ray film is optimized for image interpretation by transmitted light, sufficient contrast for reading the image by reflected light is not maintained. Therefore, the film was set up to a light box and was scanned.

Procedure:

- (1) The film is attached to cardboard which make it easy for scanning position.
- (2) The cardboard with attached film is placed on scanner.
- (3) The light box is placed on cardboard which make is clear during scanning.
- (4) Turned the light box and scanned the film.
- (5) The scanned image is saved as .tif format.

[Photo 3.23 Soft X-ray apparatus, DCTS-D003, SOFTEX, Japan]

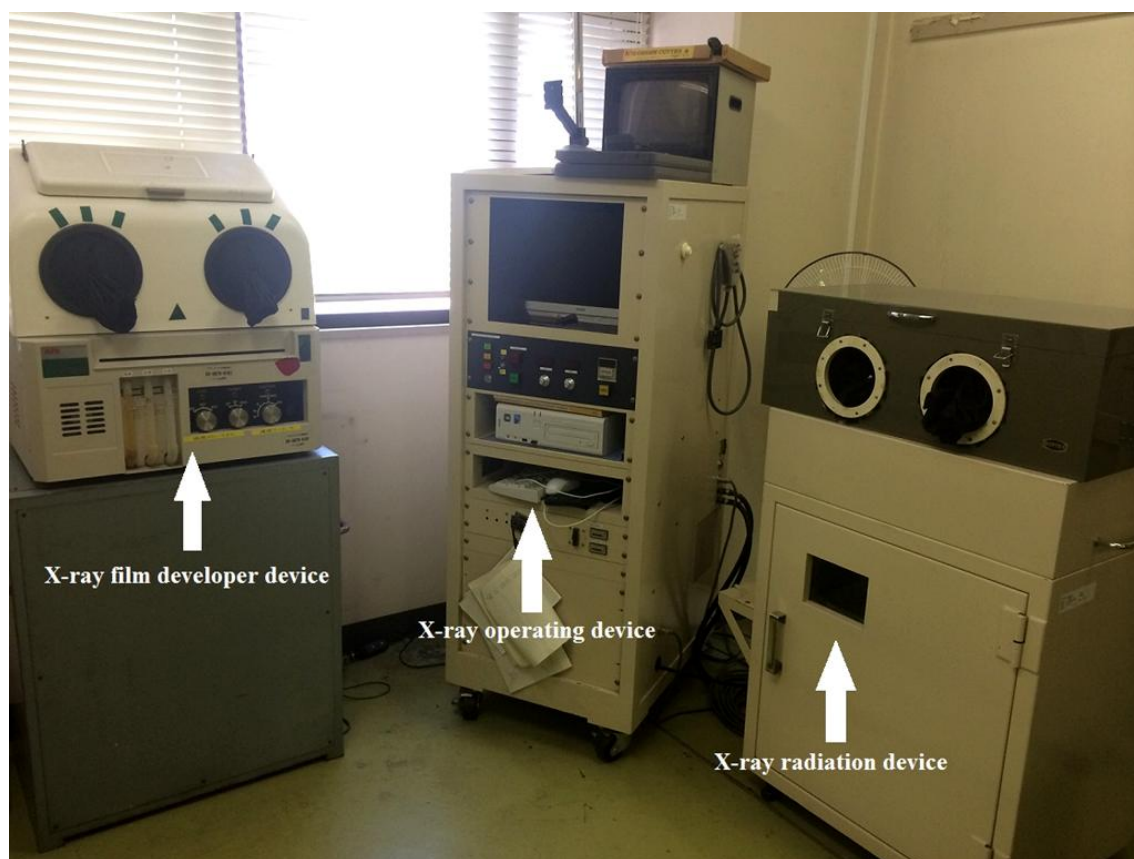


Photo 3.23 Soft X-ray apparatus, DCTS-D003, SOFTEX, Japan

3.3 Results (Case Study)

This section is merely emphasizes the application of methodology on selected three sites as “case study”.

3.3.1 Site Results

3.3.1.1 Matsusaka Broccoli Field

The **Photo 3.24** shows soil surface view and irrigation system condition of the field. As it is clear in the photo, water ponding occurred in ditches and ridge as well, and overall drainage condition of the field seems poor. The leveling condition of the entire field, particularly the ditches is not uniformed and it increases the intensity of spatial ponding.

Soil profile cross section and ridge is shown in **Photos 3.25 – 3.27**. **Table 3.4** contains the on-site soil cross section investigation data and **Fig. 3.10** presents the soil hardness distribution which was measures by “Yamanaka Soil Hardness Meter”. Based on **Fig. 3.10** of soil hardness data, on-site investigated data in **Table 3.4**, and looking to **Photos 3.25 – 3.27**, soil hardpan begins just underlying the layer I .

From 0cm – 15cm , the ridge structure is granular and from 15cm – 100cm which is composing layers I - III has massive structure and lower than this range which is layer IV has again granular structure. Sand ratio determined by hand palpation was higher in all layers.

Macropores in I layer were not significantly visible, while in layer II existing of macropores are shown in **Photo 3.28 – 3.29**. In **Photo 3.29** pores with sigh A refers to those tubular pores with diameter bigger than 1mm, those with B sign refers to tubular pores with diameter between 0.5mm – 1mm, and C refers to root made canals.

[**Table 3.4** Broccoli Field on-site soil profile cross section investigation results]

[**Fig.3.10** Soil hardness distribution in (mm)]

[**Fig. 3.11** Soil hardness distribution in (kg cm⁻²)]

[**Photo 3.24** Broccoli Field soil surface view and irrigation system condition]

[**Photo 3.25** Broccoli Field soil profile cross section]

[**Photo 3.26** Soil profile cross section and ridge]

[**Photo 3.27** Ridge close view]

[**Photo 3.28** Macropores in layer II of soil profile]

[**Photo 3.29** Detailed view of macropores]



Photo 3.24 Broccoli Field soil surface view and irrigation system condition



Photo 3.25 Broccoli field soil profile cross section



Photo 3.26 Soil profile cross section and ridge



Photo 3.27 Ridge close view



Photo 3.28 Macropores in II layer of soil profile

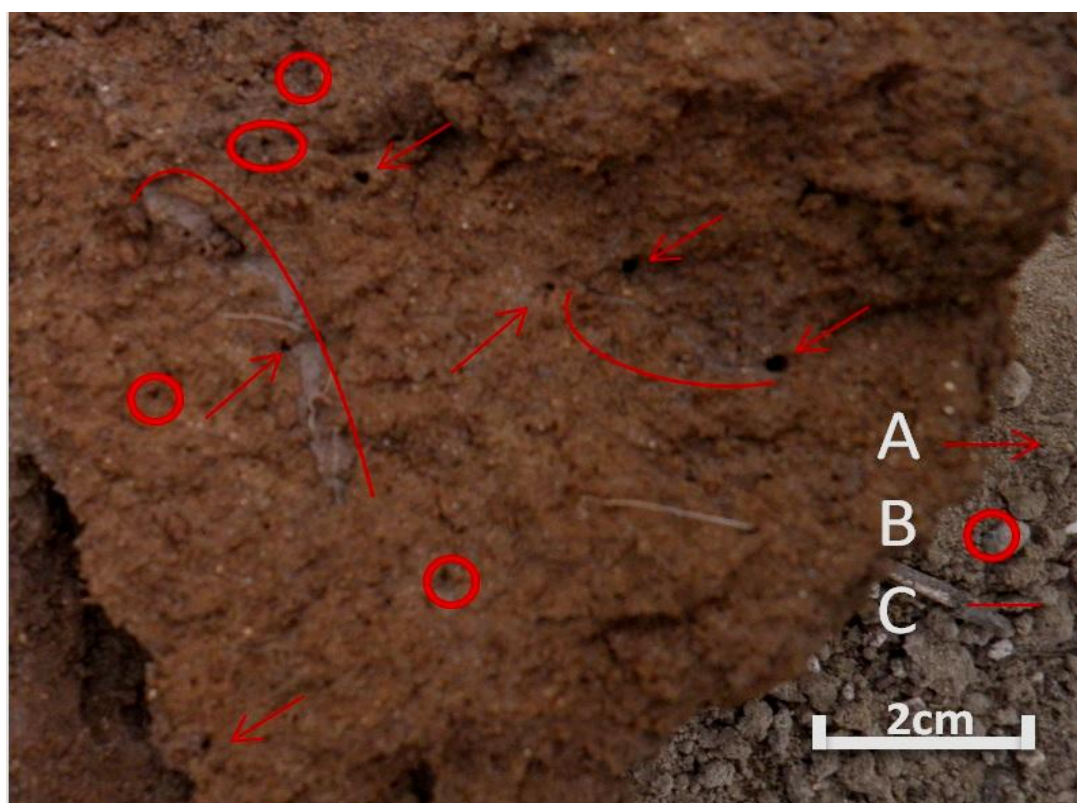



Photo 3.29 Detailed view of macropores

Table 3.4 Broccoli Field on-site soil profile cross section investigation results

Depth (cm)		Organic matter	Down Boundary		Texture	Color	Root mass	Structure	Remarks
			line	Layer					
0 - 15		Little exist	Wavy	Ridge	LS	7.5YR 3/3	Yes	granular	
15 - 22.5		None	Wavy	I	LS	7.5YR 3/4	Very few	massive	
22.5 - 50		None	Smooth	II	SL	7.5YR 3/3	-	massive	
50 - 100		None	Smooth	III	SL	7.5YR 3/4	-	massive	
100 >		None		IV	LS	7.5YR 4/3	-	granular	

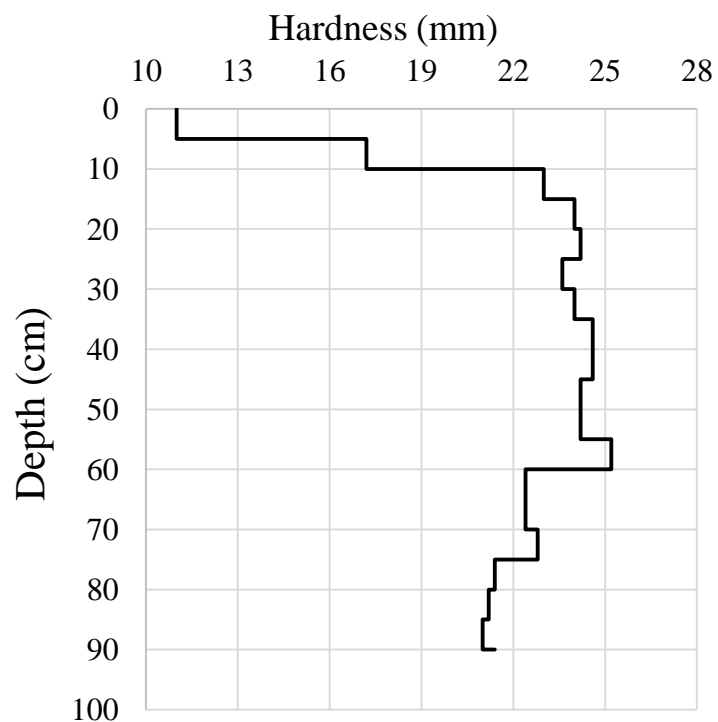


Fig. 3.10 Soil hardness distribution in (mm), Broccoli Field Matsusaka

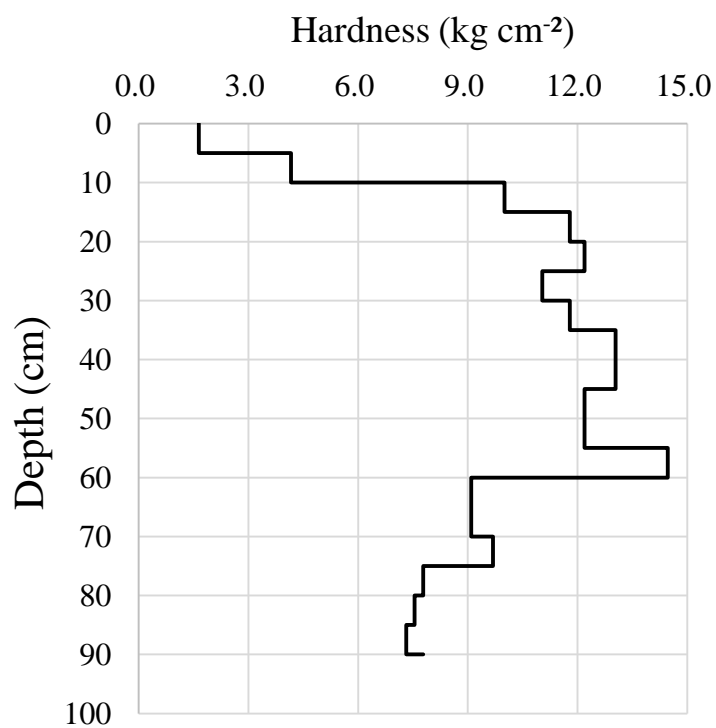


Fig. 3.11 Soil hardness distribution in (kg cm⁻²), Broccoli Field Matsusaka

3.3.1.2 Beans Field

Soil cross section is shown in **Photos 3.30 – 3.31**. Soil profile on-site investigated data is presented in Table 3.5 and soil profile hardness distribution is presented in **Fig. 3.12**.

According to hardness distribution data in **Fig. 3.12**, results of on-site soil profile investigation, and **Photos 3.30** and **3.31** the soil structure in all layers is massive and look compacted. There is few root extension in layer I of the soil and no sign of root is observed in underlying layers. The ratio of sand was high through palpation determination.

The drainage condition of the soil is very poor; this can be as a result of soil compaction. Although all layers structure seems to be compacted with massive structure, in layer II which has 3cm depth between 22cm – 25cm of soil profile shows more hardness, which limits the permeability of the soil.

Detailed site survey collected data are presented in **Table 3.5**. It needs laboratory analysis for better understanding of physical properties of the soil.

[**Table 3.5** Beans Field on-site soil profile cross section investigation results]

[**Fig. 3.12** Soil harness distribution (mm)]

[**Fig. 3.13** Soil harness distribution (kg cm^{-2})]

[**Photo 3.30** Bean Field soil profile cross section]

[**Photo 3.31** Beans Field soil profile cross section close view]




Photo 3.30 Bean Field soil profile cross section



Photo 3.31 Beans Field soil profile cross section close view

Table 3.5 Beans Field on-site soil profile cross section investigation results

Depth (cm)		Down Boundary							Remarks
		Organic matter	line	Layer	Texture	Color	Root mass	Structure	
0 - 12		Little exist	Smooth	Ridge	SL	7.5YR 4/3	Yes	massive	
12 - 22		None	Smooth	I	SL	7.5YR 3/3	Very few	massive	
22 - 25		None	Smooth	II	LS	7.5YR 4/3	-	massive	
25 - 39		None	Smooth	III	S	7.5YR 4/3	-	massive	Existence of much mica
51 >		None		IV	S	7.5YR 4/3	-	massive	Existence of much mica.

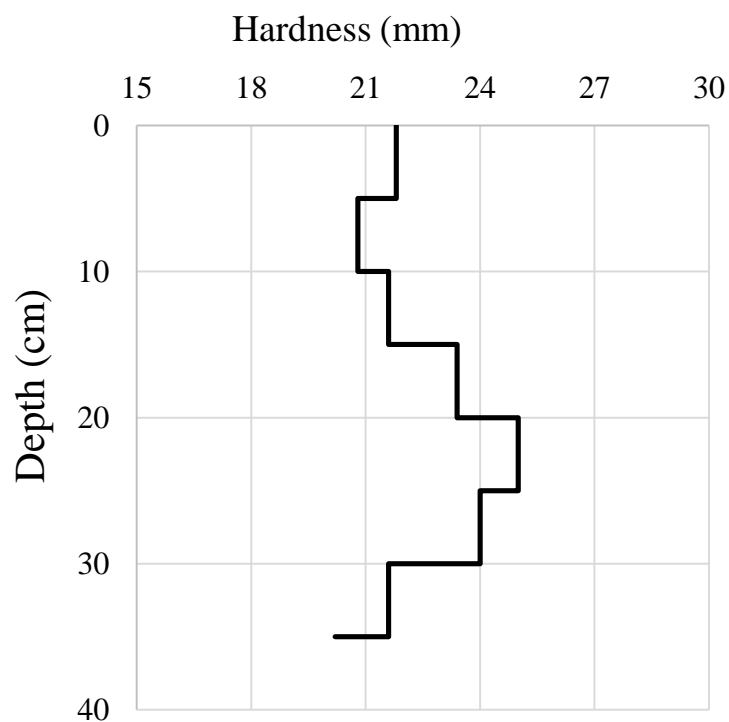


Fig. 3.12 Soil hardness distribution (mm), Beans Field Matsusaka

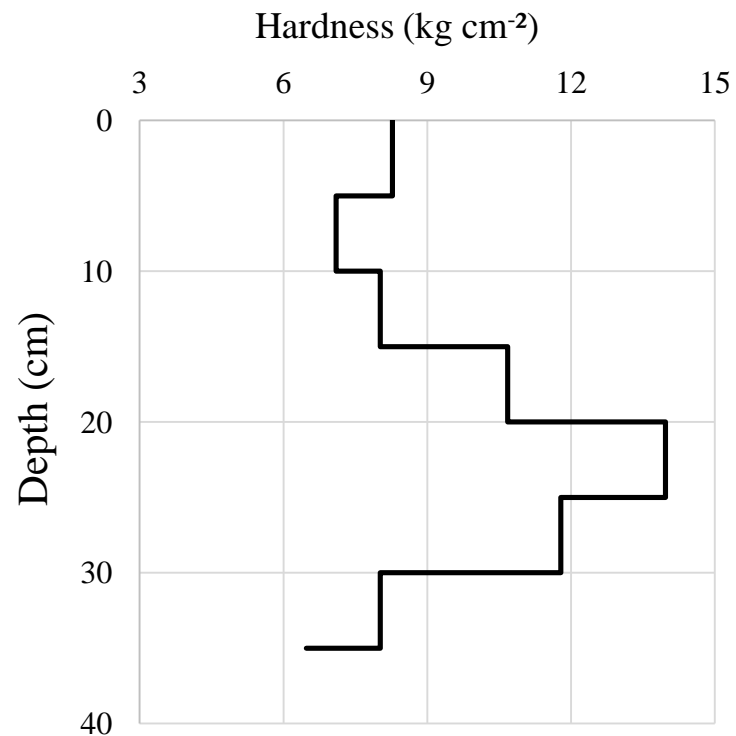


Fig. 3.13 Soil hardness distribution (kg cm⁻²), Beans Field Matsusaka

3.3.1.3 Yokkaichi Agriculture Center

Soil profile cross section is shown in **Photo 3.32**, and **Photos 3.33 – 3.34** are close view of A1 and A2 horizons. **Table 3.6** presents the result of on-site soil profile investigation, and soil hardness distribution is presented in **Fig. 3.14**.

The layers A0 and A1 are organic sandy loam soils with much slightly decomposed organic matter as root biomass. Development and distribution of root mass in A0 and A1 from 0 – 30cm depth is widely visible as shown in **Photo 3.32** and **3.33**, while it is limited in layer A2 as **Photo 3.34**, and there is no sign of root development or organic matter in layer B over 50cm deeper.

As shown in **Fig. 3.14** hardpan starts underlying layer A1 in boundary with layer A2, however it gets softer beneath layer A2. Layer A0 has granular structure with slightly decomposed sandy loam (SiL), while in layer A1 it is same texture with only difference that layer A1 structure is granular with some crumb, whereas the layer A2 has blocky structure and sandy clay loam texture (SCL), and B layer had massive structure with highly clay texture (HC). Detailed site survey collected data are presented in **Table 3.6**. It needs laboratory analysis for better understanding of physical properties of the soil.

[**Table 3.6** Yokkaichi Agriculture Center on-site soil profile cross section investigation results]

[**Fig. 3.14** Soil harness distribution (mm)]

[**Fig. 3.15** Soil harness distribution (kg cm^{-2})]

[**Photo 3.32** Soil profile cross section view]

[**Photo 3.33** Close view of layer A1]

[**Photo 3.34** Close view of subsoil layer A2]



Photo 3.32 Soil profile cross section view of Yokkaichi Agriculture Center




Photo 3.33 Close view of layer A1 Yokkaichi Agriculture Center



Photo 3.34 Close view of subsoil layer A2 Yokkaichi Agriculture Center

Table 3.6 Yokkaichi Agriculture Center on-site soil profile cross section investigation results

Depth (cm)		Organic matter	Down Boundary line	Layer	Texture	Color	Root mass	Structure	Remarks
0 - 10		Much	Wavy	A0	SiL	7.5YR 2/2	Yes (much)	granular	
10 - 30		Very much	Wavy	A1	SL	7.5YR 2/2	Yes (lesser than A0)	granular with some crumb	tubular pores
30 - 50		Little	Wavy	A2	SCL	7.5YR 3/2	Lesser	blocky	tubular pores
50>		None		B	HC	7.5YR 4/4	-	massive	tubular pores

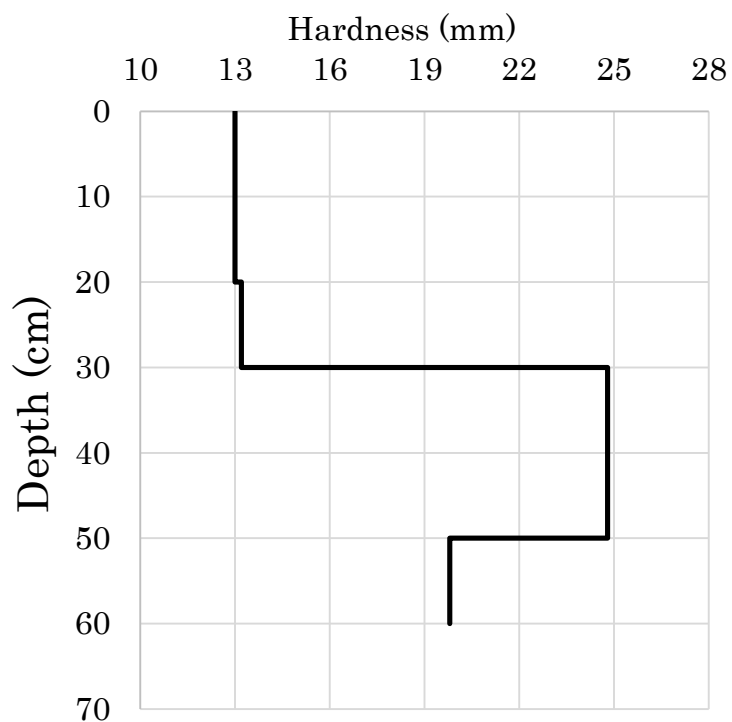


Fig. 3.14 Soil hardness distribution (mm) Yokkaichi Agriculture Center

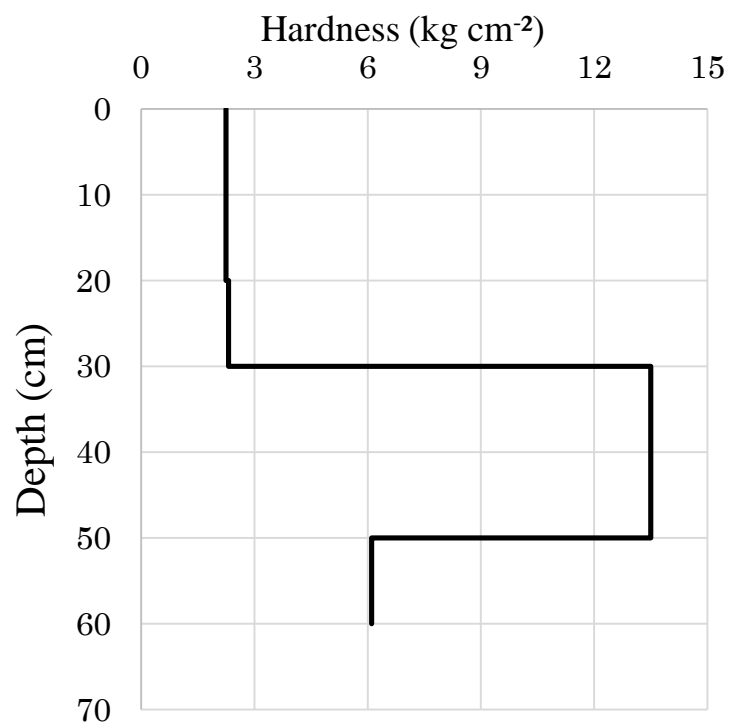


Fig. 3.15 Soil hardness distribution (kg cm⁻²) Yokkaichi Agriculture Center

3.3.2 Laboratory results

3.3.2.1 Basic soil physical properties

Results of measured basic physical properties for all three sites in **Tables 3.7 – 3.12** are presented in **Fig. 3.16 – 3.24**.

Fig. 3.16 – 3.18 presents soil three phase distribution, which; in Matsusaka Broccoli Field and Bean Field solid phase is dominated portion in all layer except for Broccoli Field layer II, while for Yokkaichi Agriculture Center the dominated phase is liquid portion.

Soil particle size distribution and textural classes based on USDA classification are presented in **Fig. 3.19 – 3.21**. In all the layers for all three sites, distribution of sand particle sizes 2mm – 0.05mm is greater than silt and clay. In Broccoli Field all layers are sandy loam. In Beans Field layers I and III are sandy loam, while II is in border between sandy loam and sandy clay loam. In Yokkaichi Agriculture Center, the surface soil A0 and A1 have sandy loam texture, it changes to sandy clay loam for sub-soils layer A2 and with clay to layer B.

[**Table 3.7** Basic soil physical properties results, “Broccoli Field” Matsusaka]

[**Table 3.8** Basic soil physical properties results, “Beans Field” Matsusaka]

[**Table 3.9** Basic soil physical properties results, “Yokkaichi Agriculture Center”]

[**Table 3.10** Particle size distribution, “Broccoli Field” Matsusaka]

[**Table 3.11** Particle size distribution, “Beans Field” Matsusaka]

[**Table 3.12** Particle size distribution, “Yokkaichi Agriculture” Center]

[**Fig. 3.16** Three phase distribution, “Broccoli Field” Matsusaka]

[**Fig. 3.17** Three phase distribution, “Beans Field” Matsusaka]

[**Fig. 3.18** Three phase distribution, “Yokkaichi Agriculture Center”]

[**Fig. 3.19** Particle size distribution, “Broccoli Field” Matsusaka]

[**Fig. 3.20** Particle size distribution, “Beans Field” Matsusaka]

[**Fig. 3.21** Particle size distribution, “Yokkaichi Agriculture Center”]

[**Fig. 3.22** Textural class (USDA), “Broccoli Field” Matsusaka]

[**Fig. 3.23** Textural class (USDA), “Beans Field” Matsusaka]

[**Fig. 3.24** Textural class (USDA), “Yokkaichi Agriculture Center”]

Table 3.7 Basic soil physical properties results, “Broccoli Field” Matsusaka

Sample name (layer)	Dry bulk density ρ_b (Mgm ⁻³)	Wet bulk density ρ_b' (Mgm ⁻³)	Particle density ρ_s (Mgm ⁻³)	Gravimetric water content w (kgkg ⁻¹)	Porosity n (m ³ m ⁻³)	Void ratio e (m ³ m ⁻³)	Degree of Saturation s (m ³ m ⁻³)
Ridge	1.32	1.73	2.68	0.31	0.51	1.03	0.82
Layer I	1.52	1.89	2.71	0.25	0.44	0.79	0.85
Layer II	1.54	1.92	2.49	0.25	0.39	0.63	0.99

Table 3.8 Basic soil physical properties results, “Beans Field” Matsusaka

Sample name (layer)	Dry bulk density ρ_b (Mgm ⁻³)	Wet bulk density ρ_b' (Mgm ⁻³)	Particle density ρ_s (Mgm ⁻³)	Gravimetric water content w (kgkg ⁻¹)	Porosity n (m ³ m ⁻³)	Void ratio e (m ³ m ⁻³)	Degree of Saturation s (m ³ m ⁻³)
Ridge	1.31	1.76	2.65	0.34	0.50	1.02	0.90
Layer I	1.47	1.87	2.68	0.28	0.45	0.83	0.89
Layer II	1.53	1.89	2.71	0.23	0.43	0.77	0.82
Layer III	1.49	1.89	2.66	0.27	0.44	0.79	0.91

Table 3.9 Basic soil physical properties results, “Yokkaichi Agriculture Center”

Sample name (layer)	Dry bulk density ρ_b (Mgm ⁻³)	Wet bulk density ρ_b' (Mgm ⁻³)	Particle density ρ_s (Mgm ⁻³)	Gravimetric water content w (kgkg ⁻¹)	Porosity n (m ³ m ⁻³)	Void ratio e (m ³ m ⁻³)	Degree of Saturation s (m ³ m ⁻³)
A1	1.14	1.66	2.54	0.46	0.55	1.23	0.95
A2	1.19	1.71	2.48	0.43	0.52	1.09	0.99
B	1.15	1.65	2.62	0.44	0.56	1.29	0.89

Table 3.10 Particle size distribution, “Broccoli Field” Matsusaka

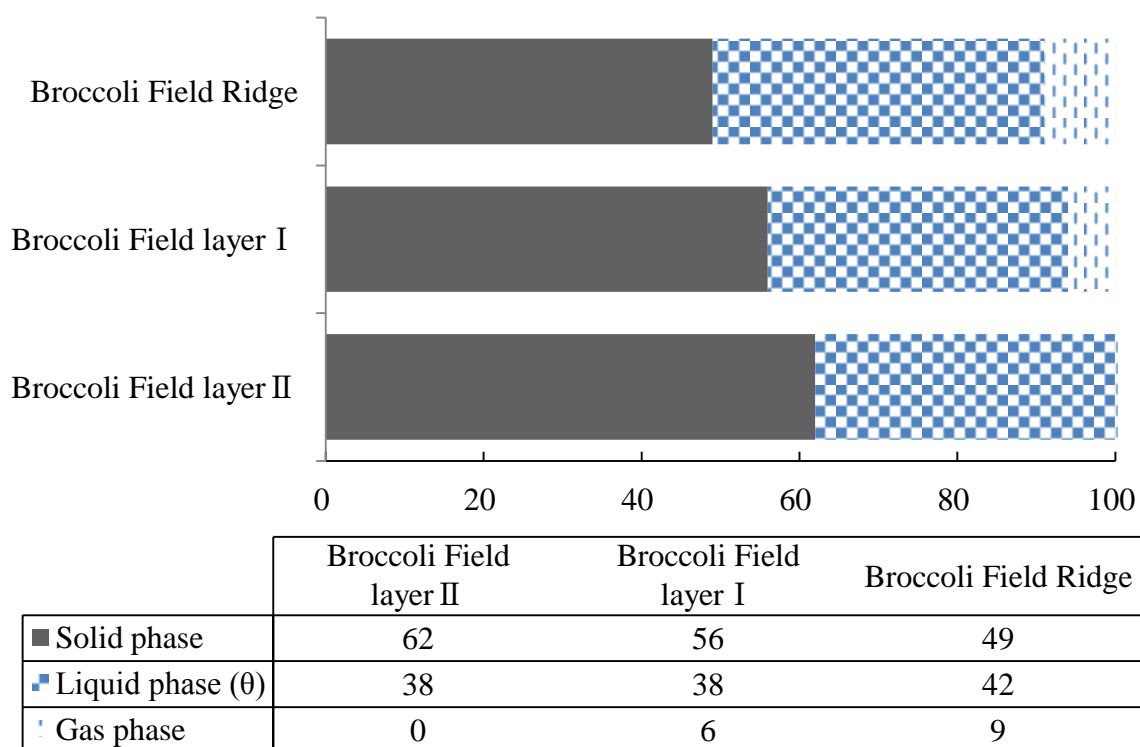
Particle Size (mm)	Ridge (%)	I (%)	II (%)	III(%)	IV(%)
9.500	100.0	100.0	100.0	100.0	100.0
4.750	100.0	100.0	100.0	100.0	100.0
2.000	94.0	99.5	99.7	99.3	99.2
0.850	89.5	92.6	95.5	96.0	97.3
0.425	82.1	88.4	89.9	90.1	91.1
0.250	70.7	76.9	81.1	78.4	78.4
0.106	44.4	50.3	53.3	50.4	43.2
0.074	34.6	40.2	45.5	42.9	35.3
0.053	30.0	33.6	43.7	36.6	29.0
0.020	18.4	31.6	37.7	26.7	26.9
0.010	13.1	25.7	31.8	21.2	21.3
0.005	10.4	23.2	26.9	17.3	17.9
0.002	7.8	19.2	22.0	12.9	13.3
0.001	6.7	16.9	18.6	10.1	11.2

Table 3.11 Particle size distribution, “Beans Field” Matsusaka

Particle Size (mm)	I (%)	II (%)	III(%)
9.500	100.0	100.0	100.0
4.750	100.0	100.0	100.0
2.000	97.3	98.1	97.3
0.850	93.0	94.8	94.5
0.425	88.5	90.6	89.2
0.250	81.4	80.7	79.0
0.106	61.1	56.6	51.1
0.074	53.4	50.2	42.5
0.053	48.9	46.7	36.9
0.020	38.1	39.8	33.1
0.010	31.5	33.4	29.0
0.005	26.9	28.7	25.4
0.002	19.5	23.5	21.5
0.001	18.9	21.0	20.0

Table 3.12 Particle size distribution, “Yokkaichi Agriculture Center”

Particle Size (mm)	A0 (%)	A1 (%)	A2 (%)	B (%)
9.500	100.0	100.0	100.0	100.0
4.750	100.0	100.0	100.0	88.0
2.000	95.4	93.5	89.7	86.2
0.850	88.4	87.4	83.5	79.9
0.425	78.1	78.2	78.5	75.9
0.250	69.5	69.7	74.4	73.0
0.106	63.3	63.8	69.4	68.8
0.074	61.1	62.0	66.9	66.8
0.053	59.3	60.3	65.0	65.0
0.020	28.1	24.6	36.4	53.6
0.010	22.8	20.2	29.4	44.3
0.005	17.8	15.9	23.0	36.8
0.002	12.0	10.9	14.8	28.5
0.001	8.0	7.3	9.5	20.2

**Fig. 3.16** Three phase distribution, “Broccoli Field” Matsusaka, (Unit: %)

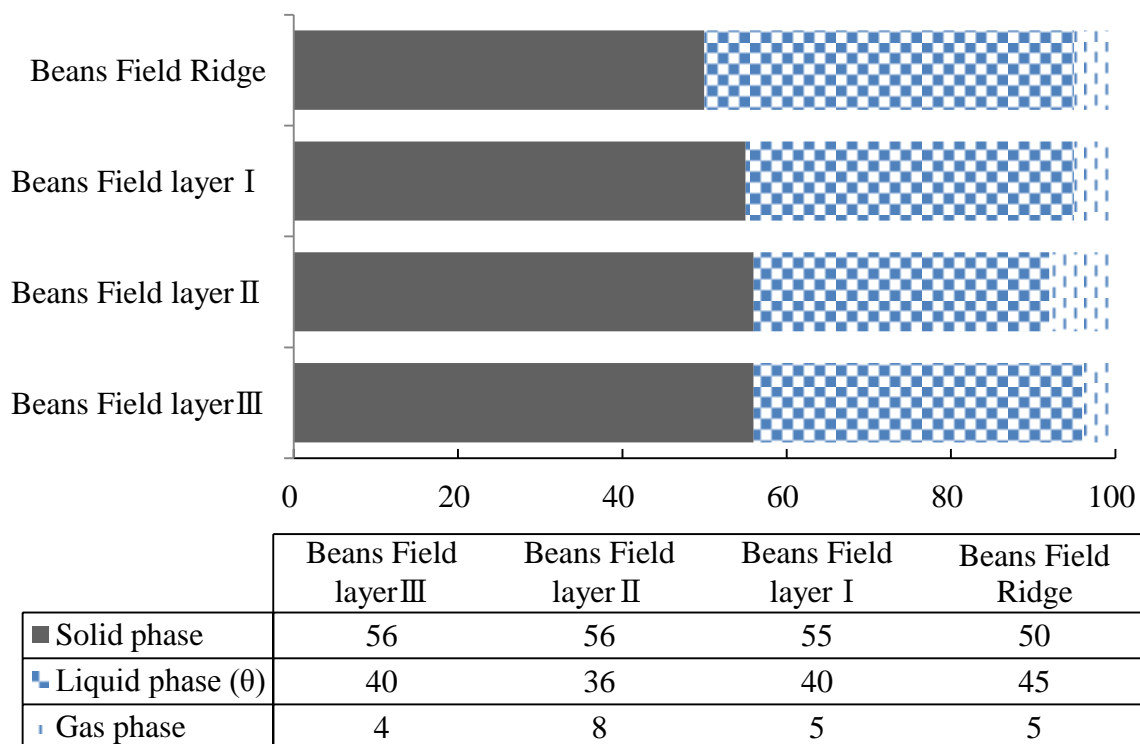


Fig. 3.17 Three phase distribution, “Beans Field” Matsusaka, (Unit: %)

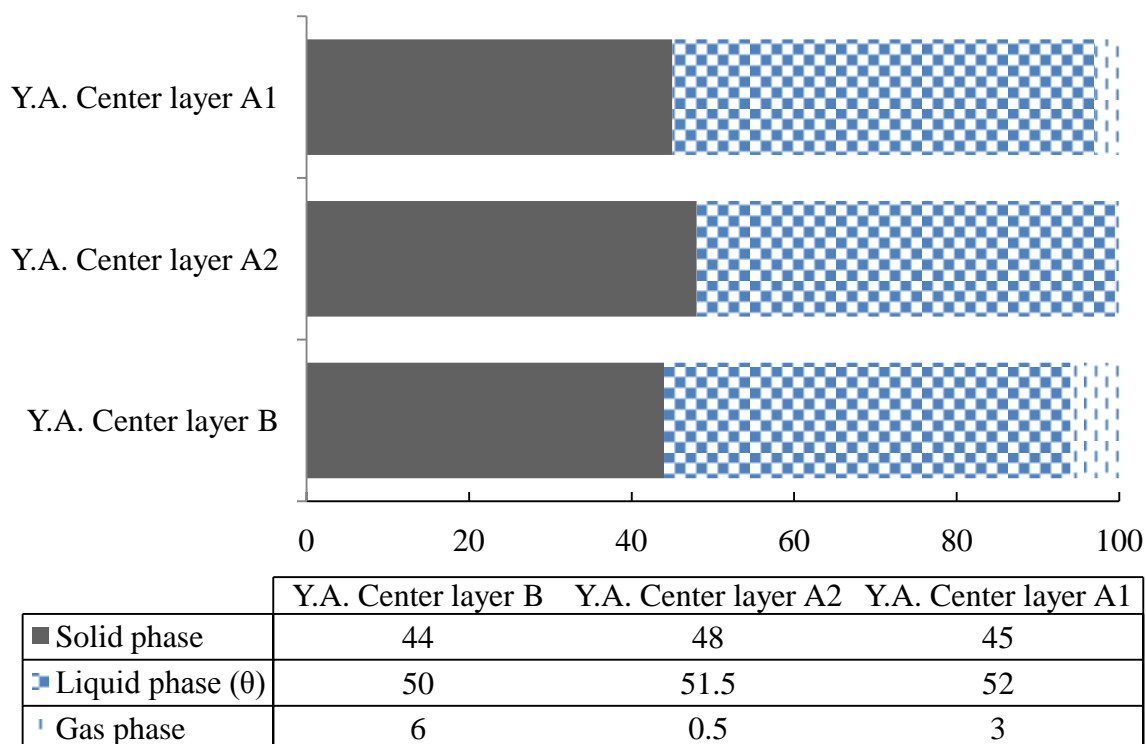


Fig. 3.18 Three phase distribution, “Yokkaichi Agriculture Center”, (Unit: %)

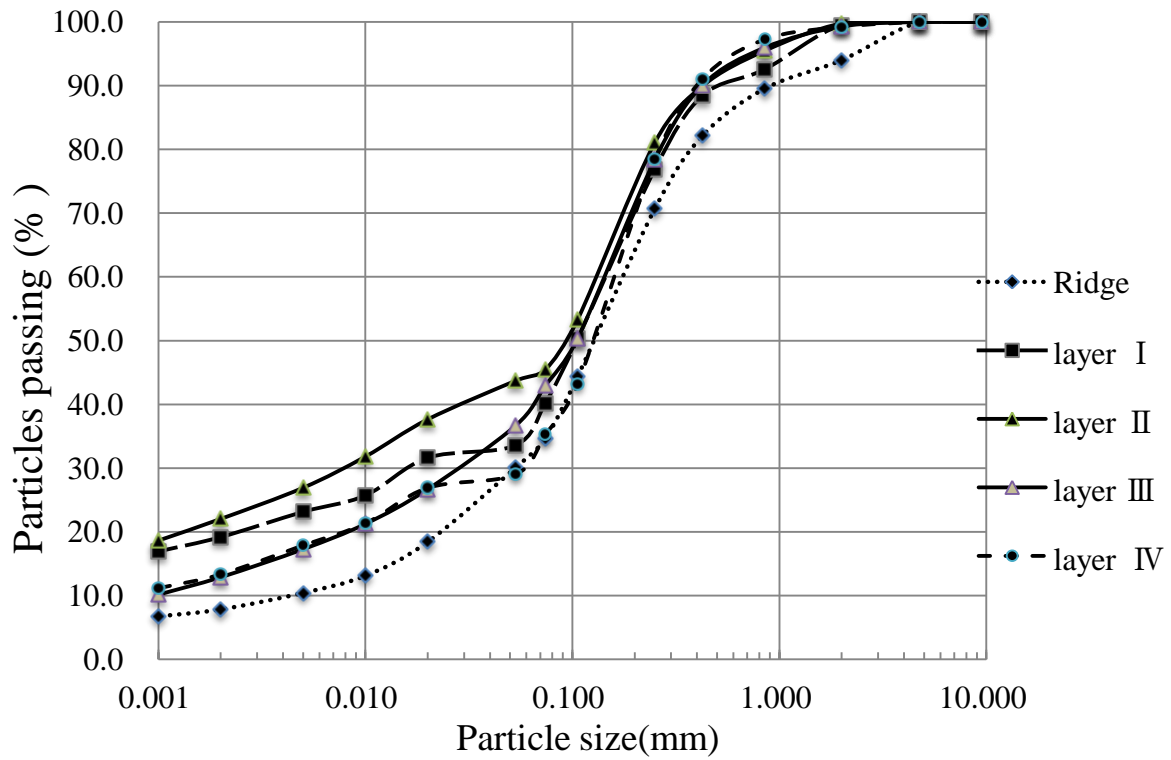


Fig. 3.19 Particle size distribution, “Broccoli Field” Matsusaka

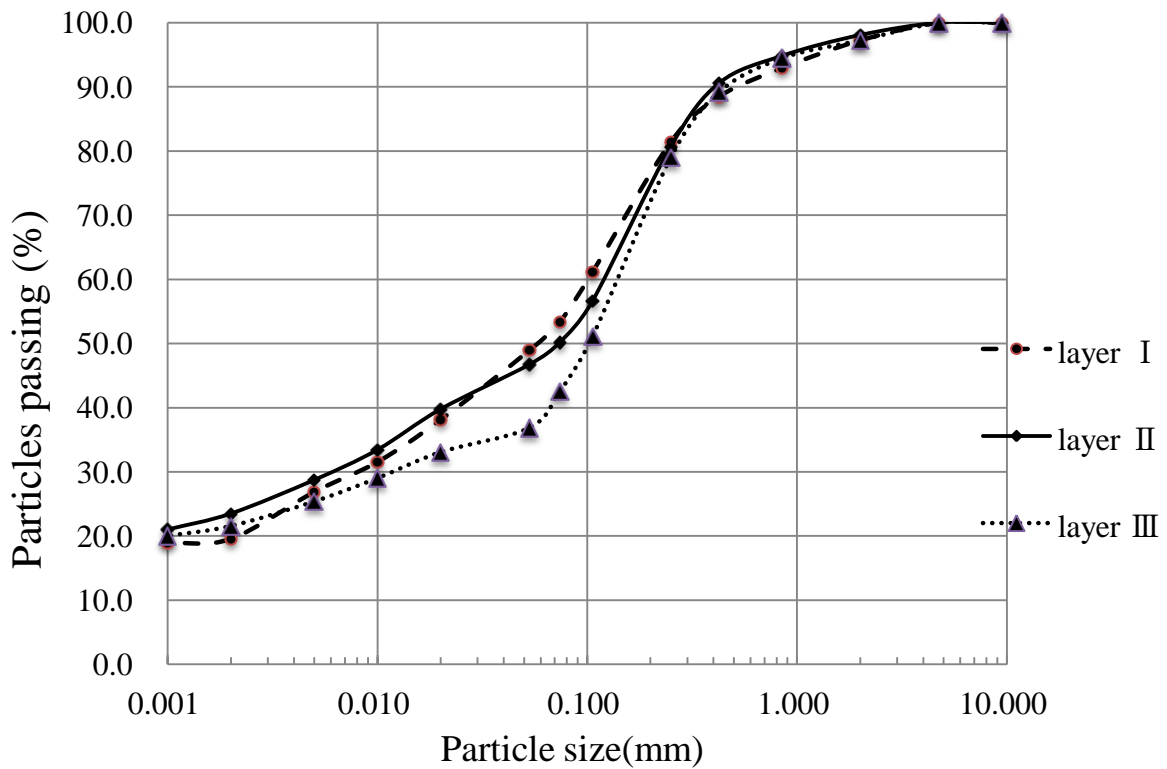


Fig. 3.20 Particle size distribution, “Beans Field” Matsusaka

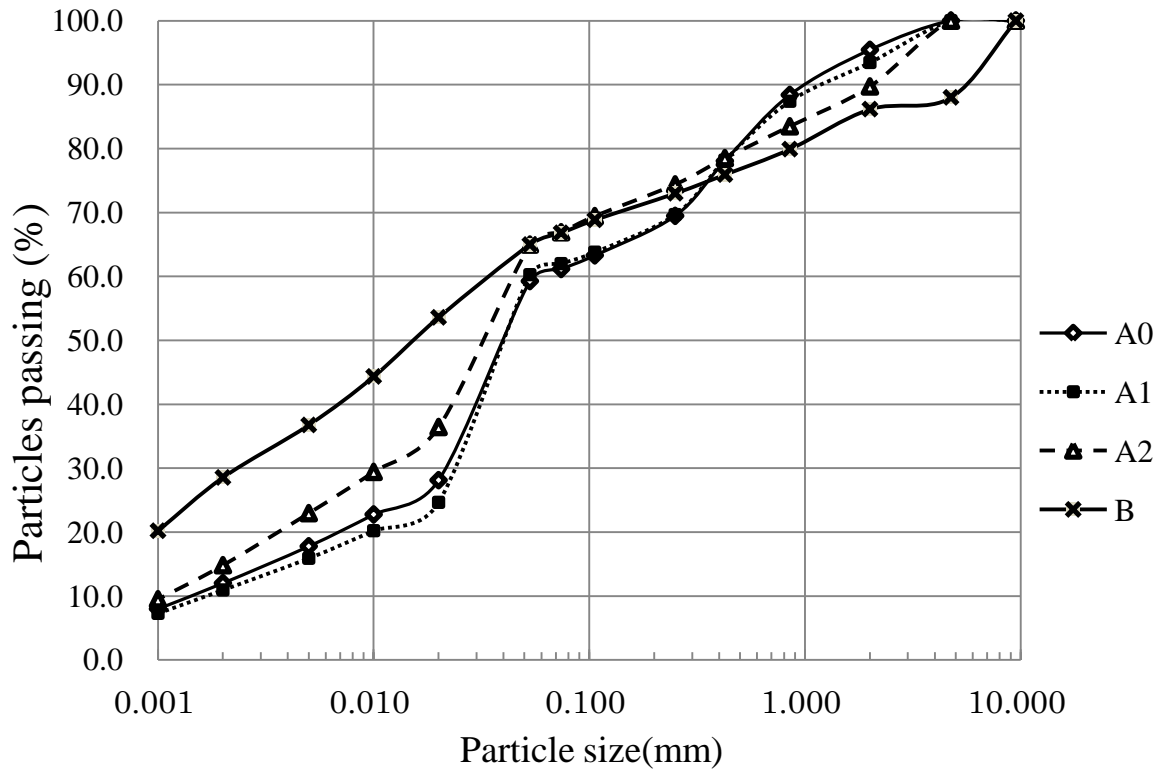


Fig. 3.21 Particle size distribution, “Yokkaichi Agriculture Center”

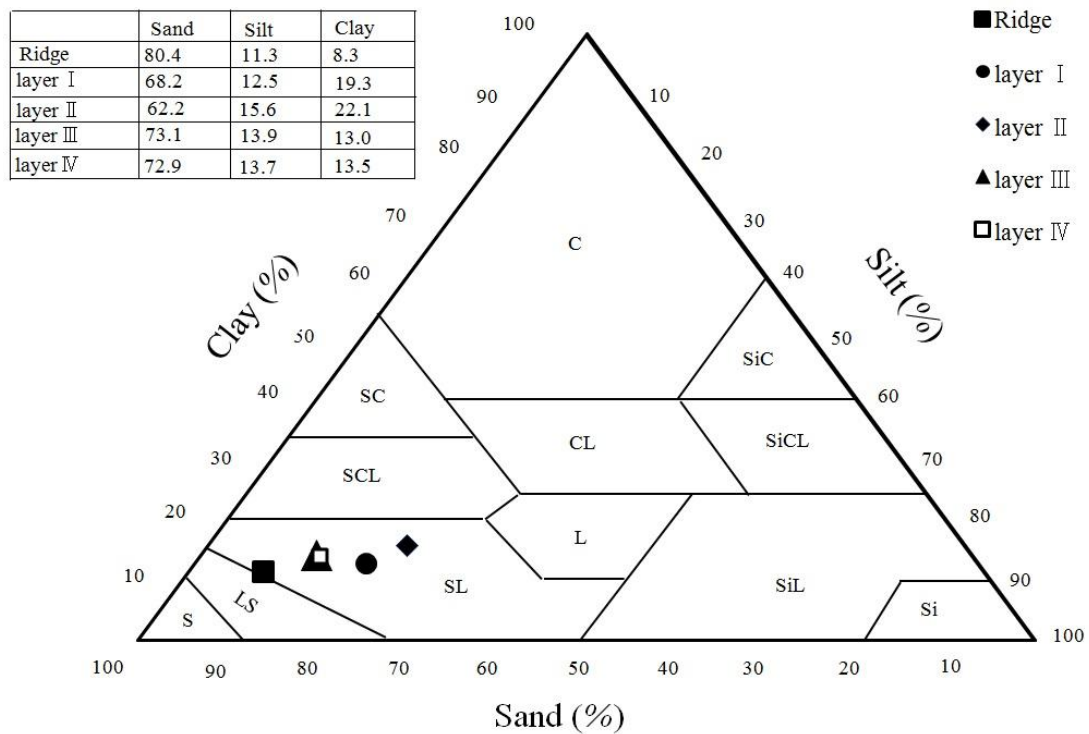


Fig. 3.22 Textural class (USDA), “Broccoli Field” Matsusaka

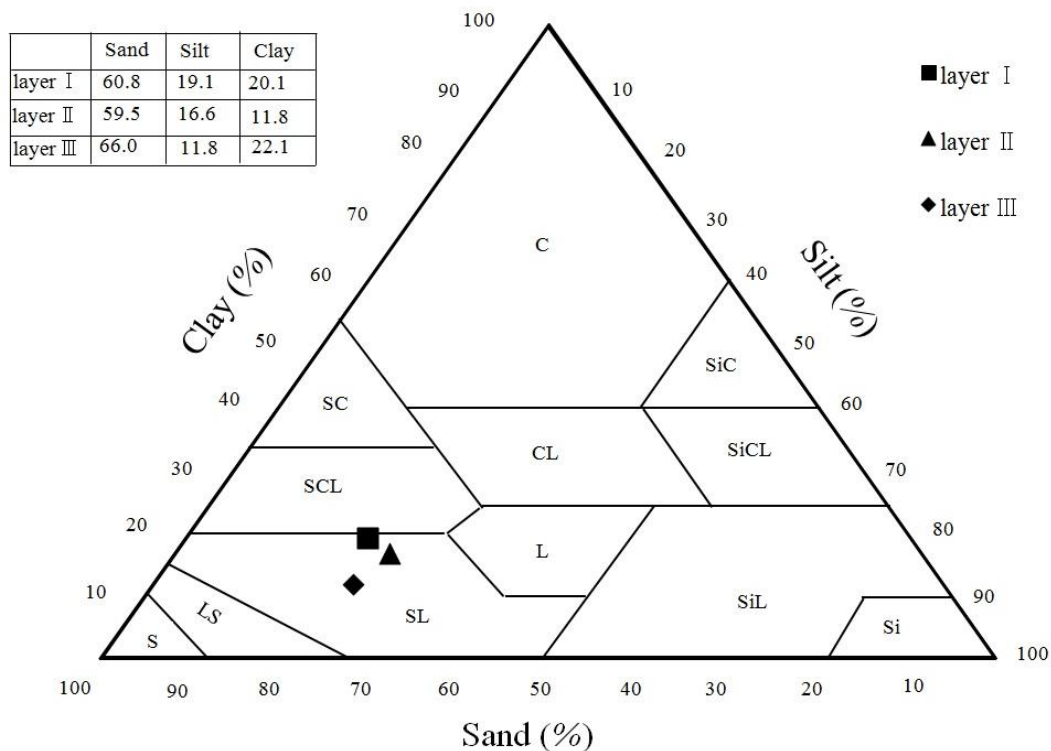


Fig. 3.23 Textural class (USDA), “Beans Field” Matsusaka

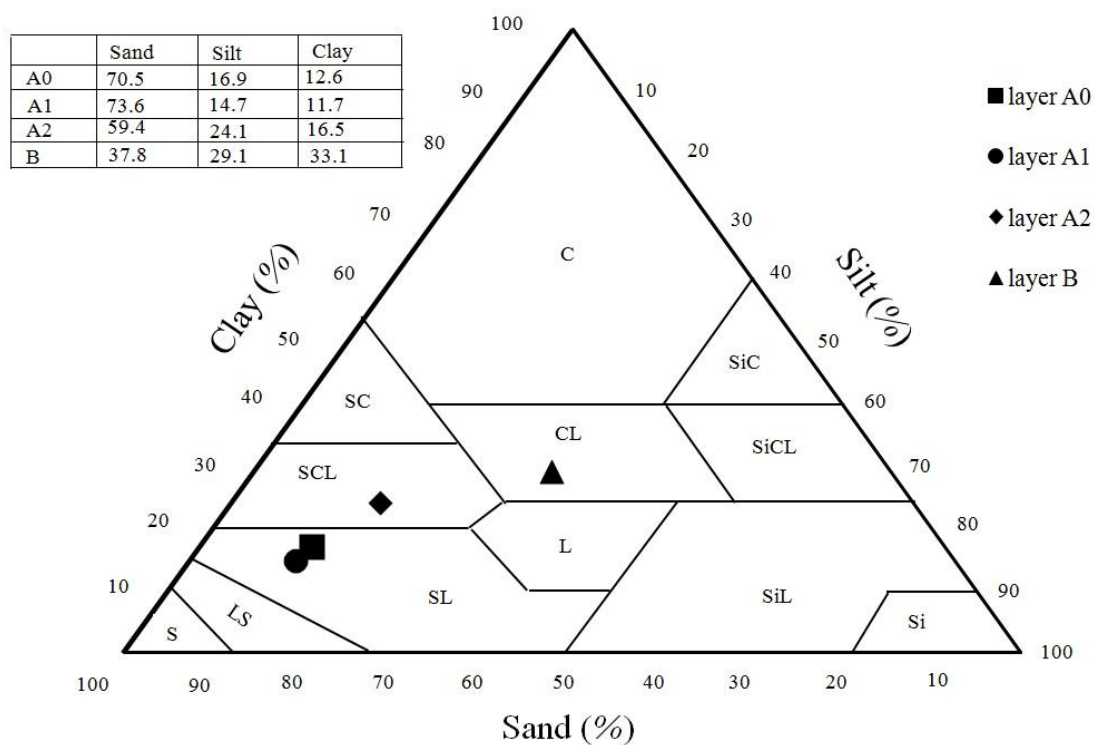


Fig. 3.24 Textural class (USDA), “Yokkaichi Agriculture Center”

3.3.2.2 Consistency

Standard description of soil plasticity index chart is presented in **Fig. 3.25**. Experimental results of soil plasticity index are presented in **Tables 3.13 – 3.14** and **Fig. 3.26 – 3.27** for Broccoli Field of Matsusaka and Yokkaichi Agriculture Center respectively. It shows low plasticity index for Broccoli Field and higher than that for Yokkaichi Agriculture Center.

[**Table 3.13** Liquid – plastic limit and Plasticity index, “Broccoli Field” Matsusaka]

[**Table 3.14** Liquid – plastic limit and Plasticity index, “Yokkaichi Agriculture Center”]

[**Fig. 3.25** Standard description of plasticity chart]

[**Fig. 3.26** Plasticity index, “Broccoli Field” Matsusaka]

[**Fig. 3.27** Plasticity index, “Yokkaichi Agriculture Center”]

Table 3.13 Liquid – plastic limit and Plasticity index, “Broccoli Field” Matsusaka

Sample name (layer)	Plastic limit L _P (%)	Liquid limit L _L (%)	Plasticity index I _P (%)
Ridge	25	31	6
Layer I	22	31	9
Layer II	23	35	12
Layer III	23	39	17
Layer IV	23	42	19

Table 3.14 Liquid – plastic limit and Plasticity index, “Yokkaichi Agriculture Center”

Sample name (layer)	Plastic limit L _P (%)	Liquid limit L _L (%)	Plasticity index I _P (%)
A0	30	51	20
A1	30	76	46
A2	40	65	26
B	35	53	17

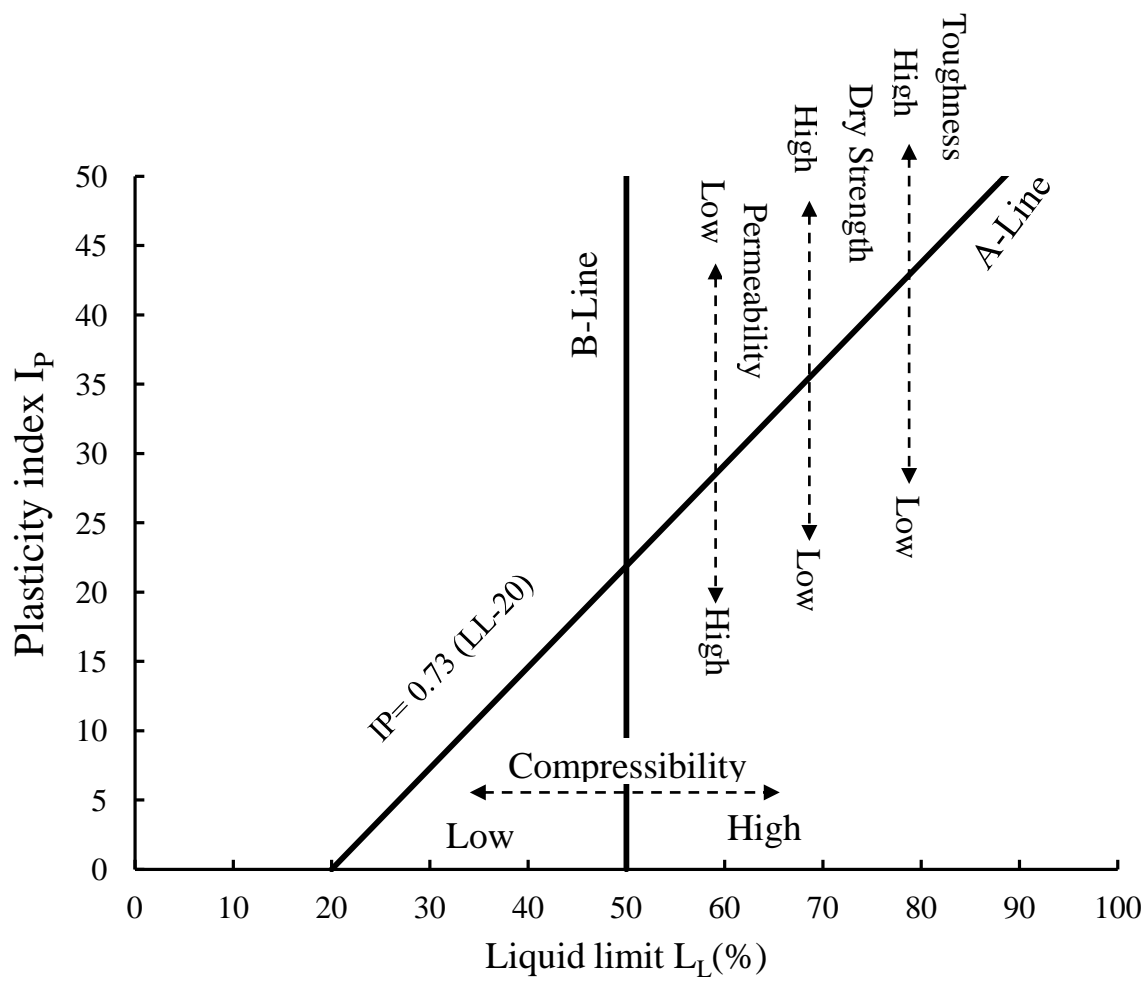


Fig. 3.25 Standard description of plasticity chart

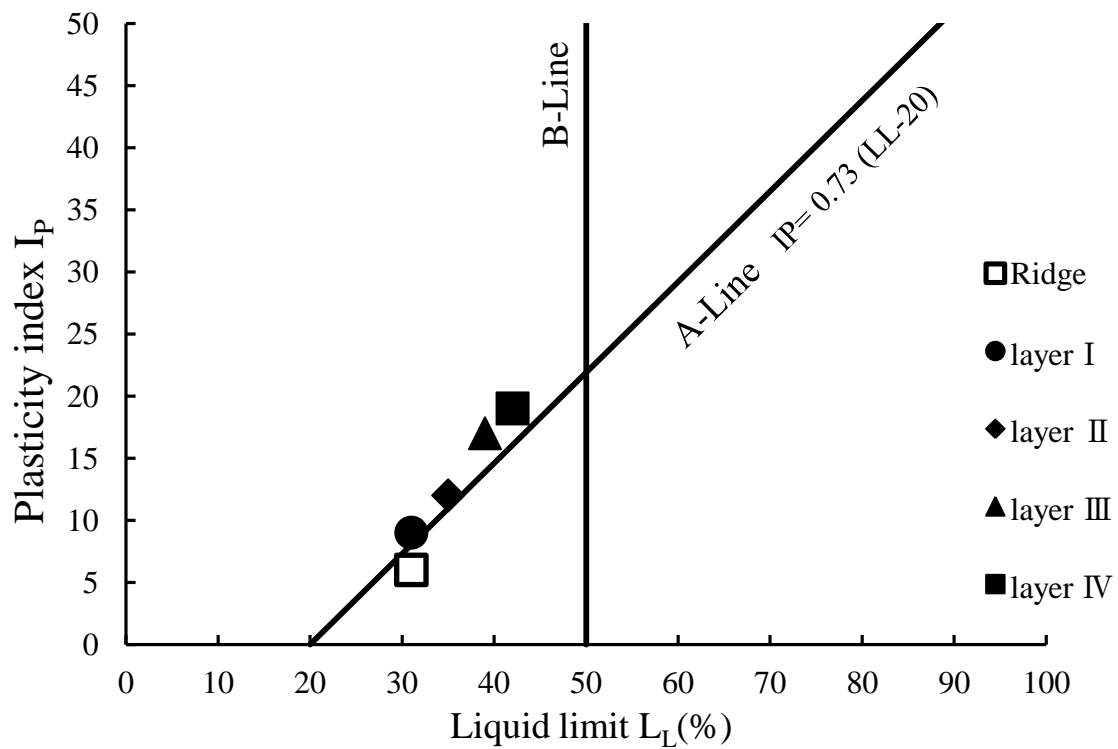


Fig. 3.26 Plasticity index, “Broccoli Field” Matsusaka

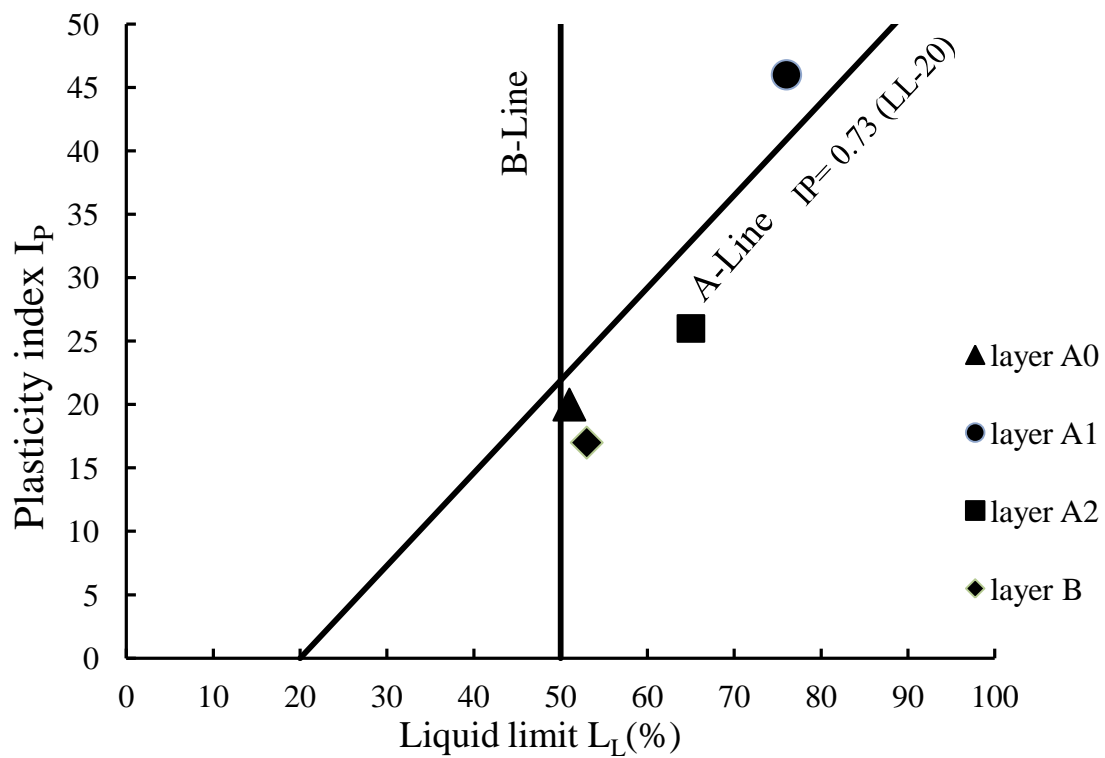


Fig. 3.27 Plasticity index, “Yokkaichi Agriculture Center”

3.3.2.3 pF – θ (soil moisture characteristics)

Soil water holding capacity in term of pF – θ ($\text{cm}^3\text{cm}^{-3}$) for Broccoli Field is presented in **Tables 3.15**, and **Fig. 3.28** shows all layers pF – θ of Broccoli Field.

Table 3.16 contains water holding capacity pF – θ ($\text{cm}^3\text{cm}^{-3}$) of Beans Field, and **Fig. 3.29** shows all layers pF – θ of Beans Field.

Yokkaichi Agriculture Center’s water holding capacity pF – θ ($\text{cm}^3\text{cm}^{-3}$) is presented in **Table 3.17** and **Fig. 3.30**.

The pF (potential of free water \log_{10}) is plotted in vertical axes and volumetric water content $\theta(\%)$ is plotted in horizontal axes.

[**Table 3.15** Broccoli Field water holding capacity and volumetric water content θ ($\text{cm}^3\text{cm}^{-3}$)]

[**Table 3.16** Beans Field water holding capacity and volumetric water content θ ($\text{cm}^3\text{cm}^{-3}$)]

[**Table 3.17** Yokkaichi Agriculture Center water holding capacity and volumetric water content θ ($\text{cm}^3\text{cm}^{-3}$)]

[**Fig. 3.28** pF-moisture characteristics curve, “Broccoli Field”, Matsusaka]

[**Fig. 3.29** pF-moisture characteristics curve, “Beans Field”, Matsusaka]

[**Fig. 3.30** pF-moisture characteristics curve, “Yokkaichi Agriculture Center”]

Table 3.15 Broccoli Field water holding capacity and volumetric water content θ ($\text{cm}^3\text{cm}^{-3}$)

		pF								
Sample	0	1	1.5	1.8	2	2.3	2.5	2.7	3.0	
Ridge (V)	0.417	0.333	0.251	0.187	0.164	0.125	0.111	0.104	0.089	
I layer (H)	0.407	0.387	0.362	0.312	0.296	0.279	0.272	0.266	0.249	
I layer (V)	0.405	0.382	0.347	0.283	0.263	0.242	0.235	0.229	0.219	
II layer (H)	0.384	0.372	0.347	0.331	0.322	0.306	0.296	0.288	0.275	
II layer (V)	0.397	0.378	0.353	0.326	0.311	0.291	0.282	0.272	0.253	

Table 3.16 Beans Field water holding capacity and volumetric water content θ ($\text{cm}^3\text{cm}^{-3}$)

		pF								
Sample	0	1	1.5	1.8	2	2.3	2.5	2.7	3.0	
Ridge (V)	0.450	0.386	0.340	0.307	0.290	0.262	0.252	0.244	0.224	
I layer (V)	0.414	0.380	0.357	0.331	0.317	0.293	0.284	0.271	0.259	
II layer (V)	0.362	0.334	0.309	0.289	0.278	0.261	0.253	0.247	0.234	
III layer (V)	0.384	0.362	0.343	0.312	0.293	0.263	0.249	0.241	0.230	

Table 3.17 Yokkaichi Agriculture Center water holding capacity and volumetric water content θ ($\text{cm}^3\text{cm}^{-3}$)

		pF								
Sample	0	1	1.5	1.8	2	2.3	2.5	2.7	3.0	
A1 (H)	0.518	0.456	0.370	0.292	0.270	0.245	0.234	0.227	0.212	
A1 (V)	0.540	0.504	0.411	0.334	0.313	0.289	0.277	0.269	0.252	
A2 (H)	0.388	0.362	0.340	0.319	0.306	0.287	0.276	0.271	0.247	
A2 (V)	0.582	0.538	0.500	0.481	0.473	0.461	0.455	0.451	0.436	
B (H)	0.472	0.453	0.411	0.386	0.374	0.357	0.349	0.345	0.330	
B (V)	0.473	0.459	0.436	0.421	0.409	0.391	0.380	0.372	0.354	

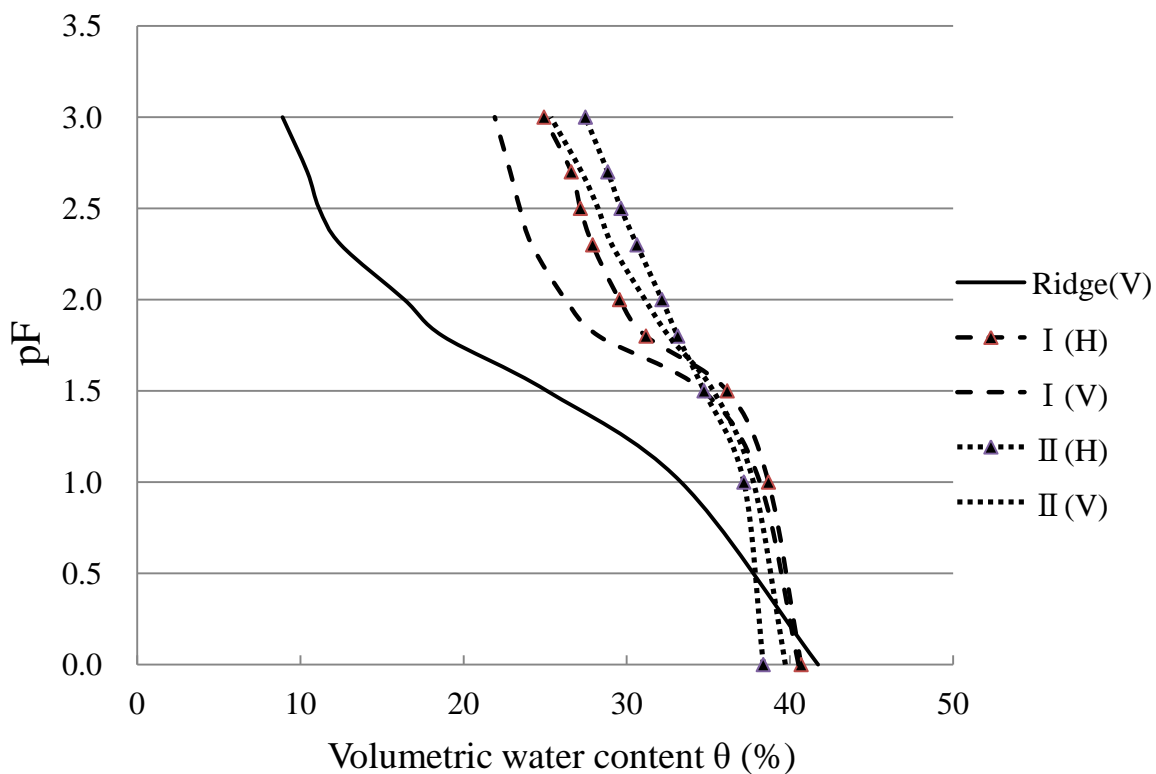


Fig. 3.28 pF-moisture characteristics curve Broccoli Field, Matsusaka

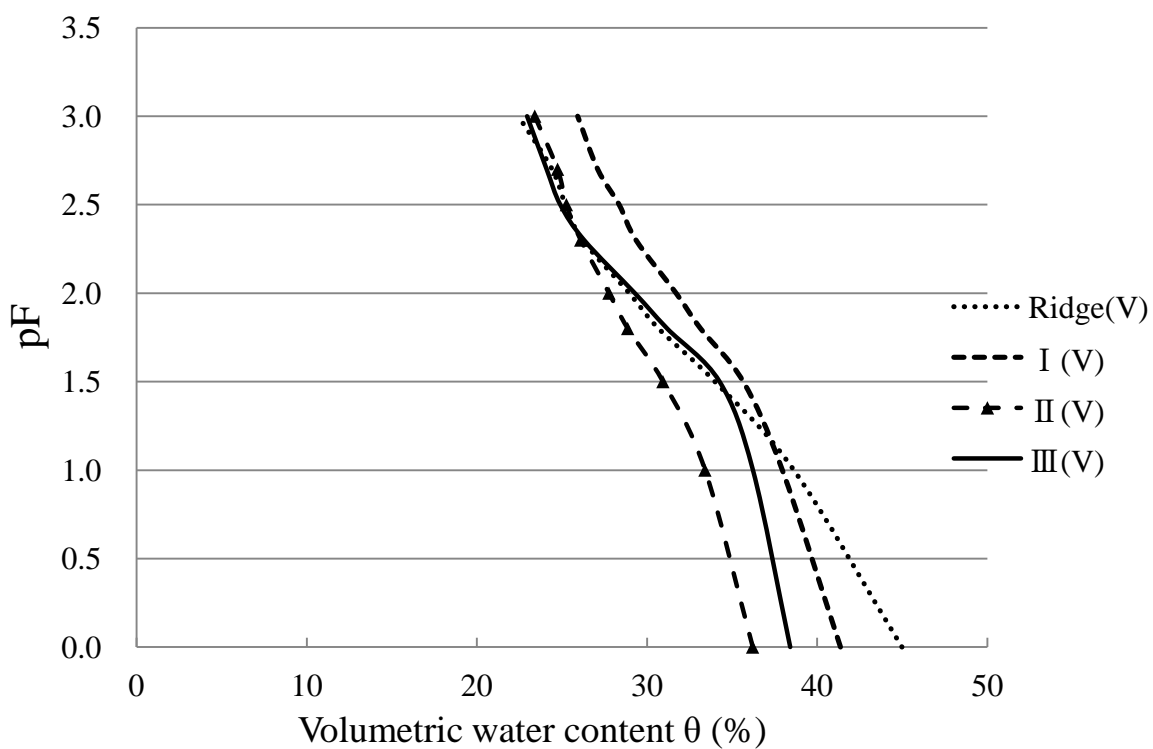


Fig. 3.29 pF-moisture characteristics curve Beans Field, Matsusaka

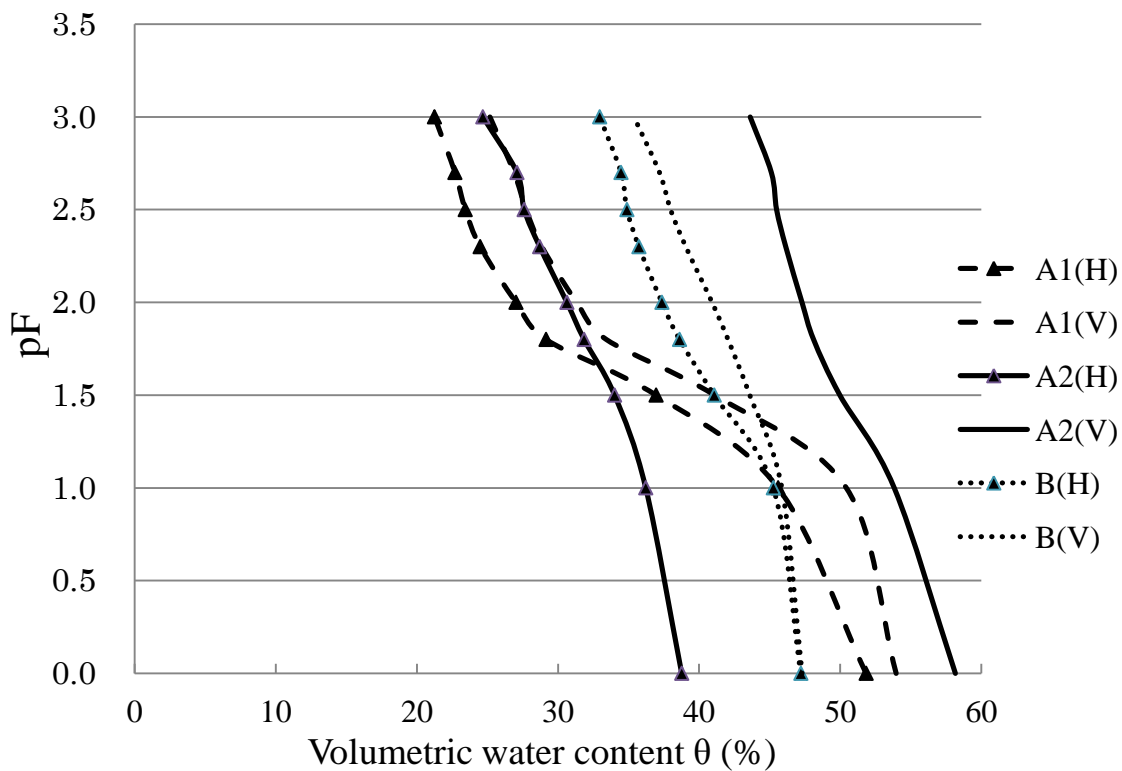


Fig. 3.30 pF-moisture characteristics curve Yokkaichi Agriculture Center

3.3.2.4 pF – θ distribution (pore size distribution)

Soil pF – θ distribution, pore size distribution, for all three sites are shown in **Figures 3.31 – 3.40**, in which $\Delta\theta/\Delta pF$ is plotted in vertical axes and pore size diameter is plotted in horizontal axes. The vertical dotted-line in almost center of the figure, pF 1.8 pores equivalent diameter 0.048mm, is the boundary between capillary pores and non-capillary pores.

[**Fig. 3.31** pF – θ distribution, “Broccoli Field ridge”]

[**Fig. 3.32** pF – θ distribution, “Broccoli Field layer I ”]

[**Fig. 3.33** pF – θ distribution, “Broccoli Field layer II ”]

[**Fig. 3.34** pF – θ distribution, “Beans Field ridge”]

[**Fig. 3.35** pF – θ distribution, “Beans Field layer I ”]

[**Fig. 3.36** pF – θ distribution, “Beans Field layer II ”]

[**Fig. 3.37** pF – θ distribution, “Beans Field layer III”]

[**Fig. 3.38** pF – θ distribution, “Yokkaichi Agriculture Center layer A1”]

[**Fig. 3.39** pF – θ distribution, “Yokkaichi Agriculture Center layer A2”]

[**Fig. 3.40** pF – θ distribution, “Yokkaichi Agriculture Center layer B”]

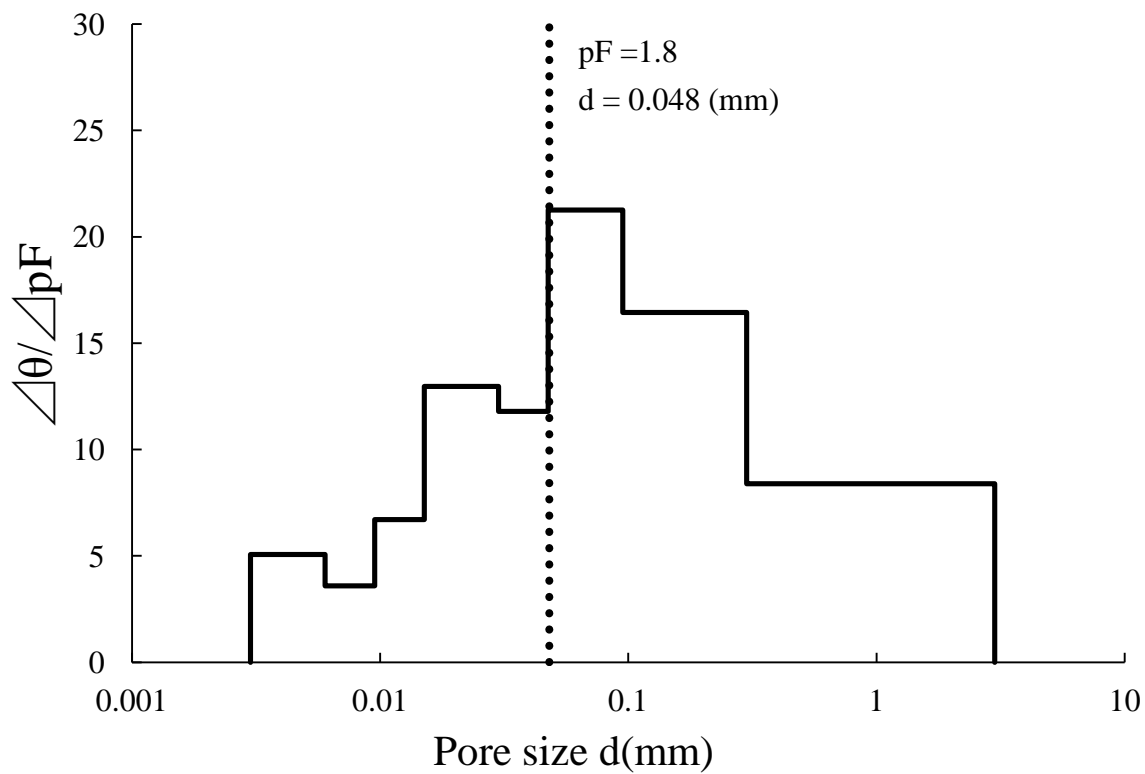


Fig. 3.31 pF – θ distribution, “Broccoli Field ridge”

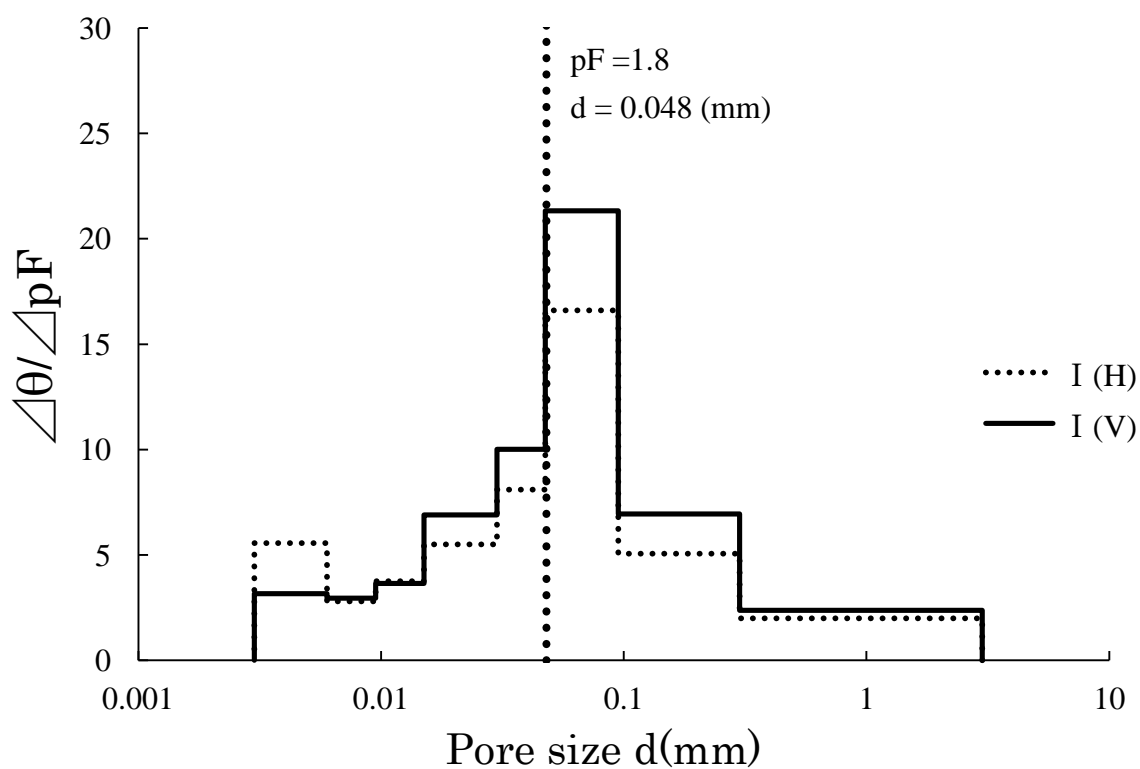


Fig. 3.32 pF – θ distribution, “Broccoli Field layer I ”

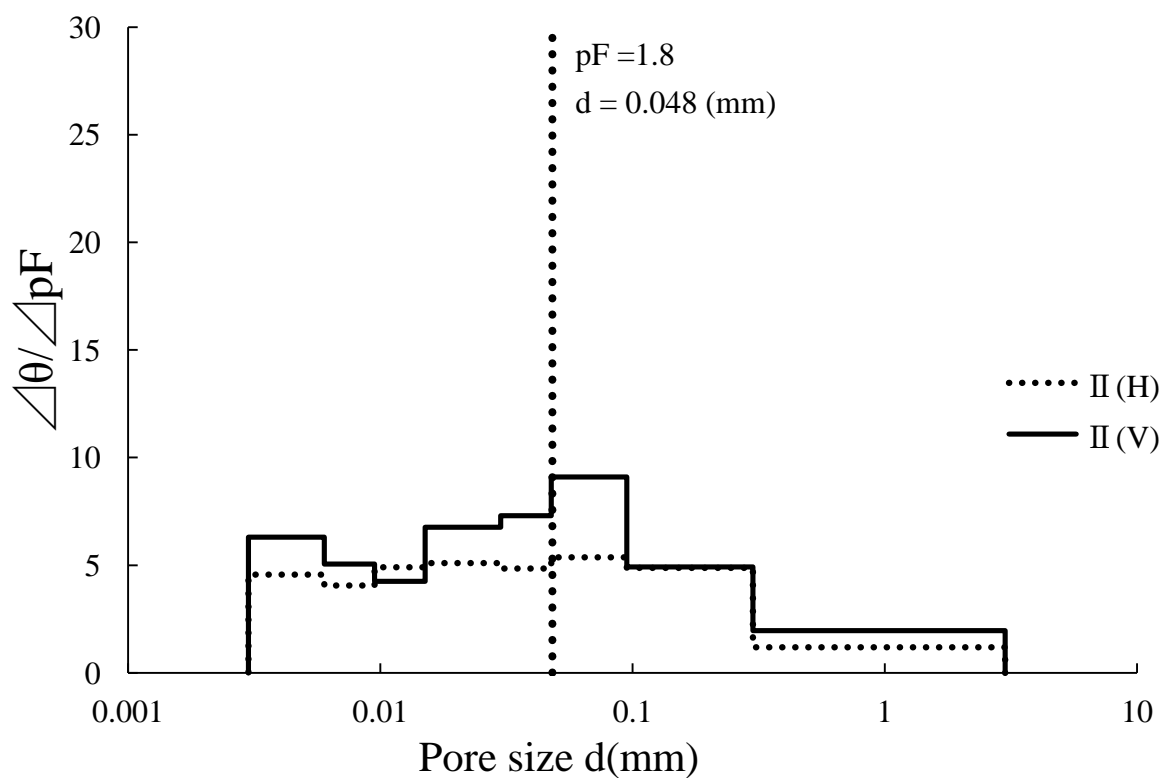


Fig. 3.33 $pF - \theta$ distribution, “Broccoli Field layer II”

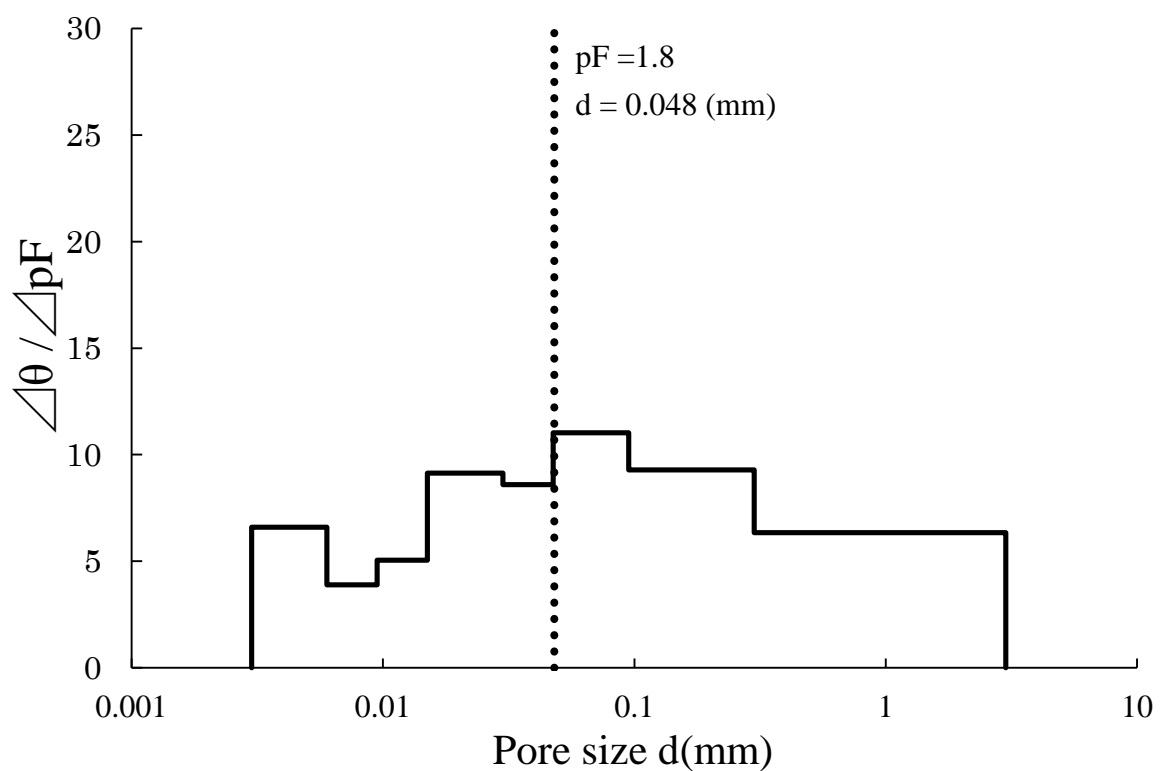


Fig. 3.34 $pF - \theta$ distribution, “Beans Field ridge”

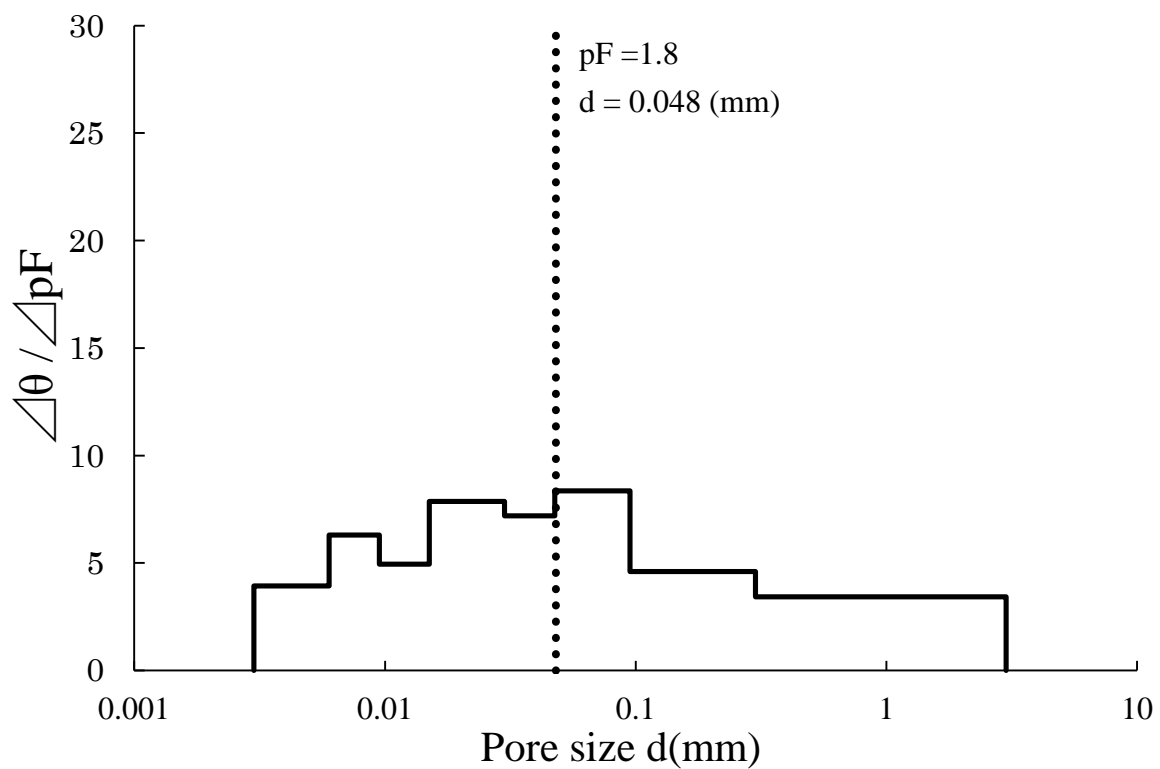


Fig. 3.35 $pF - \theta$ distribution, “Beans Field layer I ”

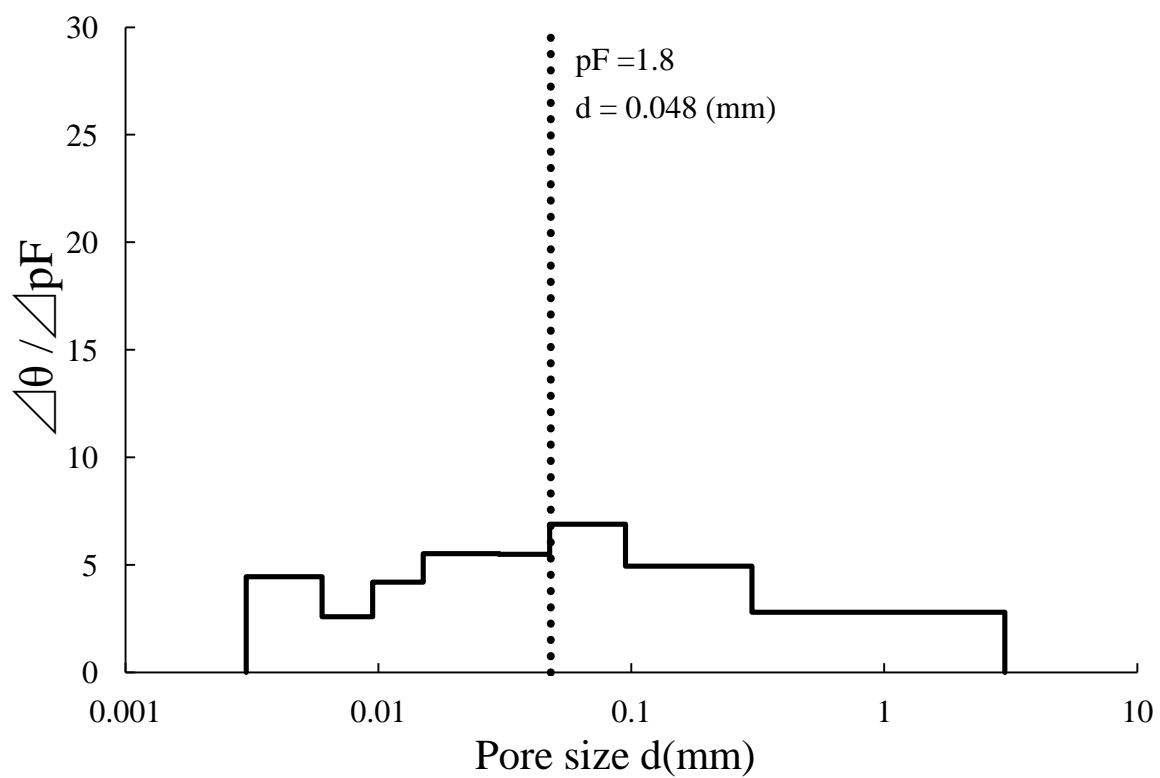


Fig. 3.36 $pF - \theta$ distribution, “Beans Field layer II ”

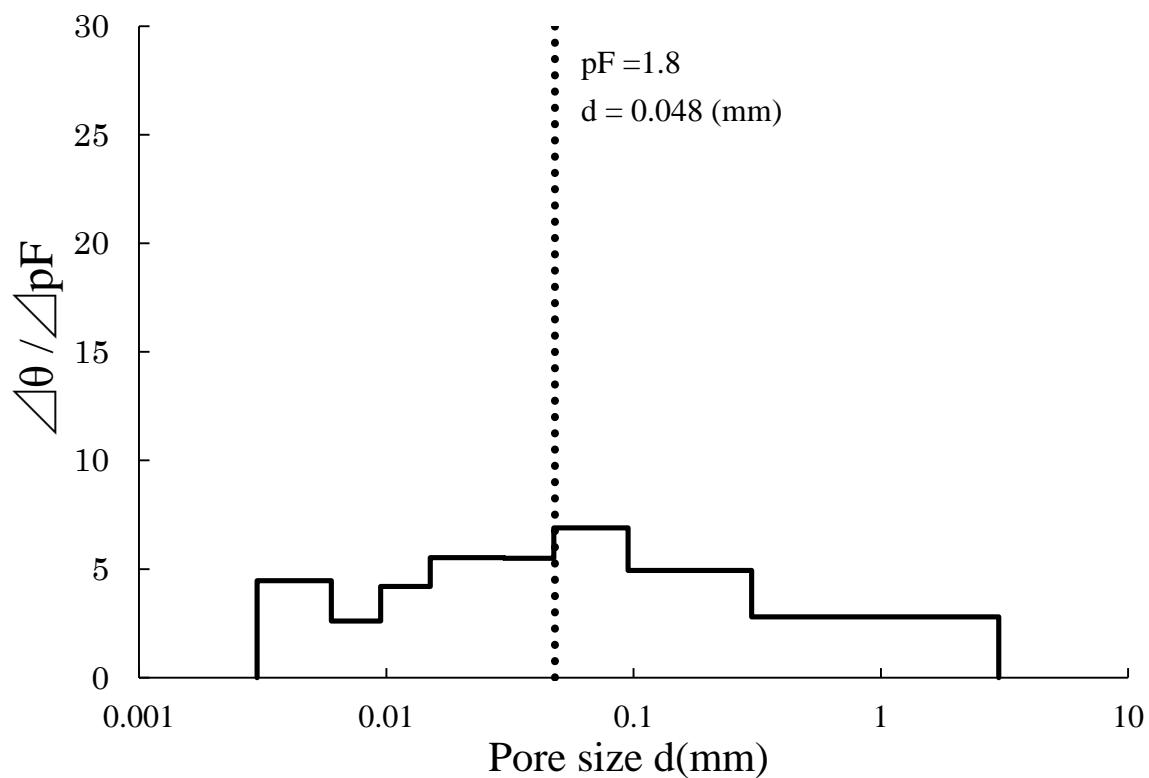


Fig. 3.37 $pF - \theta$ distribution, "Beans Field layer III"

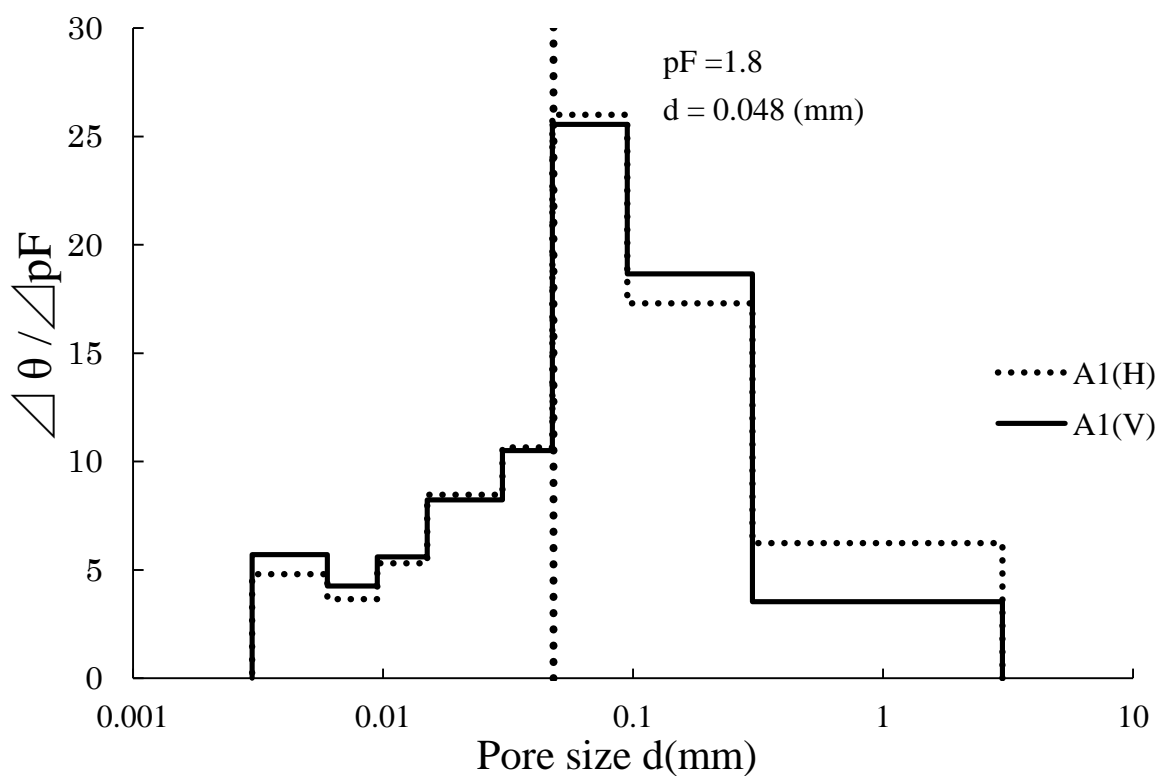


Fig. 3.38 $pF - \theta$ distribution, "Yokkaichi Agriculture Center layer A1"

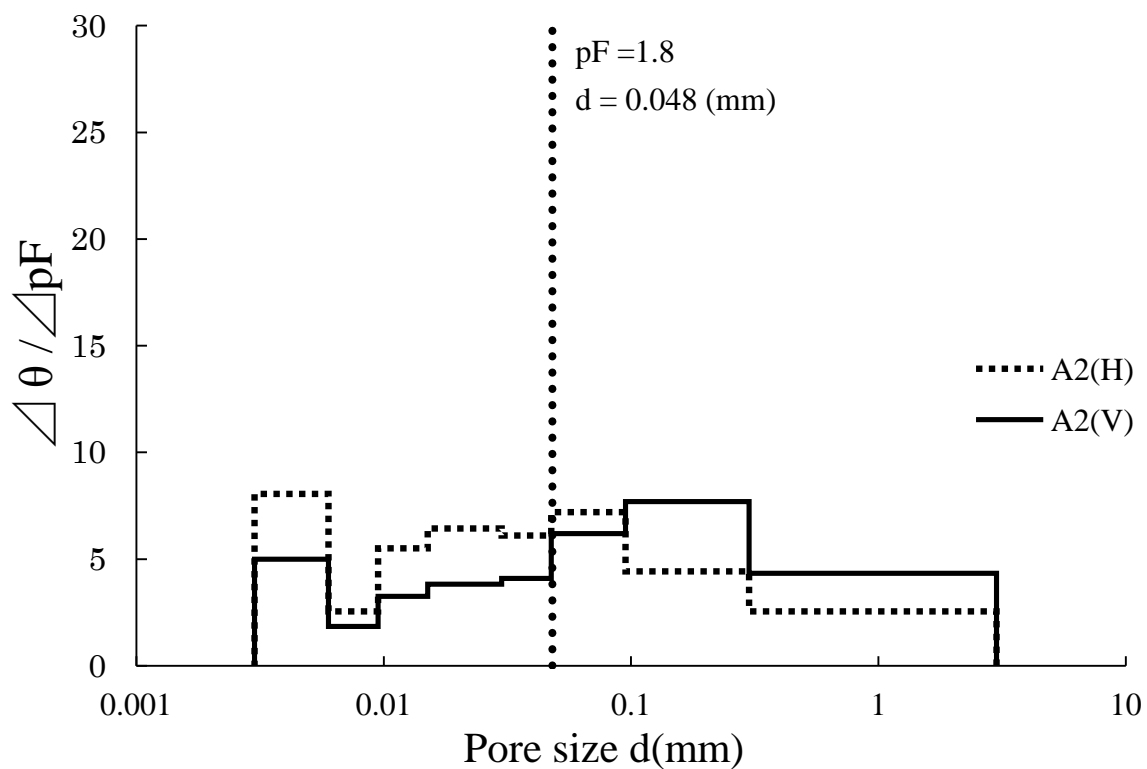


Fig. 3.39 pF – θ distribution, “Yokkaichi Agriculture Center layer A2”

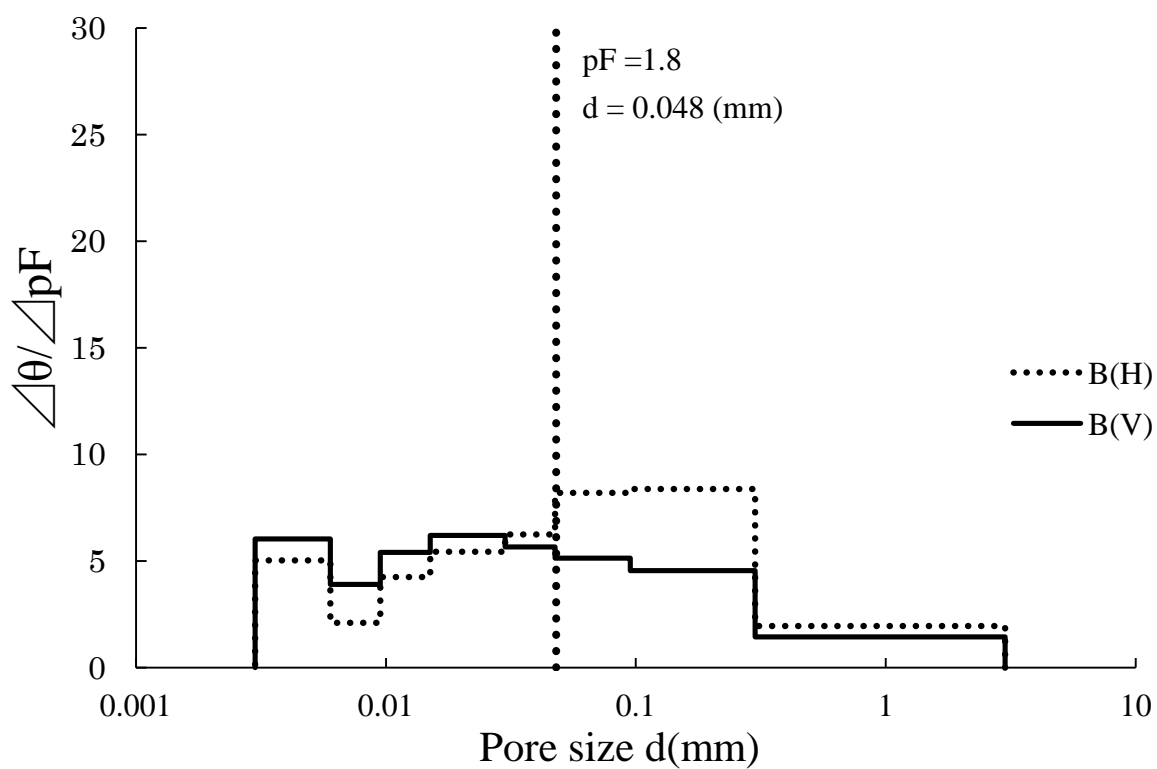


Fig. 3.40 pF – θ distribution, “Yokkaichi Agriculture Center layer B”

3.3.2.5 Permeability coefficient k_{sat} (Hydraulic conductivity)

Saturated hydraulic conductivity results for all layers are presented in **Table 3.18** and **Fig. 3.41 – 3.46**.

As shown in **Fig. 3.41** for Broccoli Filed Matsusaka, vertical direction shows higher conductivity then horizontal from surface to 25cm depth, beneath this depth it decreased sharply for vertical direction and slightly for horizontal direction.

In **Fig. 3.43** for Beans Field, Matsusaka, it is higher till 10cm depth and from 25cm depth beneath, while it decreased from 10cm – 18cm and from 18cm – 25cm depth it gets increased. When comparing to Broccoli Field, it showed totally lower hydraulic conductivity.

Based on **Fig. 3.45** for Yokkaichi Agriculture center, the hydraulic conductivity is much higher than previous two sites, especially in 0cm – 25cm depth in both direction and 45cm – 60cm depth in vertical direction.

[**Table 3.18** Saturated hydraulic conductivity k_{sat} for all sites]

[**Fig. 3.41** Saturated hydraulic conductivity k_{sat} (cm sec^{-1}), Broccoli Field Matsusaka]

[**Fig. 3.42** Saturated hydraulic conductivity k_{sat} (m h^{-1}), Broccoli Field Matsusaka]

[**Fig. 3.43** Saturated hydraulic conductivity k_{sat} (cm sec^{-1}), Beans Field Matsusaka]

[**Fig. 3.44** Saturated hydraulic conductivity k_{sat} (m h^{-1}), Beans Field Matsusaka]

[**Fig. 3.45** Saturated hydraulic conductivity k_{sat} (cm sec^{-1}), Yokkaichi Agriculture Center]

[**Fig. 3.46** Saturated hydraulic conductivity k_{sat} (m h^{-1}), Yokkaichi Agriculture Center]

Table 3.18 Saturated hydraulic conductivity k_{sat} for all sites

Sample Name	Hydraulic conductivity (k)				Ratio k_V/k_H
	V cm sec^{-1}	H cm sec^{-1}	V m h^{-1}	H m h^{-1}	
Broccoli Field, Ridge	1.0E-03	-	3.6E-02	-	-
Broccoli Filed, layer I	1.5E-03	6.0E-05	5.5E-02	2.1E-03	25.80
Broccoli Field, layer II	1.6E-05	3.2E-05	5.6E-04	1.1E-03	0.49
Beans Field, Ridge	8.6E-05	-	3.1E-03	-	-
Beans Field, layer I	4.9E-06	-	1.8E-04	-	-
Beans Field, layer II	3.6E-05	-	1.3E-03	-	-
Beans Field, layer III	9.8E-05	-	3.5E-03	-	-
YAC, layer A1	2.0E-03	3.0E-03	7.2E-02	1.1E-01	0.66
YAC, layer A2	9.1E-05	8.5E-05	3.3E-03	3.1E-03	1.07
YAC, layer B	3.0E-03	1.8E-05	1.1E-01	6.5E-04	164.73

YAC: Yokkaichi Agriculture Center

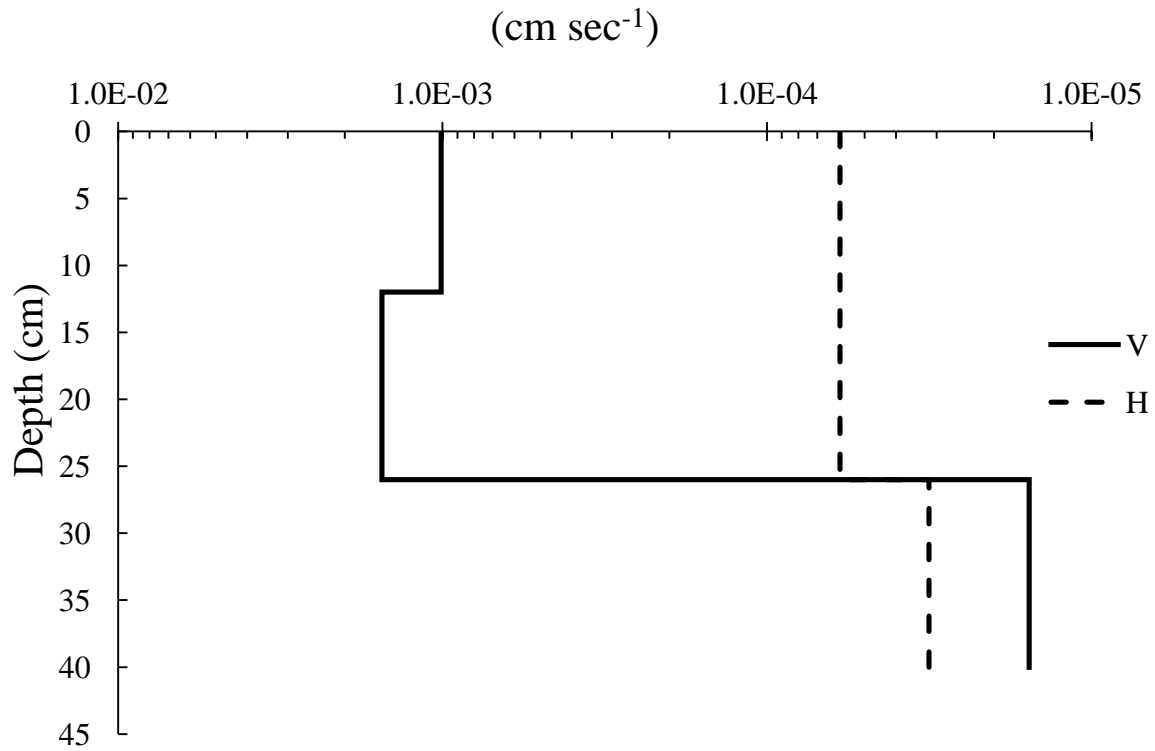


Fig. 3.41 Saturated hydraulic conductivity k_{sat} , “Broccoli Field” Matsusaka

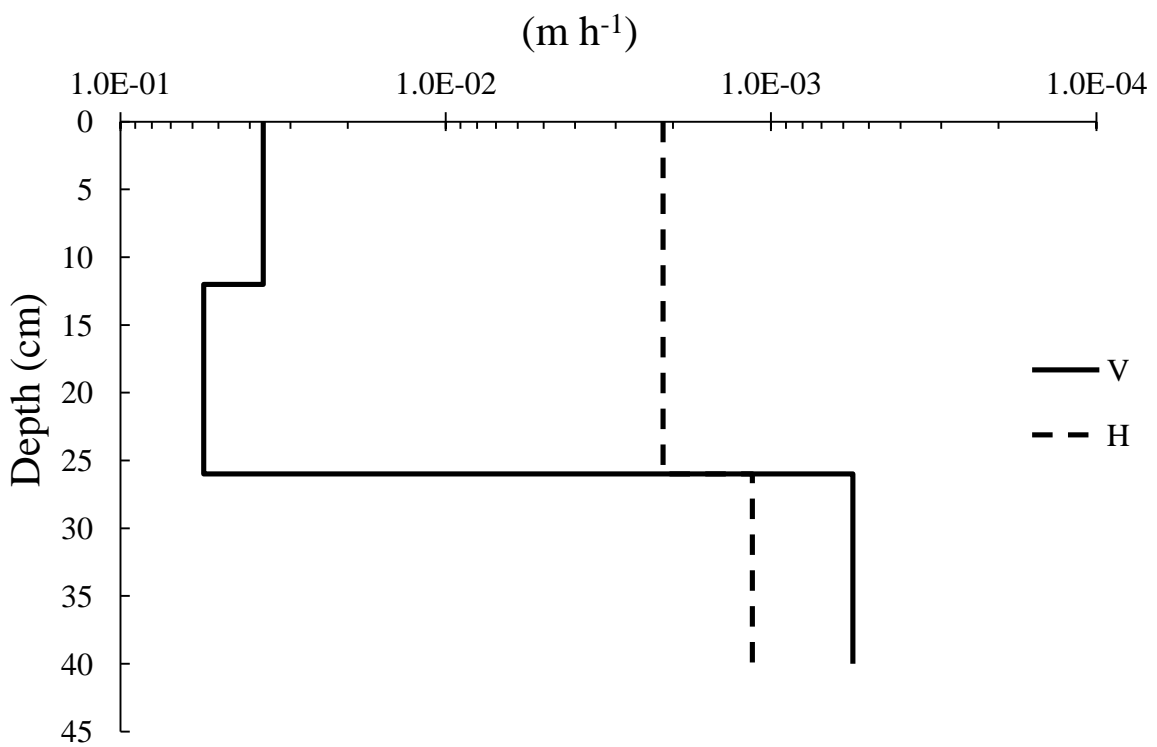


Fig. 3.42 Saturated hydraulic conductivity k_{sat} , “Broccoli Field” Matsusaka

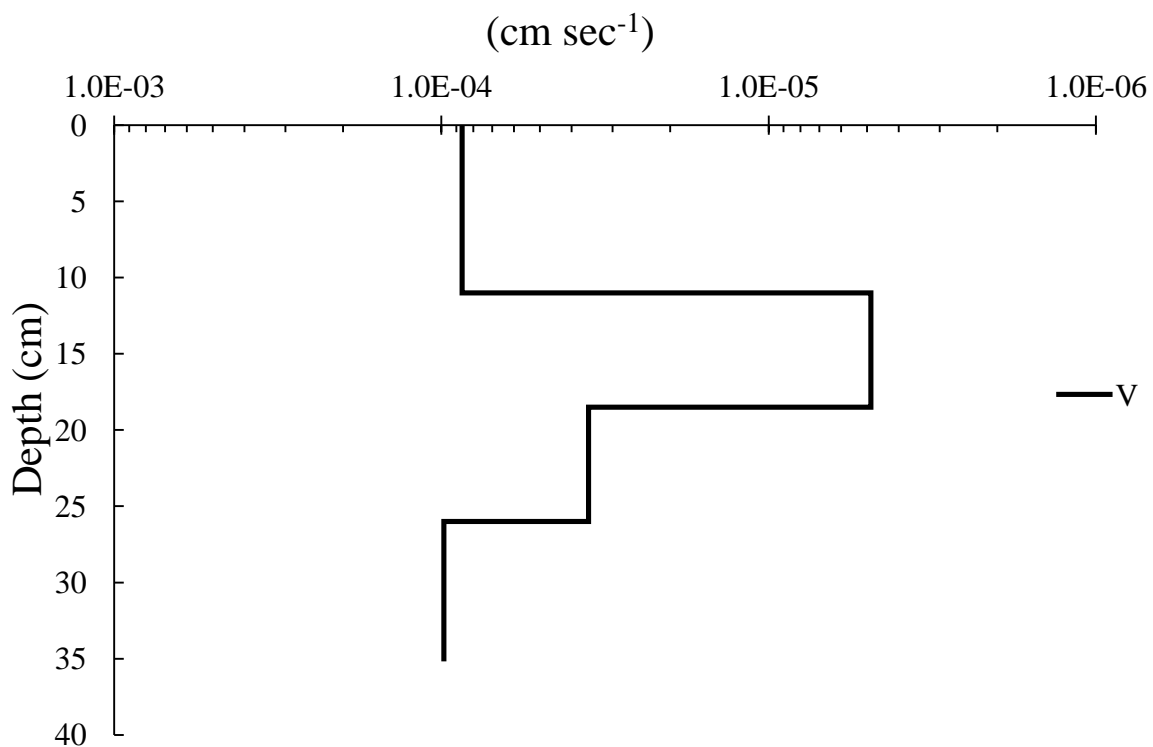


Fig. 3.43 Saturated hydraulic conductivity k_{sat} , “Beans Field” Matsusaka

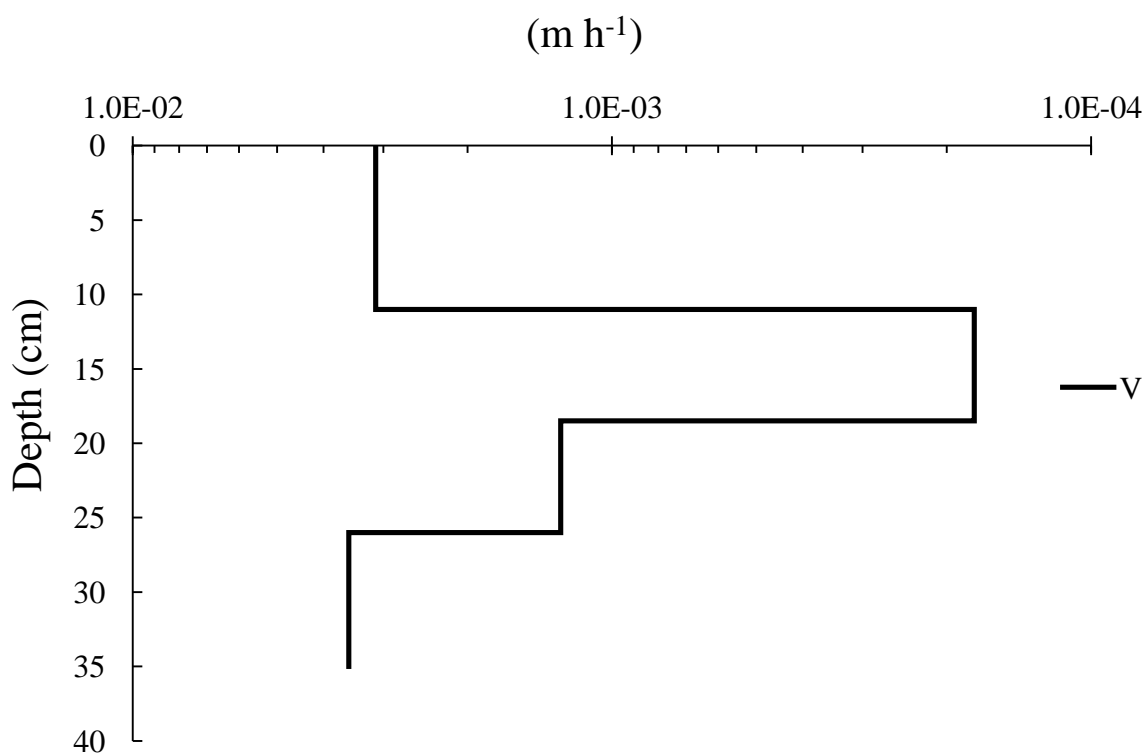


Fig. 3.44 Saturated hydraulic conductivity k_{sat} , “Beans Field” Matsusaka

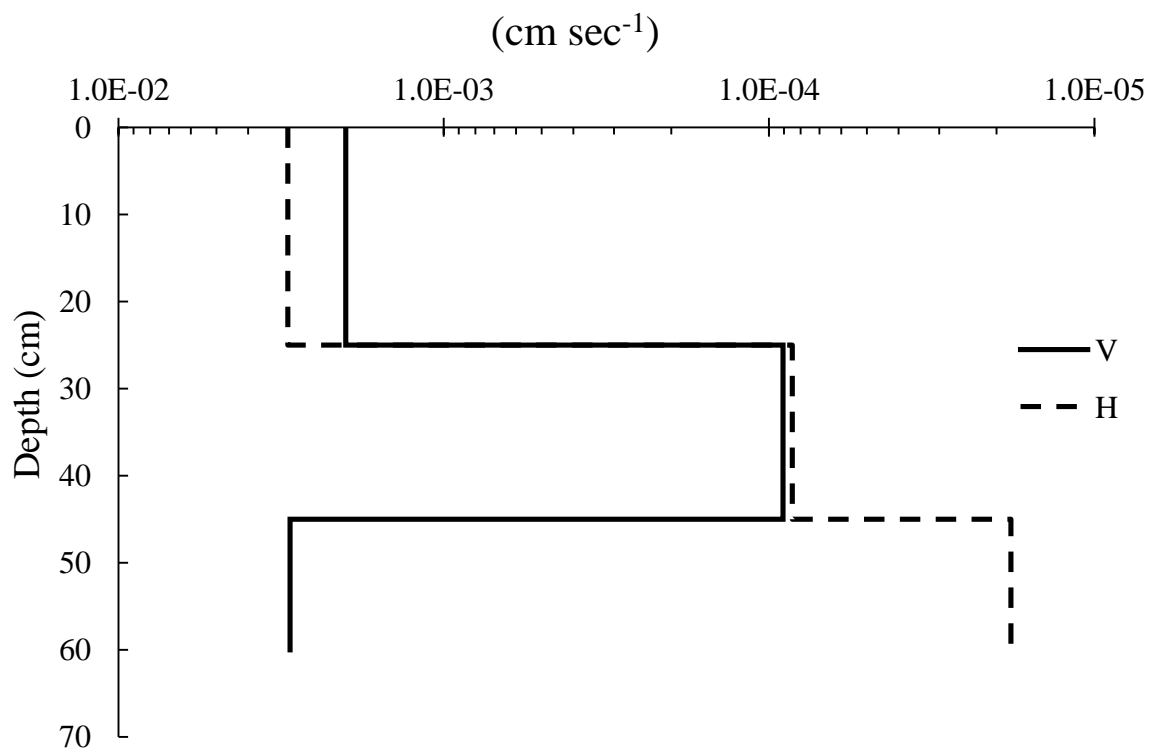


Fig. 3.45 Saturated hydraulic conductivity k_{sat} , “Yokkaichi Agriculture Center”

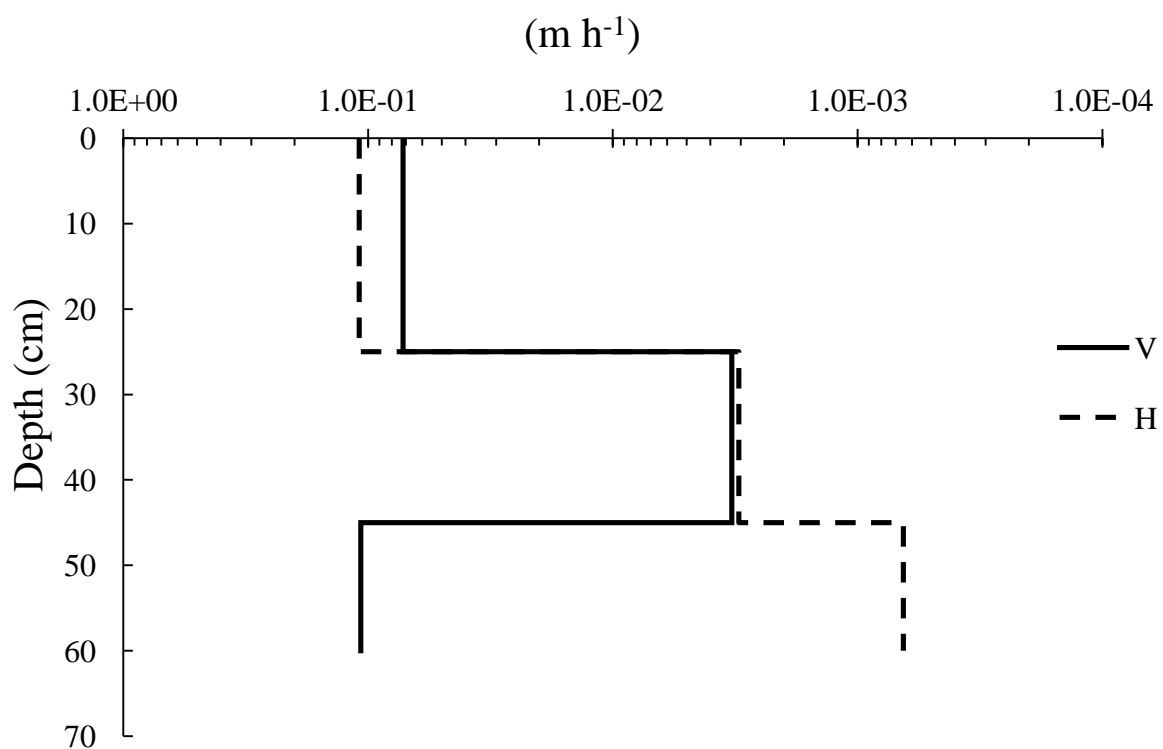


Fig. 3.46 Saturated hydraulic conductivity k_{sat} , “Yokkaichi Agriculture Center”

3.3.2.6 Drainability

The drainability, negative pressure limit (P_K), results are shown in **Fig. 3.47 – 3.56**. The commutative amount of drained water is plotted in vertical axes and load pressure is plotted in horizontal axes. The load pressure in which drainage stop by entering of air bubble in the bottom of the sample is defined as maximums diameter macropores important for drainage.

[**Fig. 3.47** Drainability, negative pressure, “Broccoli Field ridge, Matsusaka”]

[**Fig. 3.48** Drainability, negative pressure, “Broccoli Field layer I , Matsusaka”]

[**Fig. 3.49** Drainability, negative pressure, “Broccoli Field layer II , Matsusaka”]

[**Fig. 3.50** Drainability, negative pressure, “Beans Field ridge, Matsusaka”]

[**Fig. 3.51** Drainability, negative pressure, “Beans Field layer I , Matsusaka”]

[**Fig. 3.52** Drainability, negative pressure, “Beans Field layer II , Matsusaka”]

[**Fig. 3.53** Drainability, negative pressure, “Broccoli Field layer III, Matsusaka”]

[**Fig. 3.54** Drainability, negative pressure, “layer A1 Yokkaichi Agriculture Center”]

[**Fig. 3.55** Drainability, negative pressure, “layer A2 Yokkaichi Agriculture Center”]

[**Fig. 3.56** Drainability, negative pressure, “layer B Yokkaichi Agriculture Center”]

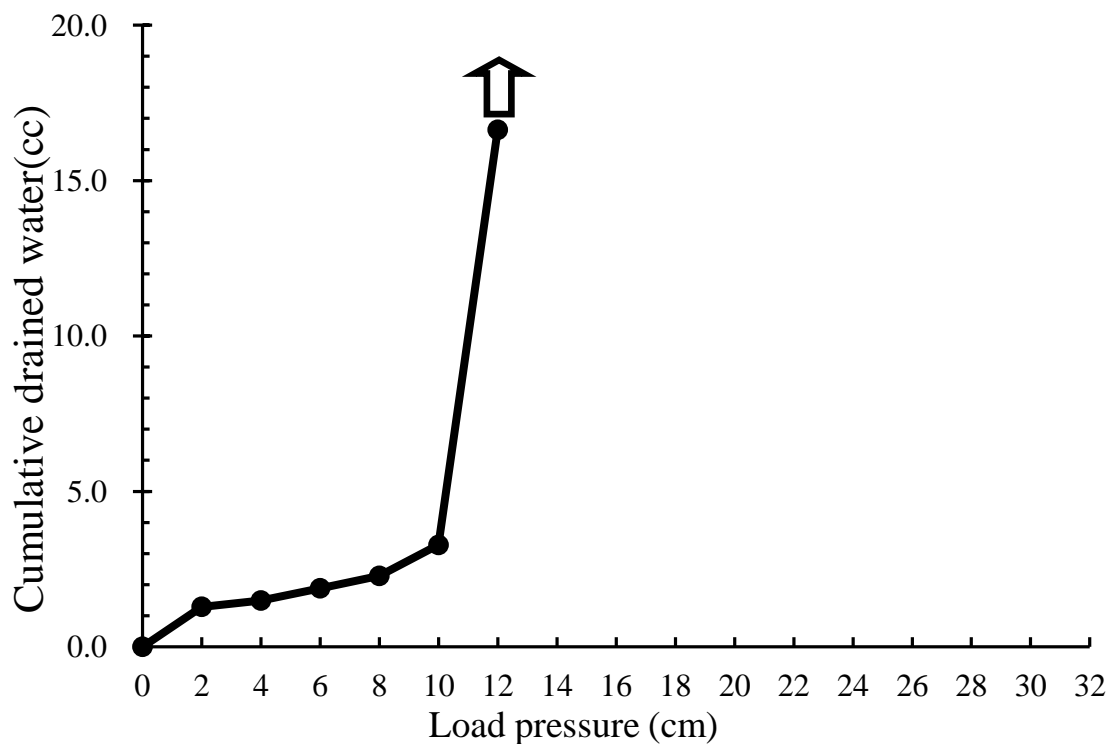


Fig. 3.47 Drainability, negative pressure, “Broccoli Field ridge, Matsusaka”

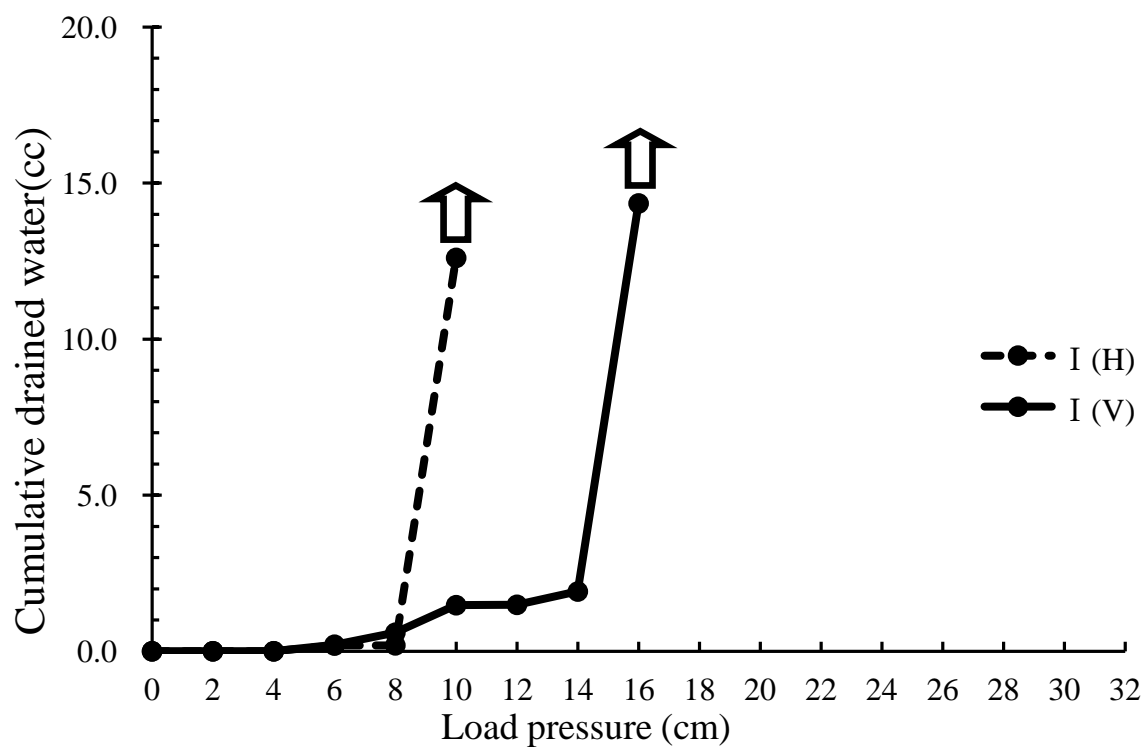


Fig. 3.48 Drainability, negative pressure, “Broccoli Field layer I , Matsusaka”

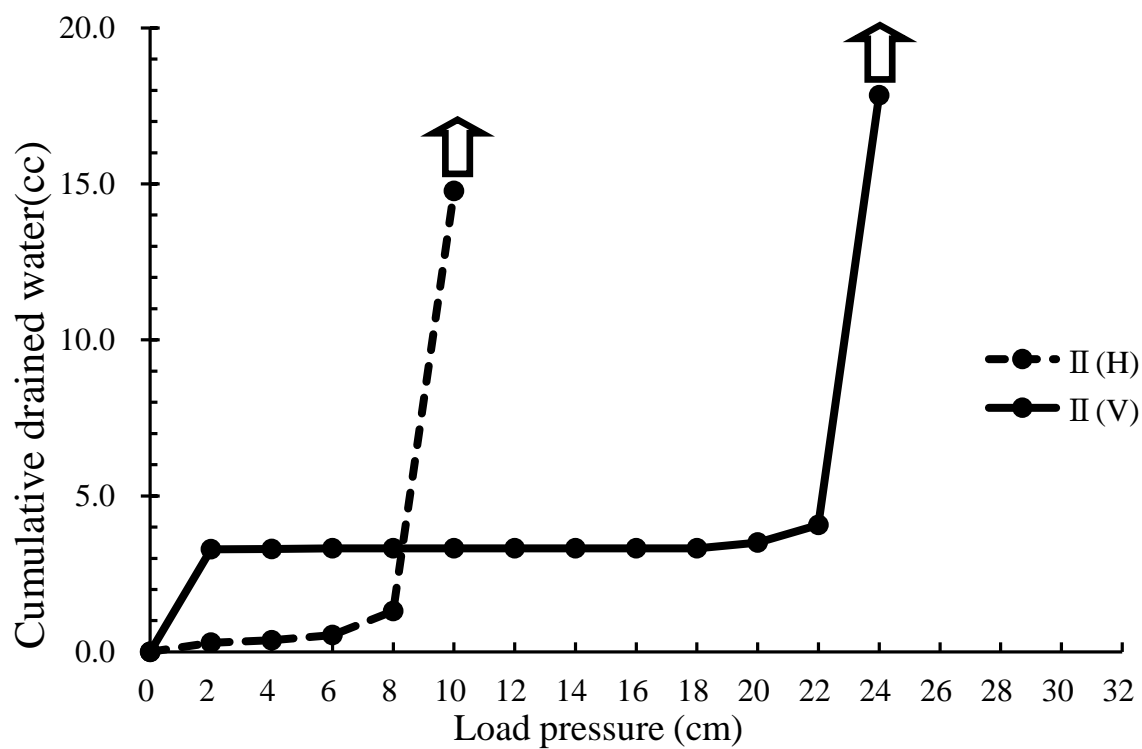


Fig. 3.49 Drainability, negative pressure, “Broccoli Field layer II, Matsusaka”

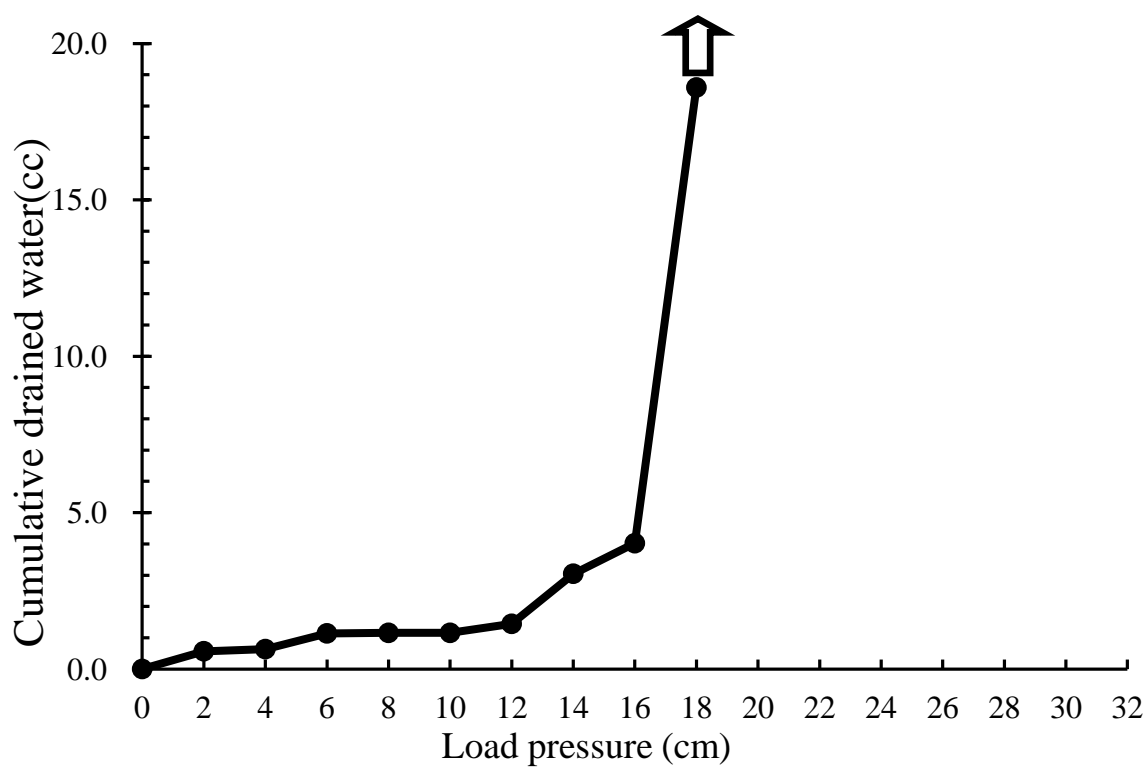


Fig. 3.50 Drainability, negative pressure, “Beans Field ridge, Matsusaka”

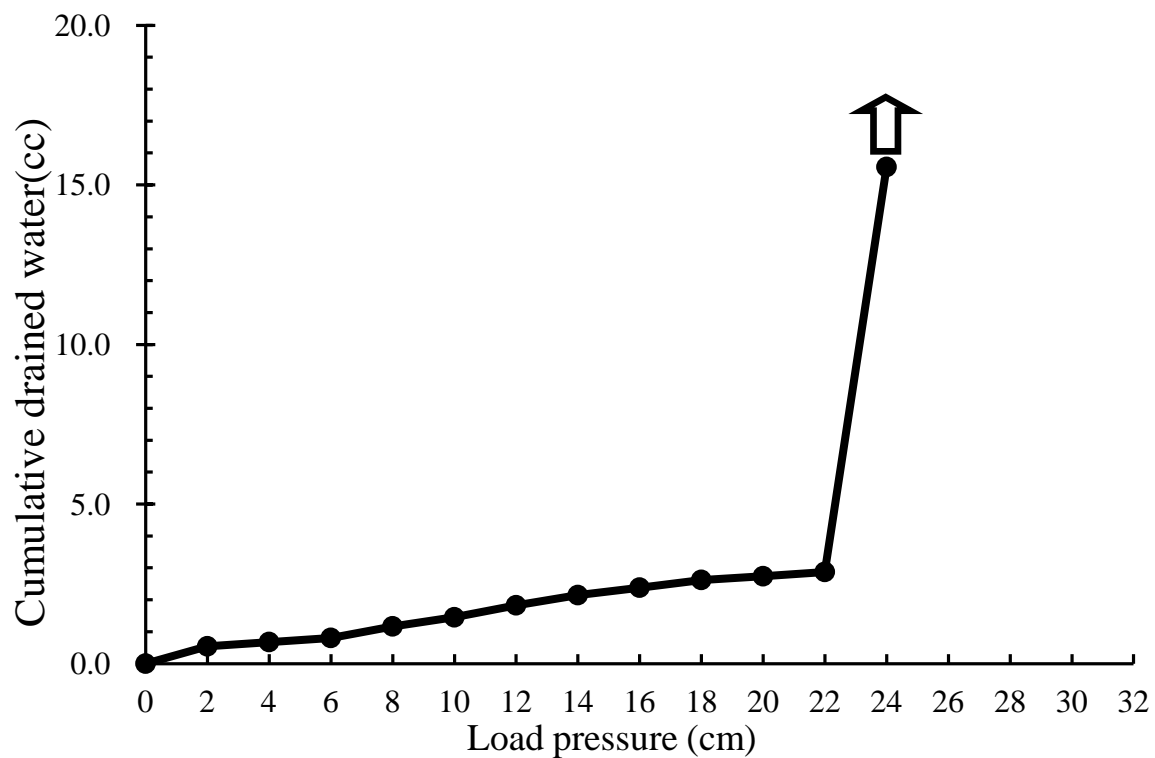


Fig. 3.51 Drainability, negative pressure, “Beans Field layer I , Matsusaka”

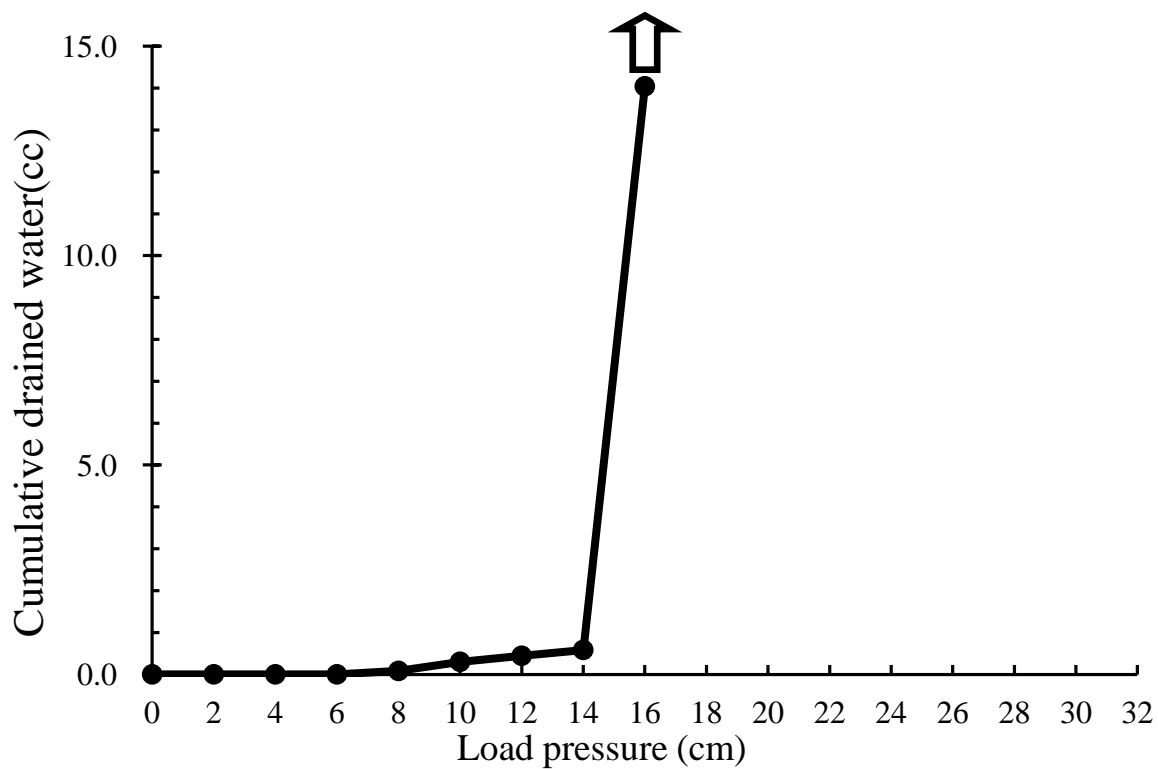


Fig. 3.52 Drainability, negative pressure, “Beans Field layer II , Matsusaka”

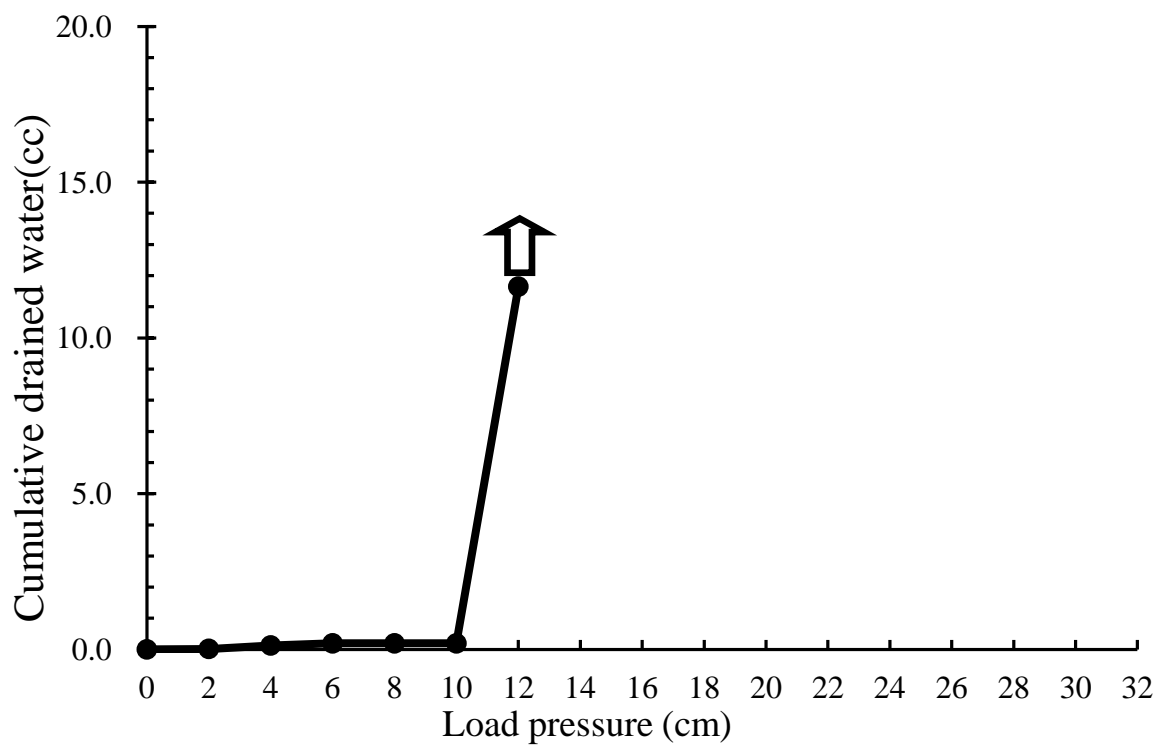


Fig. 3.53 Drainability, negative pressure, “Broccoli Field layer III, Matsusaka”

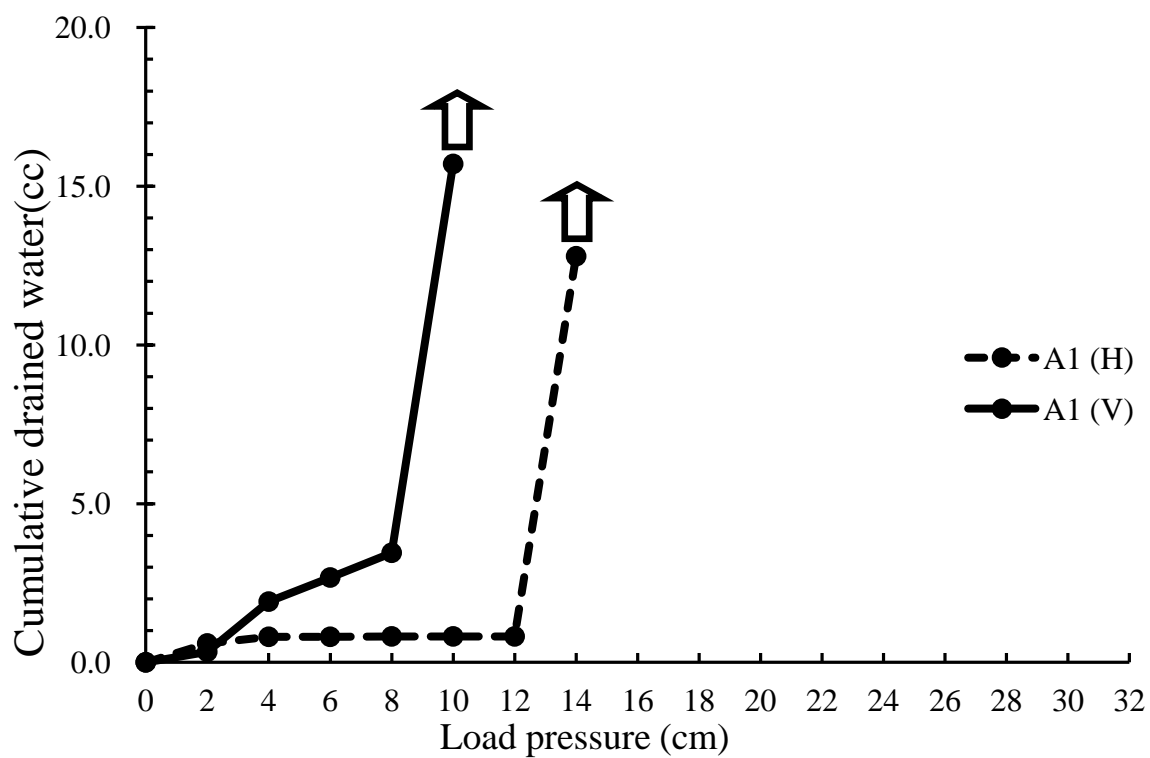


Fig. 3.54 Drainability, negative pressure, “layer A1 Yokkaichi Agriculture Center”

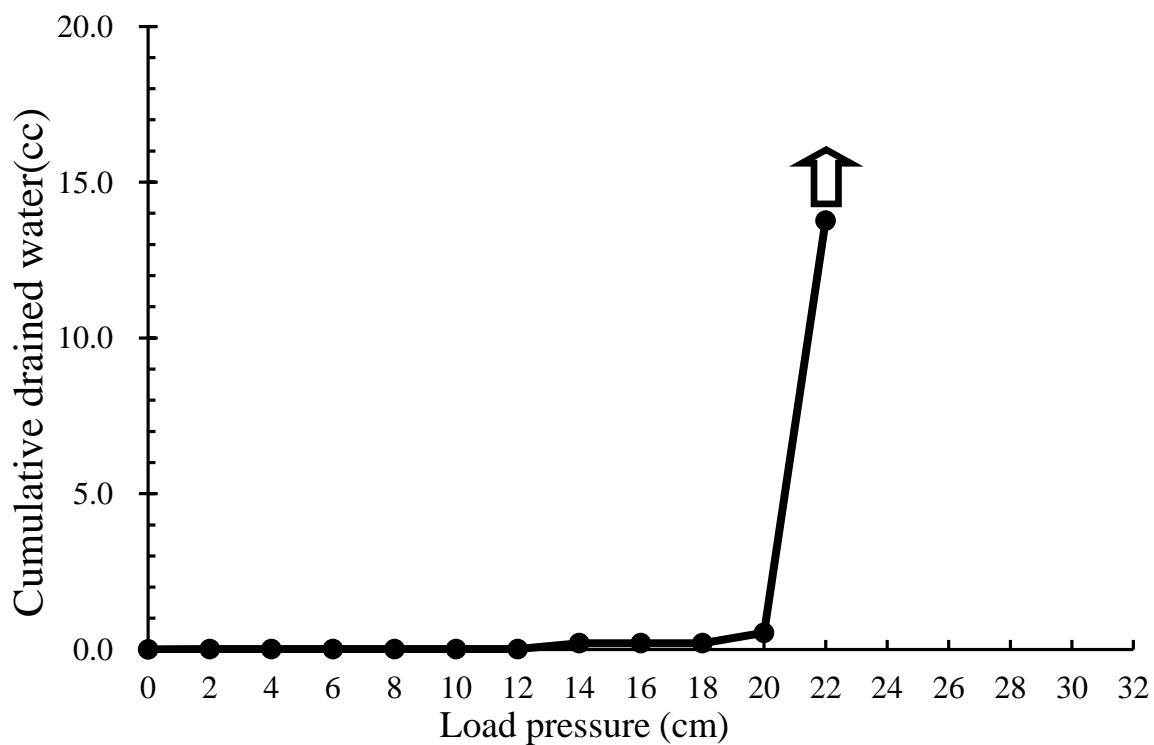


Fig. 3.55 Drainability, negative pressure, “layer A2 (H)Yokkaichi Agriculture Center”

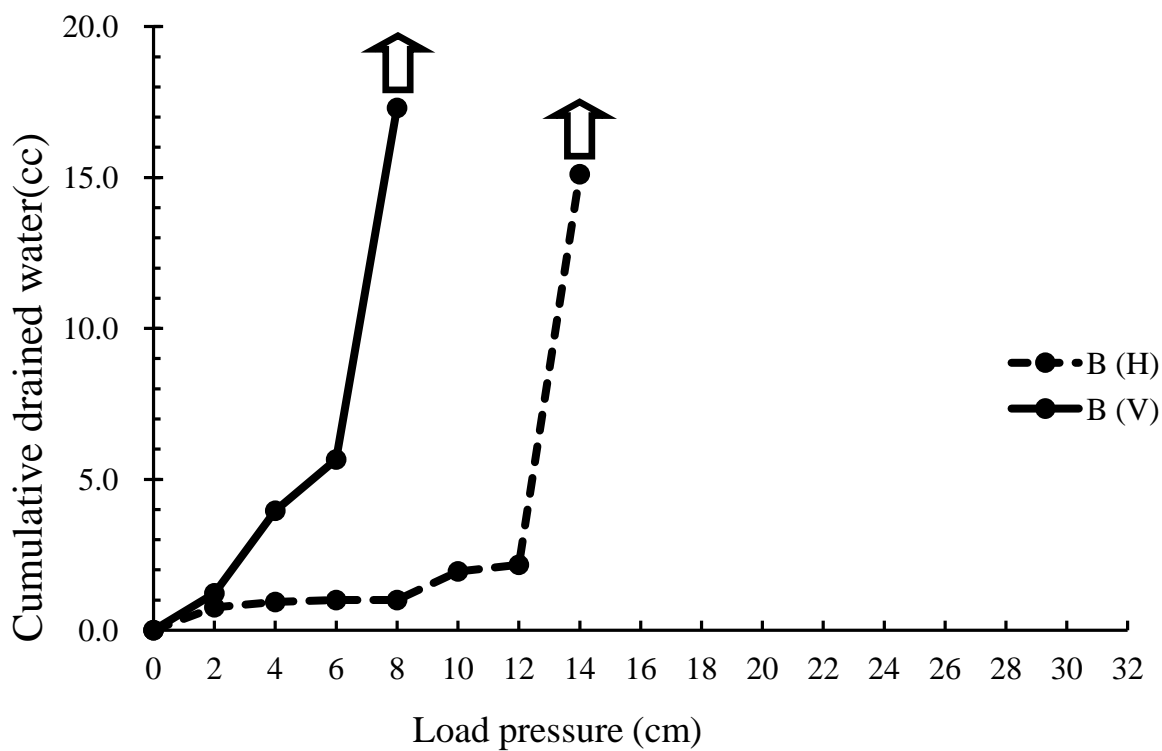


Fig. 3.56 Drainability, negative pressure, “layer A2 Yokkaichi Agriculture Center”

3.3.2.7 Soft X-ray imaging

With visual determination of macropores, Soft X-ray imaging can provide adequate information about soil macropores and their connectivity. Results of Soft X-ray imaging are shown in **Photos 3.35 – 3.44**.

Soft X-ray images which are shown in **Photos 3.35, 3.37, 3.39, and 3.41** are images of soil matrix respectively for Broccoli Field layer II (H), Beans Field ridge (V), Beans Field I (V), and Yokkaichi Agriculture Center layer B (H).

Photos 3.36, 3.38, 3.40, and 3.42 are Soft X-ray images of same locations respectively, after application of heavy liquid as contrast agent. In these images, structure of macropores is clearly visible.

Photos 3.43 and 3.44 are stereoscopic view of macropores for Broccoli Field layer II (H) and Yokkaichi layer B (H).

[Photo 3.35 Soft X-ray image without application of heavy liquid, “layer II (H) of Broccoli Filed, Matsusaka”]

[Photo 3.36 Soft X-ray image after application of heavy liquid, “layer II (H) of Broccoli Filed, Matsusaka”]

[Photo 3.37 Soft X-ray image without application of heavy liquid, “ridge (V) of Beans Filed, Matsusaka”]

[Photo 3.38 Soft X-ray image after application of heavy liquid, “ridge (V) of Beans Filed, Matsusaka”]

[Photo 3.39 Soft X-ray image without application of heavy liquid, “layer II (V) of Beans Filed, Matsusaka”]

[Photo 3.40 Soft X-ray image after application of heavy liquid, “layer II’(V) of Beans Filed, Matsusaka”]

[Photo 3.41 Soft X-ray image without application of heavy liquid, “Yokkaichi Agriculture Center layer B (H)”]

[Photo 3.42 Soft X-ray image after application of heavy liquid, “Yokkaichi Agriculture Center layer B (H)”]

[Photo 3.43 Stereoscopic view of Broccoli Field, “layer II (H) after application of heavy liquid, Matsusaka”]

[Photo 3.44 Stereoscopic view of Yokkaichi Agriculture Center, “layer B (H) after application of heavy liquid”]

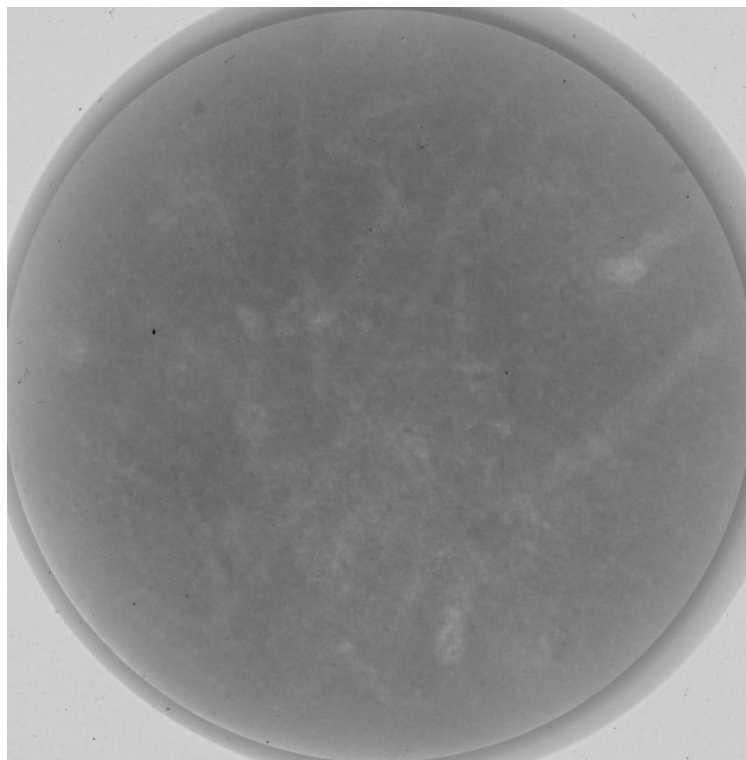


Photo 3.35 Soft X-ray image without application of heavy liquid, “layer II (H) of Broccoli Filed, Matsusaka”

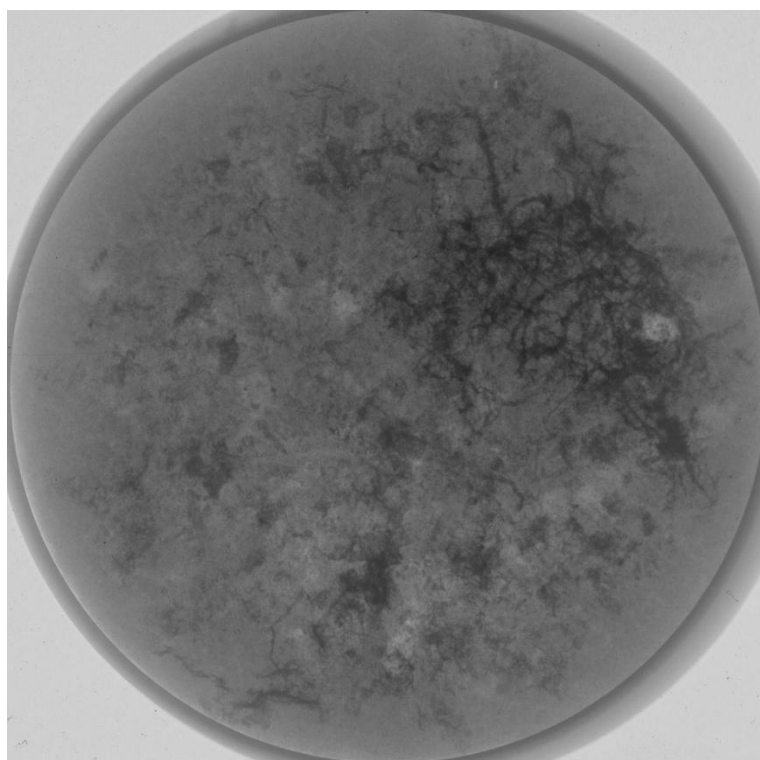


Photo 3.36 Soft X-ray image after application of heavy liquid, “layer II (H) of Broccoli Filed, Matsusaka”

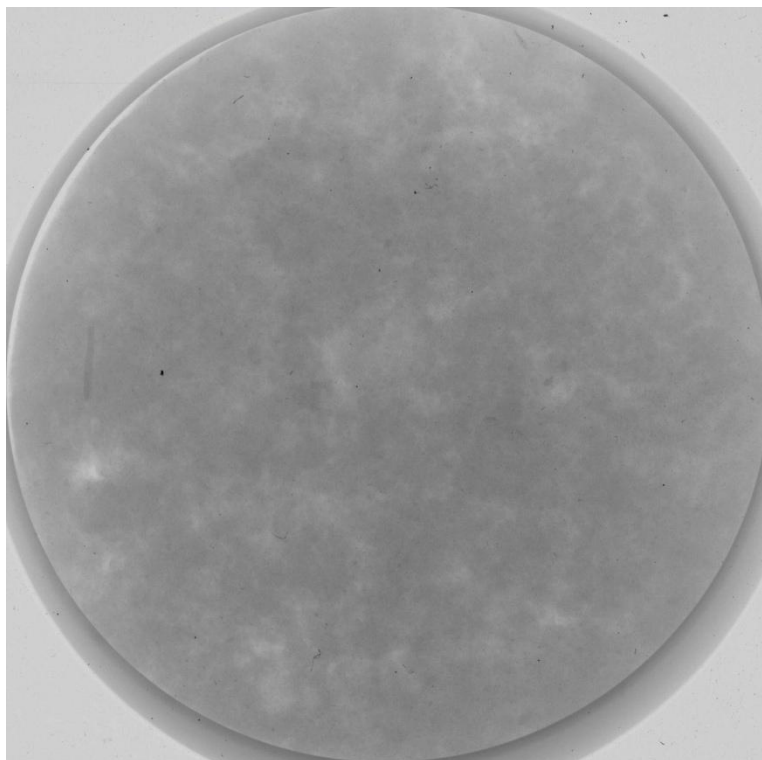


Photo 3.37 Soft X-ray image without application of heavy liquid, “ridge (V) of Beans Filed, Matsusaka”

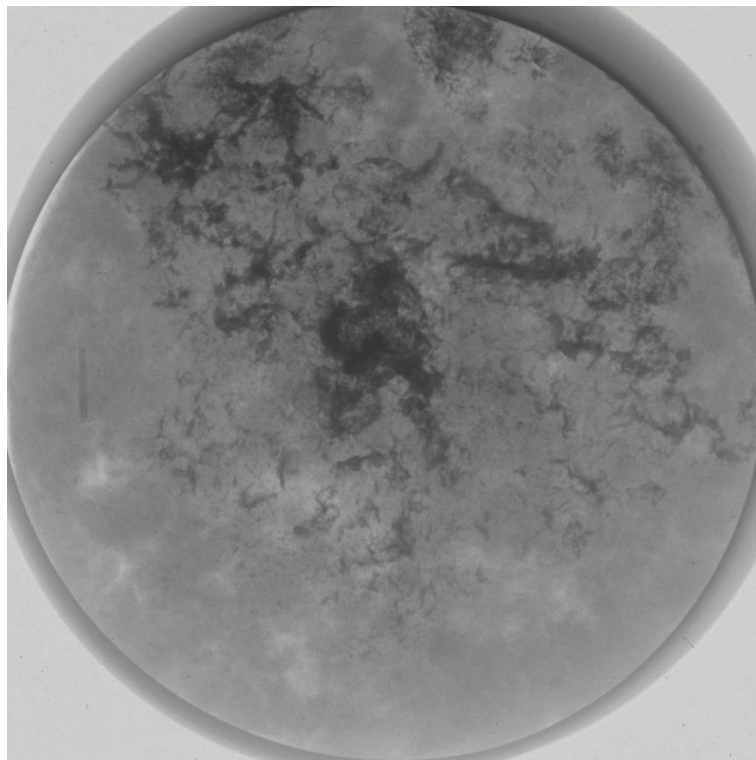


Photo 3.38 Soft X-ray image after application of heavy liquid. “ridge (V) of Beans Filed, Matsusaka”

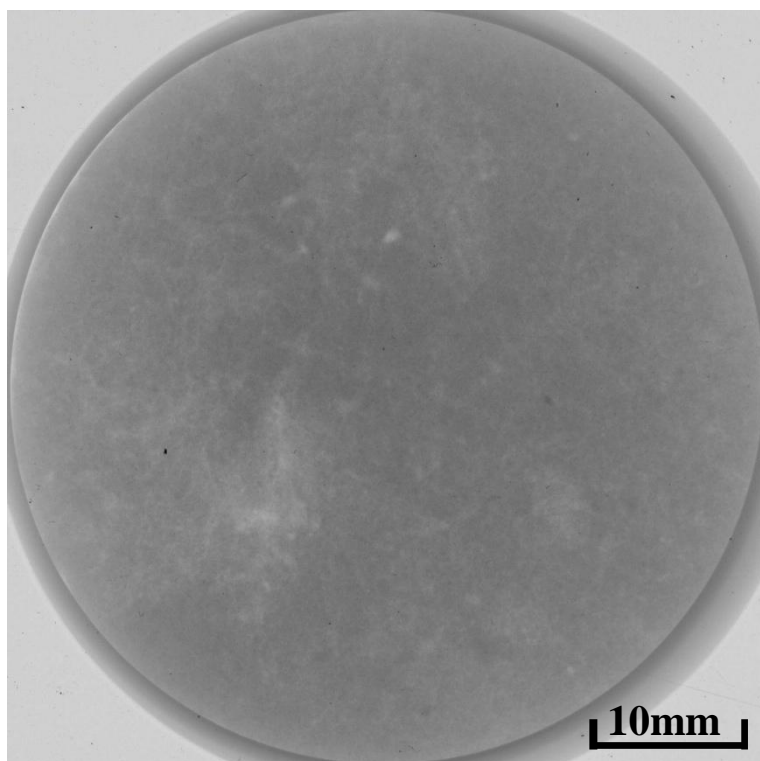


Photo 3.39 Soft X-ray image without application of heavy liquid, “layer II (V) of Beans Filed, Matsusaka”

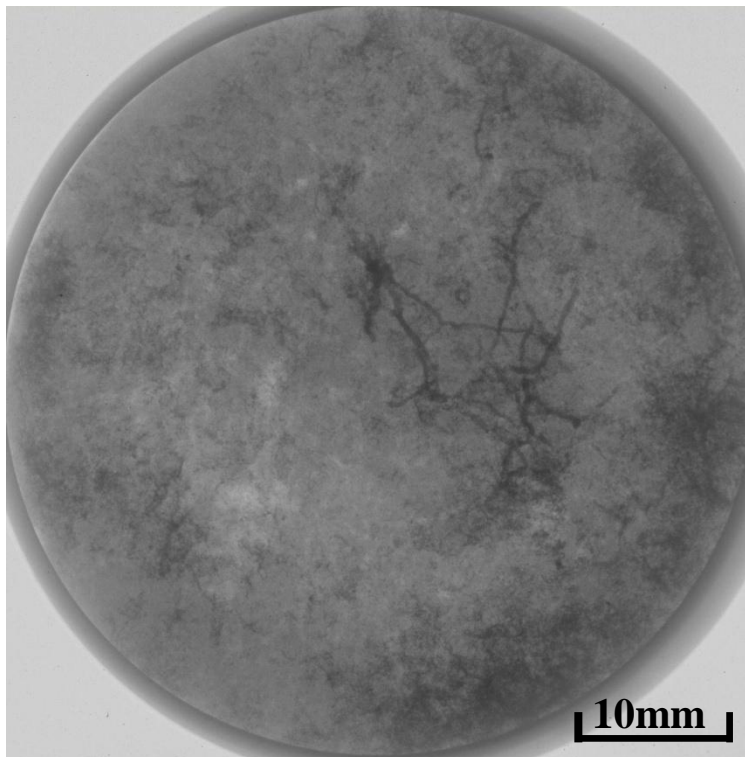


Photo 3.40 Soft X-ray image after application of heavy liquid, “layer II (V) of Beans Filed, Matsusaka”

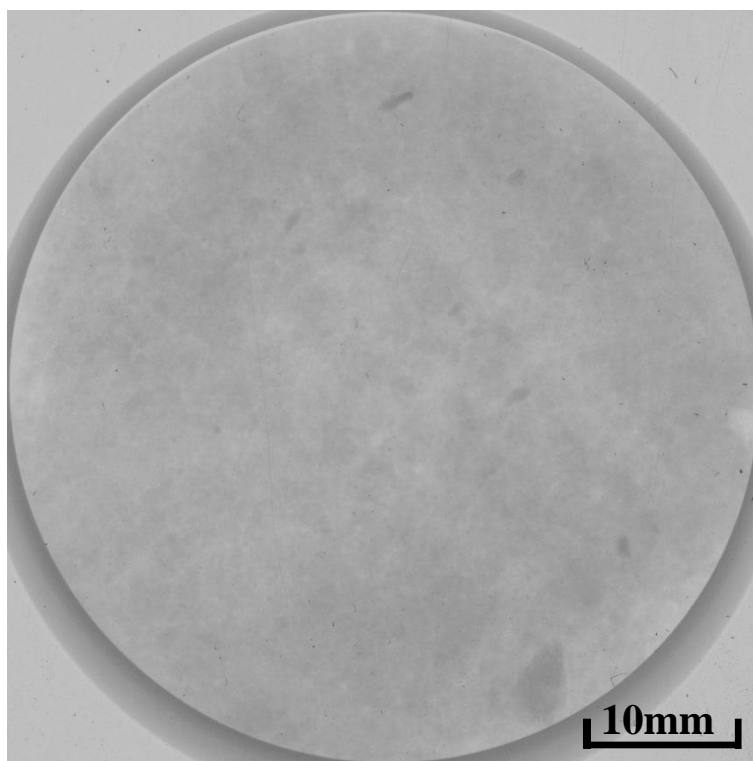


Photo 3.41 Soft X-ray image without application of heavy liquid, “Yokkaichi Agriculture Center layer B (H)”

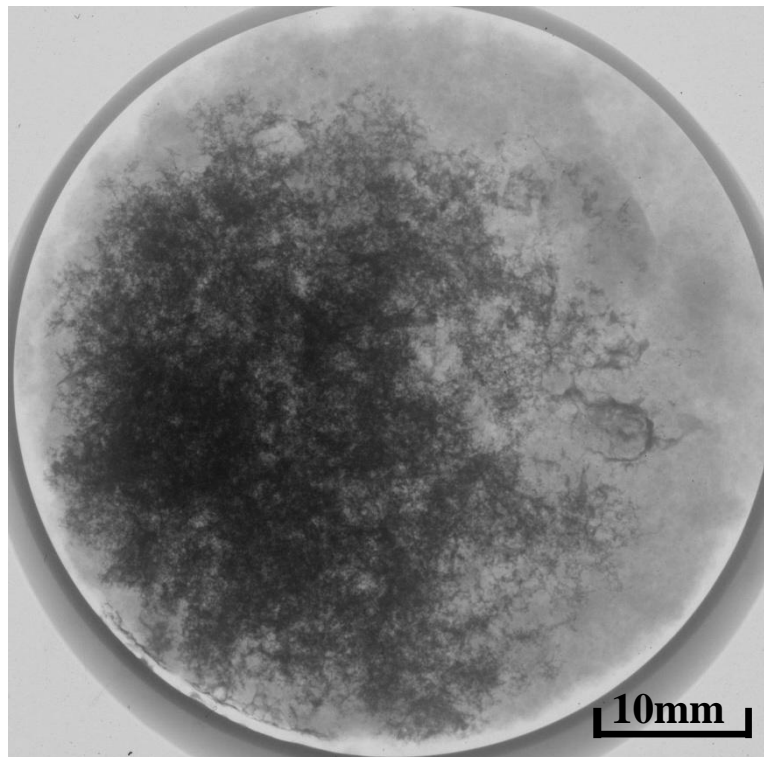


Photo 3.42 Soft X-ray image after application of heavy liquid, “Yokkaichi Agriculture Center layer B (H)”

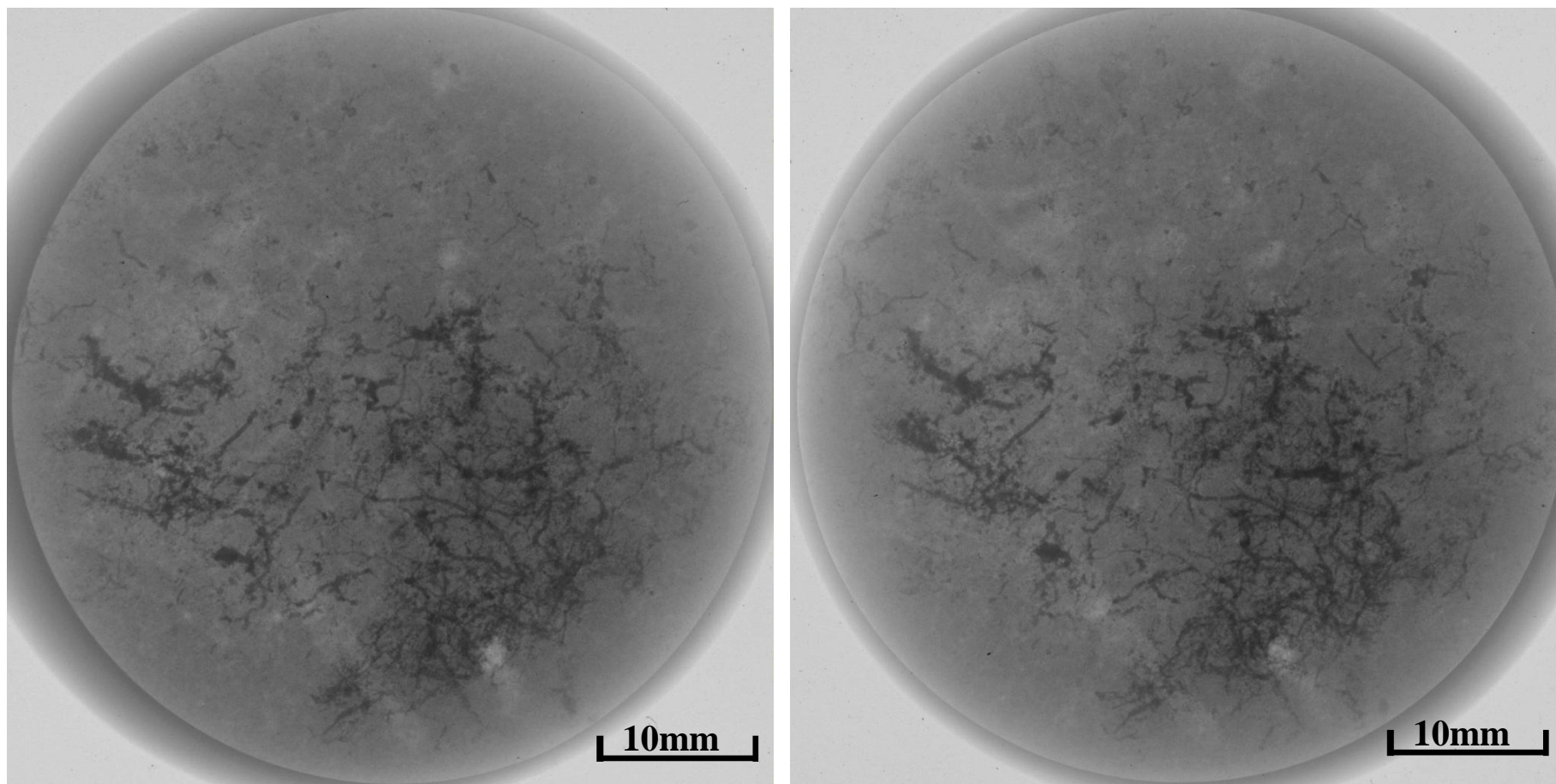


Photo 3.43 Stereoscopic view of Broccoli Field, “layer II (H) after application of heavy liquid, Matsusaka”

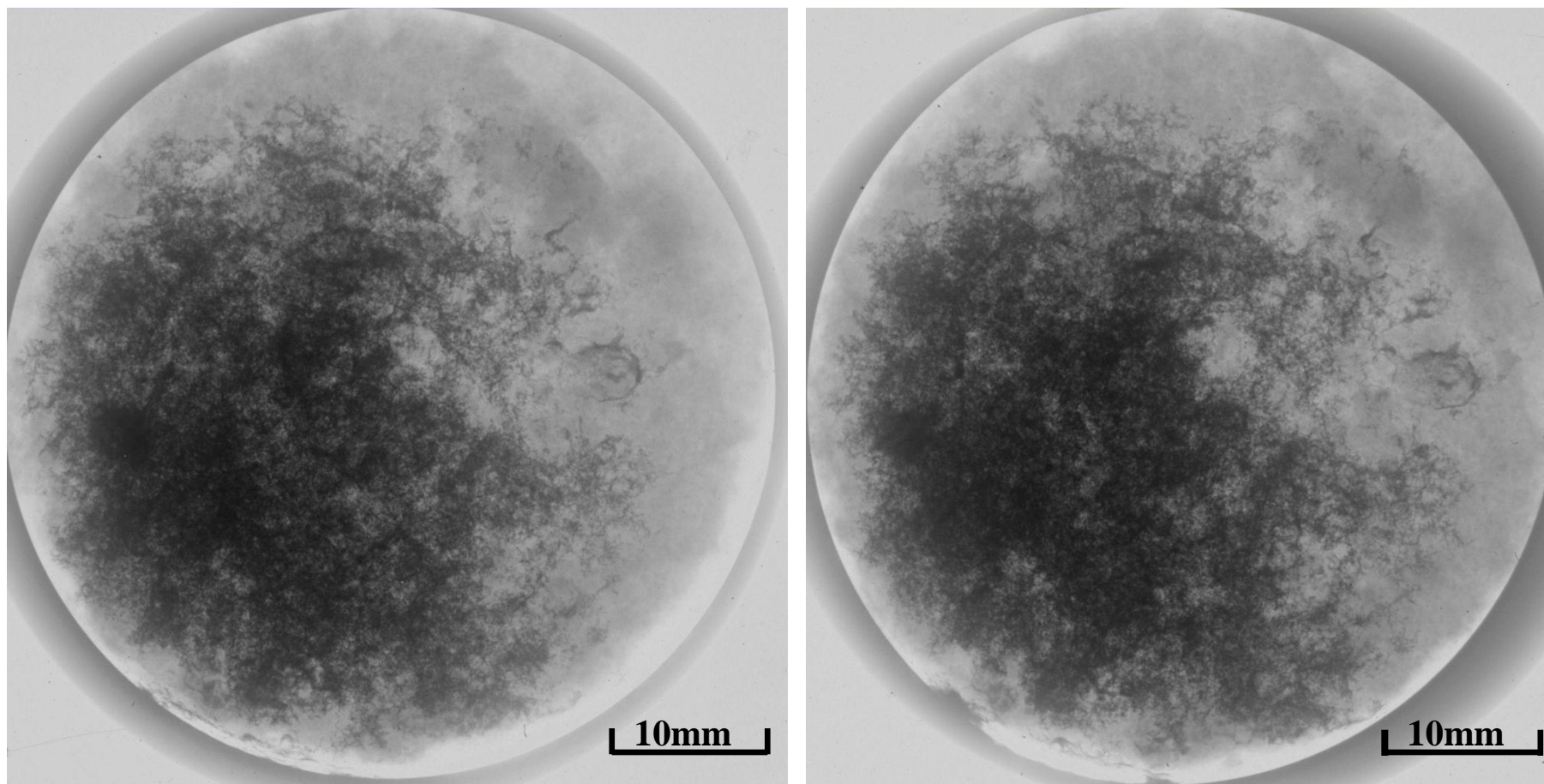


Photo 3.44 Stereoscopic view of Yokkaichi Agriculture Center, “layer B (H) after application of heavy liquid”

4. Understanding of results

4.1 Soil condition and basic physical properties

(1) Water ponding occurs in ditches and ridge as well and overall drainage condition of the Broccoli Field seems poor. The leveling condition of the entire field, particularly the ditches is not uniformed and it increases the intensity of spatial ponding. Due to lack of good drainage system, bad leveling condition, and compacted soil, as shown in **Photo 3.24**, during rainy season in Broccoli Field of Matsusaka water ponding is a challenge for production.

Even though the field surface is well leveled in Beans Field, but it also has water ponding due of lack of good drainage condition and compacted soil layers as shown in **Photo 3.30 – 3.31**.

Comparing to Broccoli Field and Beans Field of Matsusaka, Yokkaichi Agriculture Center better physical condition, no water ponding condition, and the soil is not compacted as shown in **Photo 3.32**.

(2) Macropores in I layer of Broccoli Field were not significantly visible, while in layer II existing of macropores are shown in **Photos 3.28 – 3.29**. Pores with sign A refers to those tubular pores with diameter bigger than 1mm, those with B sign refers to tubular pores with diameter between 0.5mm – 1.0mm, and C refers to root made canals. Existence of macropores in underlying layers of soil profile cross section were not much visible.

In Beans Field macropores visible to bare eye were lacking in soil profile cross section.

In Yokkaichi Agriculture Center due to plowing of A0 layer it was difficult to find macropores, while in layers A1, A2 and B macropores visible to bare eye was existing much.

(3) **Hardpan:** In Broccoli Field of Matsusaka based on **Fig. 3.10** of soil hardness data, on-site investigated results in **Table 3.4**, and **Photos 3.25 – 3.27**, soil hardpan begins just underlying layer I from layer II. The ridge has granular structure, while starting from 15cm depth, layer I, to 60cm, layer III, the structure of soil is massive and compacted with almost same hardness distribution, there is no sign of root development.

In Beans Field according to **Fig. 3.12**, **Photos 3.30 – 3.31**, and **Table 3.5** the hard pan starts from 22cm depth, beneath layer I. Including ridge, all layers have massive structure and

development of roots are limited merely to ridge and little to I layer.

According to **Fig. 3.14** of Yokkaichi Agriculture Center hardness distribution data, hardpan starts in layer A2. As clearly visible in **Photos 3.32 – 3.34**, development of roots in layer A1 and limitation of roots in layer A2, outline existence of hardpan due to compacted layer. Soil structure is granular for layer A0, granular with crumb for layer A1, blocky and compacted for layer A2, and massive for layer B, detailed results in **Table 3.6**.

Accordingly, in current condition of soil, effective soil depth for roots growth is 22cm, 22cm, and 30cm respectively for Broccoli Field of Matsusaka, Beans Field of Matsusaka and Yokkaichi Agriculture Center.

(4) As shown in **Fig. 3.16** for Broccoli Field of Matsusaka, solid phase is dominant component and it increased from 49% in ridge to 56% and 62%, respectively, for layers I and II s, whereas; dry bulk density increase from 1.32 g cm^{-3} for ridge to 1.52 g cm^{-3} and 1.54 g cm^{-3} for layer I and layer II, and porosity decrease from 51% for ridge to 44% and 39% for I layer and II layer respectively.

Soil three phase distribution of **Fig. 3.17** for Beans Field shows that except for ridge which is 50% solid and 50% liquid and gas phase, in the rest three layers dominant phase is solid phase. Dry bulk density of ridge, I, II, and III are 1.31 g cm^{-3} , 1.47 g cm^{-3} , 1.53 g cm^{-3} and 1.49 g cm^{-3} and 50%, 45%, 43% and 44% porosity respectively.

In Yokkaichi Agriculture Center, dominant phase is liquid for almost all layers. In the other word, dry bulk density of A1 is 1.14 g cm^{-3} , A2 1.19 g cm^{-3} and B 1.15 g cm^{-3} and porosity is respectively 55%, 52%, and 56%.

Hence, Yokkaichi Agriculture Center has better phase distribution which facilitates faster hydraulic conductivity, water permeability, air permeability, and root development.

(5) According to **Tables 3.10, 3.11 and 3.12** and **Fig. 3.19, 3.20, and 3.21** particle size distribution of Broccoli Field Matsusaka, Beans field Matsusaka and Yokkaichi Agriculture Center, sand particles create more than 60% for all layers, except for layer B of Yokkaichi Agriculture Center. Soil texture for all layers showed almost similar texture of sandy loam,

except for layers A2 and B of Yokkaichi Agriculture Center with sandy clay loam and clay loam respectively. Textural classes are shown in **Fig. 3.22 – 3.24**.

(6) The plasticity properties of the soil according to **Table 3.13** and **Fig. 3.26** for Broccoli Field of Matsusaka, is inorganic clay with low plasticity and cohesionless in ridge and layers I , and II , while it is inorganic clay of medium plasticity for III and IV layers. Activity-A clay properties of ridge, layers I , II , III, III, and IV are respectively normal, inactive, inactive, normal, and normal.

Plasticity properties of Yokkaichi Agriculture center as presented in **Table 3.14** and **Fig. 3.27** is inorganic silt of high compressibility and high permeability and organic clay for layers A0, A2 and B (V. N. S. Murthy, 2002), A1 has low permeability and higher dry strength and toughness. Activity-A clay properties of A0, A1 and A2 is active clay and for B is inactive clay.

For all three sites, basic physical properties are briefly presented in **Tables 4.1 and 4.2**.

[**Table 4.1** Basic physical soil properties of each layer for all sites]

[**Table 4.2** Soil phase relation and plasticity data]

Table 4.1 Basic physical soil properties of each layer for all sites

Site	Layer	Particle density (g cm ⁻³)	Bulk density (g cm ⁻³)	Particle size distribution (%)			Texture	Porosity (cm ³ cm ⁻³)	Gravimetric water content (g g ⁻¹)	Volumetric water content θ (cm ³ cm ⁻³)
				Sand	Silt	Clay				
Broccoli Field	Ridge	2.68	1.32	80.4	11.3	8.3	LS	0.51	0.31	0.40
	I	2.71	1.52	68.2	12.5	19.3	SL	0.44	0.25	0.38
	II	2.49	1.54	62.2	15.6	22.1	SL	0.39	0.25	0.38
Beans Field	Ridge	2.65	1.31	-	-	-	SCL	0.50	0.34	0.44
	I	2.68	1.47	60.8	19.1	20.1	SL	0.45	0.28	0.41
	II	2.71	1.53	59.5	16.6	23.9	SL	0.43	0.23	0.35
	III	2.66	1.49	66.0	11.8	22.1	S	0.44	0.27	0.40
Yokkaichi Agriculture Center	A1	2.54	1.14	73.6	14.7	11.7	SL	0.55	0.46	0.52
	A2	2.48	1.19	59.4	24.1	16.5	SCL	0.52	0.43	0.51
	B	2.62	1.15	37.8	29.1	33.1	CL	0.56	0.44	0.50

Table 4.2 Soil phase relation and plasticity data of all sites

Site	Layer	Soil three phase ratio (%)			Liquid-plastic (g g^{-1})			Activity A	Clay type
		Solid phase	Liquid phase	Gas phase	L_L	L_P	I_P		
Broccoli Field	Ridge	49	42	9	31	25	6	0.77	Normal
	I	56	38	6	31	22	9	0.47	Inactive
	II	62	38	0	35	23	12	0.55	Inactive
Beans Field	Ridge	50	45	5	-	-	-	-	-
	I	55	40	5	-	-	-	-	-
	II	56	36	8	-	-	-	-	-
	III	56	40	4	-	-	-	-	-
Yokkaichi Agriculture Center	A1	45	52	3	76	30	46	4.21	Active
	A2	48	51.5	0.5	65	40	26	1.76	Active
	B	44	50	6	53	35	17	0.60	Inactive

4.2 Soil pores structure

Soil pores, especially macropores, play important and inevitable role in permeability of water in soil, air permeability, hydraulic conductivity, drainability, root growth and etc., this is why when dealing with irrigation planning and practicing, macropores should be kept into the consideration.

More important for pores, which are part of total porosity, are their continuity and connectivity. Continuity and connectivity of macropores in vertical direction of soil profile improve and increase hydraulic conductivity and drainage which is important for engineering purposes and agricultural purpose, while horizontal continuity and connectivity improves moisture distribution in soil layer which is very important for agriculture especially irrigation purposes.

Here, soil pores quantification based on different prospective will be discussed separately.

4.2.1 Pore size distribution (Capillary and non-capillary pores)

(1) Non-capillary pores in vertical direction occupies much portion than capillary pores in ridge and layer I of Broccoli Field (**Fig. 3.31 – 3.32**), while in layer II capillary pores are dominant (**Fig. 3.33**). On the other hand, in horizontal direction this relation is opposite, where distribution of capillary pores are more than non-capillary pores in horizontal direction (**Fig. 5.32 – 5.34**).

Distribution of non-capillary pores for layers I and II is more downward than extending horizontally, it is 30.6% for layer I and 16% for layer II downward, vertically; while it is 23.7% for layer I and 11.4% for layer II horizontally.

Capillary pores are distributed almost equally in both horizontal and vertical direction in layer I, but in layer II it is more distributed downward.

(2) In Bean Field of Matsusaka, from ridge to layer III capillary pores are dominant (**Fig. 3.34 – 3.37**) which it is 6.6% and 7.7% in ridge and layer II and almost double of the portion of non-capillary pores in layer I and III.

(3) In Yokkaichi Agriculture Center, non-capillary pores in vertical direction is dominant in layer A1 (**Fig. 3.38**), then it almost equal to capillary pores in layer A2 (**Fig. 3.39**), and as it is shown in **Fig. 3.40** for layer B, it is less than half of capillary pores. Same relation exists in horizontal direction as well.

Distribution of no-capillary pores in both vertical and horizontal direction showed almost equal in layer A1, in layer A2 it is more distributed vertical, while in is more in layer B.

Capillary pores are equally distributed vertically and horizontally in layer A1, while in A2 it is more distributed horizontally and in layer B the ration of vertical distribution to horizontal is 1.17.

Among these three sites, Beans Field has more portion capillary pores of its total porosity in all layers, except for ridge layer of Broccoli Field with 40% of capillary pores and layer A1 of Yokkaichi Agriculture Center with same percentage distribution. In the other word, Bean Field all layers, ridge layer of Broccoli Field and layer A1 of Yokkaichi Agriculture Center has more water holding capacity than the rest layers.

Non-capillary pores are dominant in Broccoli ridge and Yokkaichi Agriculture Center layer A1 comparing to rest of layers, this implies that saturated hydraulic conductivity and aeration in these two layers are more than the rest.

Briefly the results of **Fig. 3.31 – 3.40** are presented in **Table 4.3**.

[**Table 4.3** Pore size distribution (capillary and non-capillary pores) for all sites]

Table 4.3 Pore size distribution (capillary and non-capillary pores) for all sites

Sample name	Capillary pores			Non-capillary pores		
	H (%)	V (%)	V/H	H (%)	V (%)	V/H
Broccoli Field Ridge	–	40.1	–	–	46.1	–
Broccoli Field layer I	25.7	26.9	1.04	23.7	30.6	1.29
Broccoli Field layer II	23.5	29.7	1.26	11.4	16.0	1.40
Beans Field Ridge	–	33.3	–	–	26.7	–
Beans Field layer I	–	30.3	–	–	16.4	–
Beans Field layer II	–	22.3	–	–	14.6	–
Beans Field layer III	–	34.3	–	–	16.4	–
Y. A. Center layer A1 (Yokkaichi)	32.9	34.3	1.04	49.5	47.8	0.96
Y. A. Center layer A2 (Yokkaichi)	28.6	18.0	0.62	14.2	18.2	1.28
Y. A. Center layer B (Yokkaichi)	23.1	27.2	1.17	18.5	11.1	0.6

4.2.2 Significant microspores' diameter for drainage

From results of **Fig. 3.47 – 3.56** of drainability, macropores sizes significant for drainage was derived and according to section 2.3.3 pores were classified based on their slope of curves and are presented in **Table 4.3**.

(1) Accordingly, macropores significant for drainage and aeration in Broccoli Field of Matsusaka in the vertical direction from ridge to layer II downward their equivalent diameter decrease to half from 0.25mm for ridge to 0.125mm for layer II. In ridge and layer I there are macropores of (c) group, “conical shape”, while in layer II they shape change to (f) group, “cylindrical”. Since both groups have concave curve, they response to higher load pressures in their group.

(2) In Beans Field the diameter of macropores having active role in drainability fluctuating in size and shape. In ridge they are classified in cylindrical (d) group with 0.16mm diameter, cylindrical (f) group with 0.125mm in layers I, II and III has 0.187mm and 0.25mm diameter respectively and both are in (c) group conical shapes.

(3) In Yokkaichi Agriculture Center, pore shape and size change in each layer and even in same layer different direction. Pore diameter and shape for layer A1 is 0.3mm conical (b) group for vertical direction and 0.214mm conical (c) group for horizontal direction. In layer A2 it takes cylindrical shape (e) group with 0.136mm diameter for horizontal direction. In B layer it gets bigger diameter for vertical direction with 0.375mm as (a) group conical shape, and 0.214mm diameter for horizontal direction as (c) group.

Yokkaichi Agriculture Center layer B vertical direction has (a) group with 0.375mm diameter macropores, classified in conical shape convex curve which drain fast with lower load pressure.

Broccoli Field layers I and II horizontal direction, and Yokkaichi Agriculture Center layer A1 vertical direction have (b) group with 0.3mm diameter macropores, classified in

conical shape straight slope curve. These pores drain uniformly with change in load pressure.

Macropores of Broccoli Field ridge (V), Broccoli Field layer I (V), Beans Field layers II and III (V), and Yokkaichi Agriculture Center layer A1 and layer B (H), have (c) group conical concave curve. In another word, these pores drain in last stage of load pressure of their group.

Yokkaichi Agriculture Center layer A2 (H) only has cylindrical (e) group properties. This group pores as discussed in section 3.3 drain suddenly in ultimate load pressure.

And finally macropores of Broccoli Field layer II (V) and Beans Field layer I (V) classifies as (f) group cylindrical properties with concave curve.

[**Table 4.4** Significant Pore size diameter and groups for drainage]

Table 4.4 Significant minimum equivalent pore size diameter and groups for drainage

Layer	Equivalent pore diameter (mm)	Pore group
Broccoli Ridge	0.25	c
Broccoli layer I (H)	0.3	b
Broccoli layer I (V)	0.187	c
Broccoli layer II (H)	0.3	b
Broccoli layer II (V)	0.125	f
Beans Ridge	0.16	c
Beans Field layer I	0.125	f
Beans Field layer II	0.187	c
Beans Field layer III	0.25	b
YAC layer A1 (H)	0.214	c
YAC layer A1 (V)	0.3	b
YAC layer A2 (H)	0.136	e
YAC layer B (H)	0.214	c
YAC layer B (V)	0.375	a

YAC: Yokkaichi Agriculture Center

4.2.3 Soft X-ray macropores imaging

In soil not only size and existence of macropores are important, but also channeling and connectivity are very important for mass flow in soil. Visual determinations of macropores in undisturbed soil sample were implemented by Soft X-ray imaging for better understanding of soil pores importance and dynamic.

Photo 3.36 is represented in **Photo 4.1**. In the image which is magnified pore channel of different sizes can be easily distinguished. The white color means the existence of heavy liquid in pores and the black color represent soil matrix. The whiter the color, soil pores, the darker the color, soil matrix. The maximum pore channel visible is 0.5mm and connectivity of pores in vertical direction is mostly exists in one quarter of the core. Macropores are mostly distributed individually, while non-capillary pores are distributed in bundles.

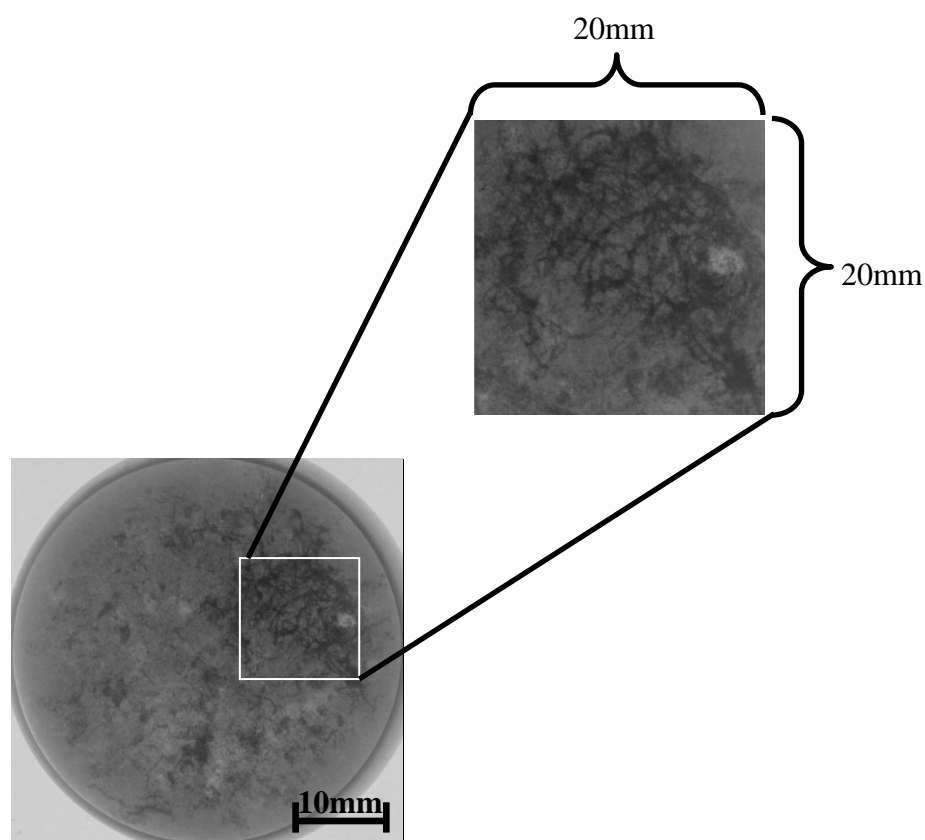


Photo 4.1 Soft X-ray image, visual view of vertical distribution and connectivity of pores in Broccoli Field layer II

Photo 3.38, sample taken from vertical direction, show pores channeling and connectivity in horizontal direction of Beans Field ridge layer (**Photo 4.2**). Capillary pores exist as bundles which shows as big white area, while non-capillary pores exist comparably with very low ration. Distribution of pores in this layer do not concentrated only in one quarter and as it can be seen in original image (**Photo 3.38**), pores are distributed in almost 70% of the core with different intensity.

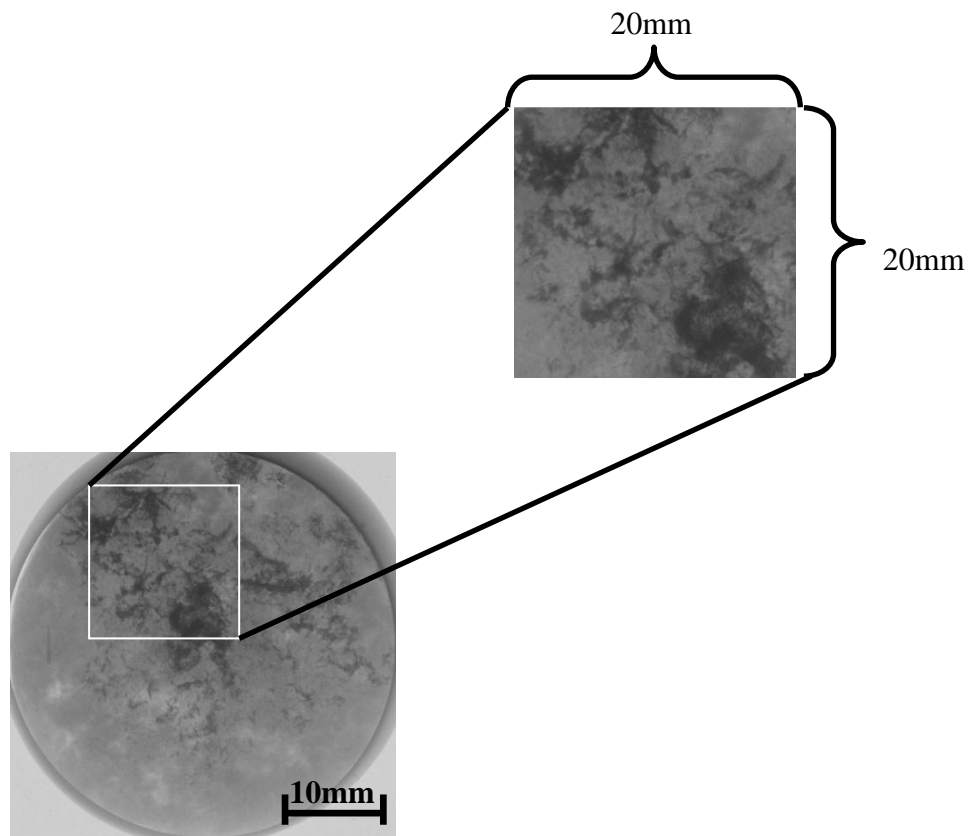


Photo 4.2 Soft X-ray image, visual view of horizontal distribution and connectivity of pores in Beans Field ridge layer

Photo 4.3 present horizontal pore size distribution and connectivity in layer I. It can clearly be seen that non-capillary pores are distributed in center of the sample, while capillary pores occupied around of the sample. Size of macropores distributed horizontally ranges from 0.125mm to 0.5mm.

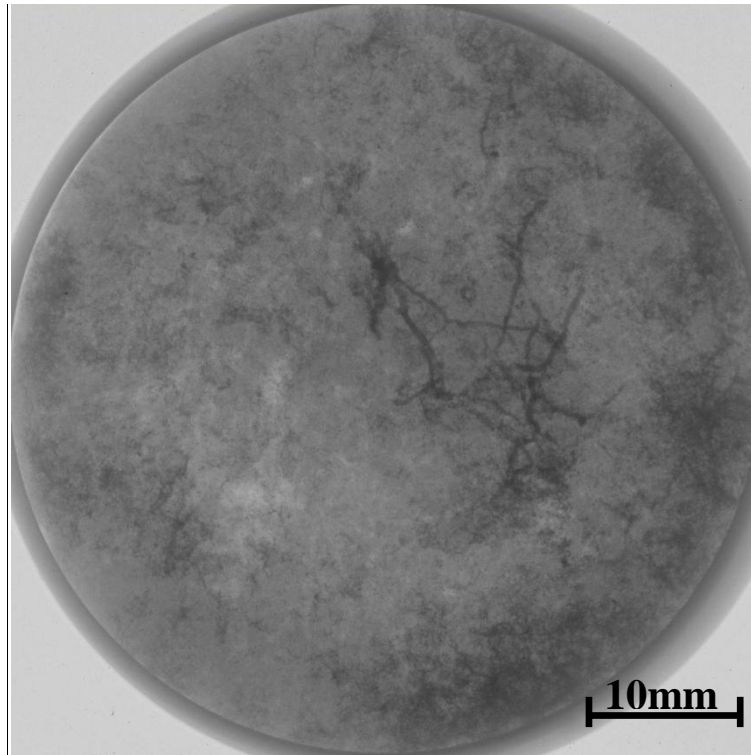


Photo 4.3 Soft X-ray image, visual view of horizontal distribution and connectivity of pores in Beans Field layer I

Vertical distribution of pores and connectivity for Yokkaichi Agriculture Center layer B is shown in **Photo 4.4**, as porosity of this layer is 56% and it shows much capillary pores. Even macropores exists, but due to much intensity of capillary pores they are not visible.

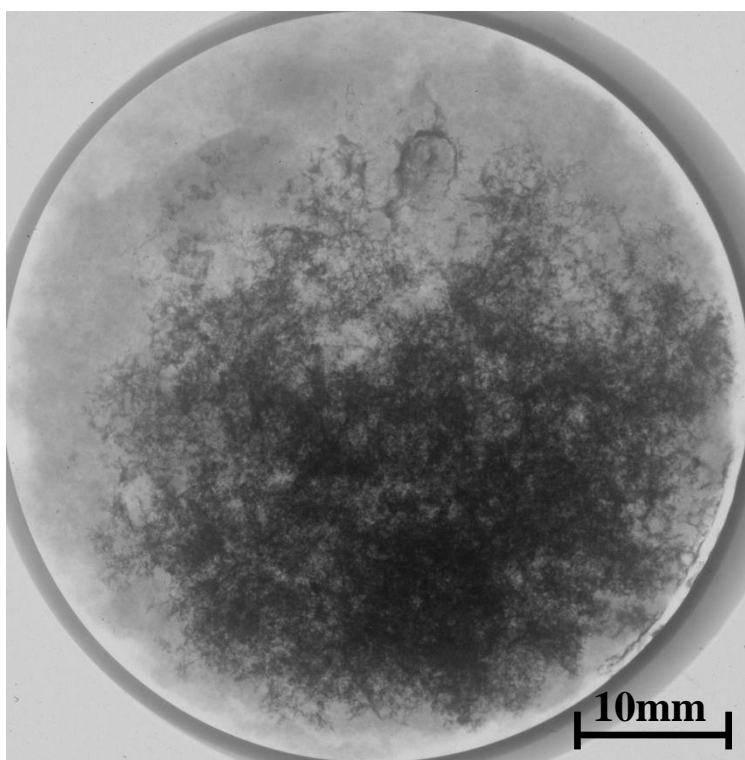


Photo 4.4 Soft X-ray image, visual view of vertical distribution and connectivity of pores in layer B of Yokkaichi Agriculture Center

4.3 pF – θ (Readily Available Soil moisture)

In irrigation planning availability of water in effective root zone and effective soil depth is important to know for accurate application of irrigation water.

(1) As discussed earlier about effective root zone depth, it is 22cm for the Broccoli Field which stands 15cm ridge and 7cm for the layer I. The readily available water (moisture), differences between pF 1.8 – pF 3.0 for each of these two layers are 0.098mm mm^{-1} and 0.064mm mm^{-1} respectively, according to **Table 3.15** and **Fig. 3.28**. For ridge layer the readily available water (moisture) is 14.7mm and for layer I is 4.48mm, and totally the readily available water (moisture) for 22cm depth of soil, ridge layer and layer I, is 19.18mm which should be applied in each period of irrigation on proper time, provided no other proposes are behind irrigation.

(2) According to results for Beans Field in **Table 3.16** and **Fig. 3.29**, readily available water (moisture) for effective root zone 22cm, 12cm ridge layer and 10cm for layer I, are 0.083mm mm^{-1} and 0.072mm mm^{-1} , respectively, for ridge and layer I. The total readily available moisture in effective root layer before hardpan layer starts is 17.16mm which correspond 9.96mm for ridge and 7.2mm for layer I.

(3) In Yokkaichi Agriculture Center, effective root soil layer is 30cm, 10cm layer A0 and 20cm layer A1, and in A2 layer hardpan layer starts. Based on **Table 3.17** and **Fig. 3.30**, the water holding capacity of soil in layer A1 is 0.08mm mm^{-1} and we assume equal intensity for A0 layer. The total readily available water (moisture), for the effective soil depth is 24mm.

Even though all three sites have same texture, but the water holding capacity among them are different and even it is changing in same Field among different layers.

These changes are mainly related to distribution of capillary pores. As described in **Table**

4.3, the ratio of capillary pores in downward and lateral direction are not much different for Broccoli Field layers I and II and it provides adequate water movement between the capillary pores in both direction, especially lateral direction which is important for effective soil layer and water availability for plants.

For Yokkaichi Agriculture Center layer A1 distribution of capillary pores are almost equal and in layer A2 it changes with much distribution for lateral direction and lesser in downward direction.

4.4 Water flow in soil

The hydraulic conductivity of saturated soil depends on the size and distribution of pores in the soil (G. S. Campbell, 1985). Soil pores play significant role in infiltration and redistribution. Infiltration, hydraulic conductivity and drainability of a soil is governed by non-capillary pores, while redistribution in soil bulk is governed both by non-capillary and capillary pores. Infiltration and redistribution of water in soil greatly affect soil water balance and solute transport in soil.

Saturated hydraulic conductivity of a soil more than 1md^{-1} (meter per day) is more than adequate for most agricultural soils, while less than 0.01md^{-1} is problematic in some cases (P. Kooreaar, 1987).

(1) As presented data in **Table 4.3**, ratios of non-capillary pores from total porosity in vertical direction to horizontal direction are 1.29 and 1.40 for layers I and II of Broccoli Field. In the other word, it implies that movement of water is much downward in these two layers during saturated hydraulic conductivity. Based on results of **Table 3.18** and **Figure 3.45** the Saturated hydraulic conductivity for this site downward shows 0.87md^{-1} for ridge, 1.32md^{-1} for I layer, and decreases to 0.013md^{-1} for layer II. For lateral direction it is 0.05md^{-1} for layer I and 0.02mh^{-1} for layer II.

However, pore diameter is another indicative of water movement and distribution; accordingly, **Table 4.4** shows that minimum pore diameter significant in drainage is almost double in lateral direction than downward direction. Therefore even the portion non-capillary pores in lateral direction are lesser, but their bigger diameters encourage lateral distribution of water in soil bulk, and since hydraulic conductivity decreases in layer II there will be more pressure from surface due to gravitational force and water will be forced to redistributed laterally.

(2) In Beans Field non-capillary pores occupies small portion of total porosity in vertical

direction with small pore diameters significant for drainage and hydraulic conductivity, and based on Soft X-ray images of Bean Field for ridge and layer I **Photos 4.2** and **4.3**, the lateral distribution of macropores are negligible.

The saturated hydraulic conductivity starts with 0.0746 md^{-1} in ridge, it drastically decrease to 0.0042 md^{-1} for first layer and it increases again in layers II and III with 0.0306 md^{-1} and 0.0849 md^{-1} , respectively.

(3) For Yokkaichi Agriculture Center the saturated hydraulic conductivity downward shows 1.728 md^{-1} for layer A1, it drastically decreases to 0.078 md^{-1} for layer A2, and greatly again increase to 2.567 md^{-1} for layer B. For lateral direction it is 2.607 md^{-1} for layer A1 and with drastic decrease to 0.073 md^{-1} for layer A2, and 0.015 md^{-1} for layer B.

According to **Tables 4.3** and **4.4** non-capillary pores ratio has sharp descending gradient from 47.8% of total porosity for layer A1 to 18.2% for layer A2 and 11.1% for layer B; however, their minimum significant pore diameter showed the much higher in layer B downward direction.

Due to sandy texture for all sites, it showed for most layers high hydraulic conductivity. According to P. Kooreaar (1987), downward capability of saturated hydraulic conductivity for Broccoli Field I layer (V), Yokkaichi Agriculture Center layer A1 (V & H) and layer B (V) are more than adequate, while ridge layer (V) of Broccoli Field has high. Broccoli Field {layer I (H), layer II (V) and (H)}, Beans Field (ridge, layer II, and layer III), and Yokkaichi Agriculture Center {layer A2 (V and H), layer B (H)} has low saturated hydraulic conductivity, and finally the Beans Field I layer has the lowest hydraulic conductivity, which is problematic for water movement in soil.

For Broccoli Field layer II limit the vertical movement of water, in Beans Field layer I and in Yokkaichi layer A2.

5. New approaches to be added to upland agriculture in Afghanistan

In order to tackle water scarcity and food production in arid, semi-arid and continental climates where water is a limited resource, like Afghanistan, more emphasis is needed on efficient use of water resources. This involves multi-disciplinary approaches and cover from watershed management to end user application efficiency. Charles Batchelor (1999), Hamdy et al., (2003), and Dennis Wichelns (2004) mentioned that innovations in both the technology and policy dimensions of water resource management are needed to achieve desired improvements in irrigation practices and water use decisions; furthermore, practical practices itself is as important as mentioned above dimensions. The concept of irrigation efficiency much focuses on application efficiency in field on how to minimize water loss and increase output.

As discussed in detail about importance of soil resources, especially upland, for irrigation water use efficiency, new approaches have to be considered for improvement of current low water use efficiency. A well designed soil based integrated approaches that cover both field and laboratory analysis is proposed to be implemented for irrigation planning in Afghanistan.

Investigation of soil profile in order to determine its physical quality for production and its suitability for agricultural practices is very important in irrigation.

An investigation plan should answer all aspects of concern related to the field. The physical conditions of soil can provide information about effective soil depth, natural drainage condition, hardpan layer and some other physical properties which are critical in planning and application of irrigation.

Furthermore, by the time it is investigated about soil physical properties and profile cross-section, other information about topography, general leveling condition of the field,

water availability and source of water, and existing factors which may affect the irrigation practices should be collected.

Selection of points for investigation in the field is very important and it needs the investigator to have good knowledge of field survey and data collection. The point selected for investigation should be a great representative of the field which its characteristics represent the general field condition and adequate amount of samples of disturbed and undisturbed soil is needed for laboratory analysis based on purpose behind the research.

Laboratory experiment can provide detail result information about those properties which is difficult to characterize in field. For example, characterizing macropores, water holding capacity, permeability and hydraulic conductivity of soil, help in accurate decision on plotting of field, irrigation rate and frequency which result in increase of water use efficiency and decrease of water loss.

Such detailed investigation and research will provide the opportunity to increase the total irrigated area through better water use efficiency and result in more production.

The land resources of Afghanistan can be use for commercialization of agriculture and attraction of foreign currency through export of products. However, detailed investigation on large scale land resources of Afghanistan can answer whether they have potential for production and agriculture?.

6. General discussion

The methodology, both field investigation and laboratory experiments, applied on three selected sites as case study for developing a detailed soil based irrigation plan for Afghanistan, highlight the importance of this model and help in comprehensive understanding of soil properties and capabilities on transportation, redistribution, and retention of irrigation water for crops. Besides that, some part of this model is useful in characterizing soil water transport in environmental aspects and hazard prevention aspects.

(1) The field and laboratory results showed that natural drainage condition in two fields, Broccoli Field and Beans Field, is poor and it needs to be developed. Lack of a natural drainage system and compaction is counted as main source of the problem.

In dry land agriculture, this might not seem to be a problem, because during the cropping season there is sometime the precipitation intensity is negligible, and mostly no precipitation at all occurs. Also irrigation water is not much available to create water logging for long period of time. However, construction of a subsurface drainage system will facilitate in removal of excess water, whether applied by irrigation or rainfall, from effective root zone and effective soil depth.

(2) The soil hardpan exists in shallow depth with maximum 30cm for Yokkaichi Agriculture Center and around 22cm for other two fields. In two field of Matsusaka solid phase is dominant and as a result bulk density increases and total porosity decreases.

Shallow hardpan limits development of root growth in soil and decreases hydraulic conductivity of water, and as a consequence water logging and less nutrient and water availability for plant due to small effective soil depth occurs.

According to the literature for general characteristics of Afghanistan soil, the organic content of soils are very low even negligible, as mineral soils it is expected that their bulk density is higher and total porosity is lower, however it need detailed analysis. Deep plow and

application of organic amendment can improve the porosity of the soil, break the hardpan and solve compaction problem at the same time, since organic content has lower bulk density.

(3) Non-capillary pores, macropores, their total volume, diameter and connectivity play important role in soil. In structured soils water may flow through the macropores even before soil effective layer is saturated, resulting from preferential phenomenon (K. Beven and P. Germann, 1982). They facilitate soil aeration and ease water movement in soil. Vertical continuity and connectivity of non-capillary pores are important for increase hydraulic conductivity downward and also increase exchange of gasses between soil and atmosphere, while lateral continuity and connectivity increase water distribution. Distribution of macropores was different in even same field between different layers.

For Matsusaka Fields the ridge layer showed considerable percent of macropores and in Yokkaichi Agriculture Center till 30cm soil depth almost 50% of total porosity was occupied by macropores.

(4) Distribution of capillary pores, which play important function in retaining water for crop use between pF 1.8 – pF 3.0, showed not significant and as the result less water available for crops in most of the layers. In the range of effective soil layer the percentage of capillary pores occupied high percentage of total porosity in Broccoli Field ridge, while it was good in ridge layer of Beans Field and layer A1 of Yokkaichi Agriculture Center, and low to other layers. Cropping pattern can affect both non-capillary and capillary pores. For improving capillary pores condition in soil, crops with fibrous root system can develop the condition of capillary for future land use. As was discussed about A1 layer of Yokkaichi Agriculture Center, the water holding capacity was the highest among all layers, on the other hand the Photo of A1 layer showed the intensity of fibrous roots in this layer and this indicated importance of fibrous roots for improving capillary water in soil and water holding capacity.

(5) Soil readily available moisture, water, between ranges of pF 1.8 – pF 3.0, which is the amount of water that is retained in soil capillary pores and easily can be easily used by

plant, showed less for all the layers of three Fields, except for layer A1 of Yokkaichi Agriculture Center.

The reasons for low water holding capacity are sandy loam texture, high bulk density, lower total porosity, and very low organic content in case of Matsusaka Fields. The reason behind exception of Yokkaichi Agriculture Center is high organic content in layer A0 and layer A1, lower bulk density and higher porosity.

Based on these data it is easy to measure and allocate rate and frequency of irrigation, with high efficiency and lowest possible water loss.

In areas where facing water scarcity, management of water and improving irrigation water use efficiency can be ensured when such accurate and data about soil water holding capacity is presented. However, in Afghanistan allocation of water, frequency and rate of irrigation are practiced based on availability of water.

(6) Saturated hydraulic showed more than adequate for Broccoli layer I and Yokkaichi Agriculture Center layer A1 (V & H direction) and layer B (V). It was high in ridge layer of Broccoli Field, while Broccoli Field (layer I (H), layer II (V & H), Beans Field (ridge, layer II, and layer III), and Yokkaichi Agriculture Center (layer A2 (V & H), layer B (H)) has low saturated hydraulic conductivity, and finally the Beans Field layer I has the lowest hydraulic conductivity, which is problematic for water movement in soil.

Understanding of saturated hydraulic conductivity of the soil helps in proper management of irrigation, distribution efficiency, and other agronomic and farm practices, as designing of plot size and irrigation water flow rate control, provided if applicable.

Hydraulic conductivity which has direct dependency on macropores size and distribution is important in water movement between soil layers, redistribution of water in the soil, recharging of underground aquifer. Importance of hydraulic conductivity, soil pores geometry and volume is not only limited to above mentioned issues, but also can provide good knowledge about watershed management, erosion control, management of surface runoff, and

preserving underground water quality from pollutant transport by water. Fig. 6.1 shows overall understanding that the model provide and which questions they answer for planning of irrigation with expected result.

Such comprehensive detailed investigation model is not only good for irrigation planning, but it is also important in distribution efficiency and minimizing water loss due to deep percolation; therefore, this model is required to be implemented in Afghanistan and current irrigation practices have to be improved in order to increase food production toward self-sufficiency.

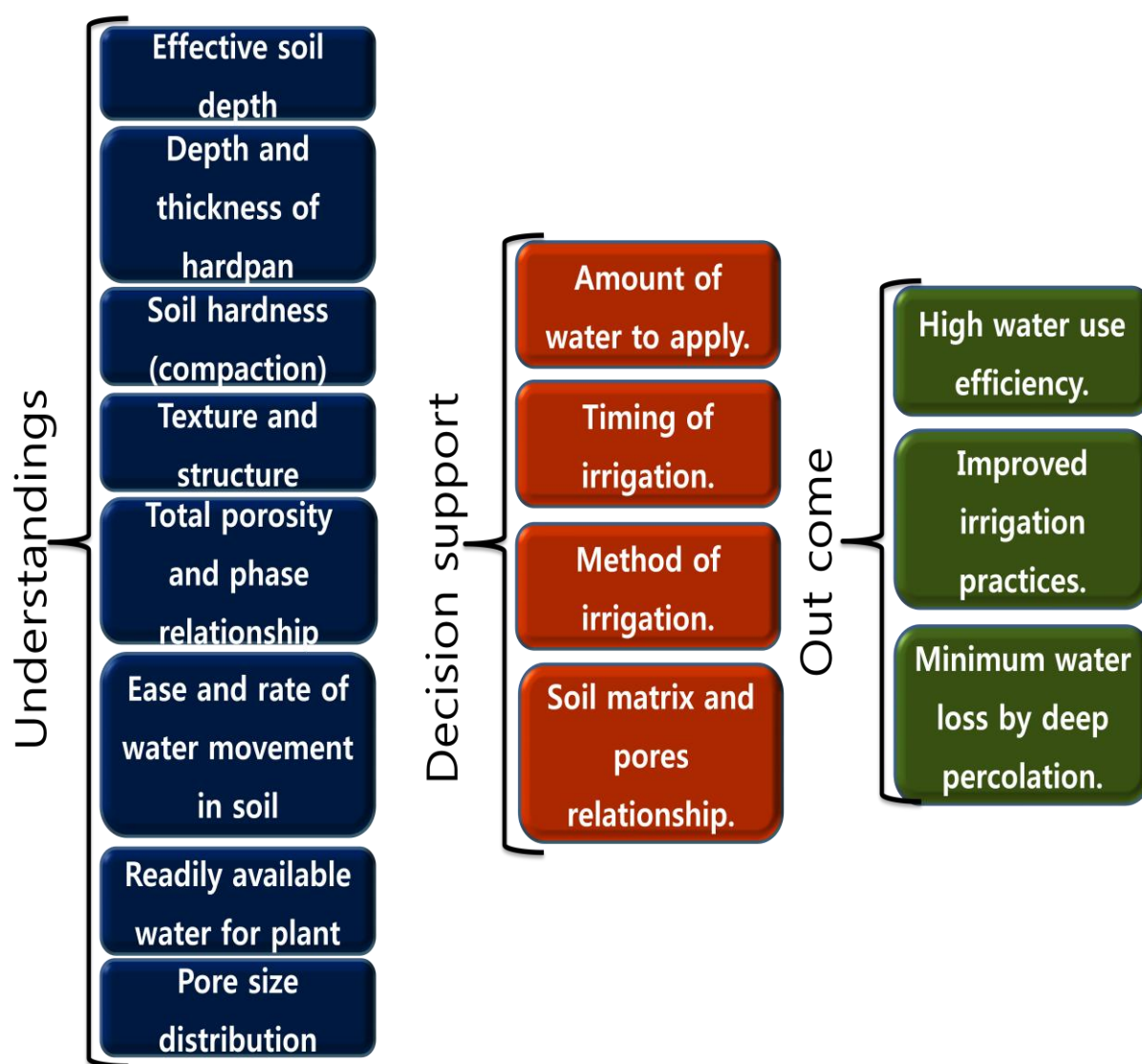


Fig. 6.1 Brief importance of the model and its suitability.

Acknowledgement

I would like to express my deep gratitude to my academic supervisor Professor Hajime NARIOKA for his valuable time spent in teaching, advising, supporting and encouraging me through this period of study. Furthermore, I would like to thank Professor Takamitsu KAJISA for his all time support and Associate Professor Kenji OKAJIMA for their detailed review of this thesis and providing useful comments, and thanks from all other professors in Division of Environmental Science and Technology.

Special appreciations and regards are presented to my family members who emotionally supported me and accepted difficulties for me during this period of time, and I dedicate this thesis especially to my Mother, my life partner Sonita Saleh Rahmany, my cute children Ahmad Sohrab Jan and Satin Jan.

I am grateful that I was blessed with a great young and motivated friend, Mr. Homayoon Ganji, who supported me emotionally and encouraged me during tough period of research and writing thesis.

I thank my great laboratory members who supported and helped me during laboratory work especially Miss Minayo GOTO for her hard-working and supportive nature, and Mr. Mamoru YOSHIDA.

I would like to thank all my brothers and friends for encouraging me and periodic support they provided.

Achievement of this honor was financially supported by JICA PEACE-Project and thanks from JICA staff who facilitated communication from beginning of the program till end.

February, 2015

Abdul Saboor Rahmany

References

- (1) A. J. Franzluebbers, 2002, Water infiltration and soil structure related to organic matter and its stratification with depth, *ELSVIER, Soil & Tillage Research*, 66:197–205
- (2) A. L. Paraskevopoulos and A. Singels, 2014, Integrating soil water monitoring technology and weather based crop modelling to provide improved decision support for sugarcane irrigation management, *ELSVIER, Computers and Electronics in Agriculture* 105, 44–53
- (3) A. W. Warrick, 2002, *Soil physics companion*, CRC PRESS, pp. 49 - 80
- (4) Akyuz, F.A., Scherer, T., Morlock, D., 2008. Automated Irrigation Scheduling Application of the North Dakota Agricultural Weather Network. In: *Proceedings of the International Meeting on Soil Fertility Land Management and Agroclimatology*. Turkey, pp. 777–785
- (5) Alfered R. Conklin, Jr., 2005, *Field Sampling Principles and Practices in Environmental Analysis*, MARCEL DEKKER, INC. pp. 51 – 141
- (6) Ali Morad Hassanli , Mohammad Ali Ebrahimizadeh , Simon Beecham, 2009, The effects of irrigation methods with effluent and irrigation scheduling on water use efficiency and corn yields in an arid region, *ELSVIER, Agricultural Water Management* 96, 93–99
- (7) B. Yaron, E. Danfors, and Y. Vaadia, 1973, *Arid Zone Irrigation*, Springer, pp. 1
- (8) B.A. George, S.A. Shende, N.S. Raghuwanshi, 2000, Development and testing of an irrigation scheduling model, *ELSEVIER, Agricultural Water Management* 46,121-136
- (9) Blake, G., Schlichting, E., Zimmermann, U., 1973, Water Recharge in a Soil with Shrinkage Cracks, *Journal of Soil Science Society of America*, 37: 669-672
- (10) Busch, J., Abourached, C., Hutchinson, K., Sayde, C., Hillyer, C., English, M., 2009. A
- (11) C.B. Hedley, P.Roudier, I.J. Yule, J. Ekanayake, S. Bradbury, 2013, Soil water status

- and water table depth modeling using electromagnetic surveys for precision irrigation scheduling, *ELSEVIER*, *Geoderma*, 199 (2013) 22-29
- (12) CFC (Civil-Military Fusion Center), 2012, *Afghanistan in Transition*, Executive Summary, Irrigation, Profit & Alternative Crops, pp. 2-12.
- (13) CSO (Central Statistics Organization), 2013~14, *Afghanistan Statistical Yearbook*
- (14) Charles Batchelor, 1999, Improving water use efficiency as part of integrated catchment management, *ELSEVIER*, *Agricultural Water Management* 40, 249-263
- (15) Charles Hillyer et al., 2009 Web-Based Advisory Service for Optimum Irrigation Management. In: *Proceedings of the World Environmental and Water Resources Congress*, pp. 1–10.
- (16) *Climatemaps*, 2014, *Afghanistan climate*
- (17) Coppola et al., 2008, Transport in preferential flow domains of the soil porous system: Measurement, interpretation, modeling and upscaling, *ELSEVIER*, *Journal of Contaminant Hydrology*
- (18) Daniel Hillel, 2003, *Environmental Soil Physics*, Academic press, pp. 131-161
- (19) Dennis Wichelns, 2004, New Policies are needed to encourage improvements in irrigation management, *ASCE*, *Journal of Irrigation and Drainage* 130, 366-372
- (20) Derdour, H., Angers, D. A., and Laverdiere, M. R., 1993, Characterization of the pore space of a clay soil: Influence of soil constituents and tillage practices, *Canadian Journal of Soil Science*, No. 73, pp. 299-307
- (21) Dipak Sarkar & Abhijit Haldar, 2005, *Physical and Chemical Methods in Soil Analysis*, *NEW AGE*, pp 34-76
- (22) E. BARTON WORTHINGTON (editor), 1977, *Arid Land Irrigation in Developing Countries*, Environmental Problems and Effects, Based on the International Symposium, 16-21 February 1976, Alexandria, Egypt, *PERGAMON PRESS*, pp.15-20
- (23) *FAO*, 2014, *Afghanistan Country Pasture/Forage Resource Profiles*

- (24) Freddie R. Lamm, James E. Ayars, Francis S. Nakayama, 2007, *Microirrigation for Crop Production :Design, Operation, and Management*, ELSVIER, pp. 29-36
- (25) Future Direction International (FDI), 2011, *Afghanistan's Food and Water Security Challenges*
- (26) G.S. Campbell, 1985, *Soil Physics with Basics*, ELSVIER, pp. 40 – 48
- (27) Goodwin, I., O'Connell, M.G., 2008. The future of irrigated production horticulture –world and Australian perspective. *Acta Horticulturae* 792, 449–458.
- (28) Greenland, D.J., 1977, Soil damage by intensive arable cultivation: temporary or permanent?, *Phil. Trans. Roy Soc. London, B*, 281:193–208.
- (29) H. Ganji, A. S. Rahmany, T. Kajisa, M. Kondo, H. Narioka, 2014. Comparison of the Crop Water Need between Actual Wind Condition and Zero Wind Simulation; Wind Velocity within 24-Hour Interval in Herat, Afghanistan. ISSAAS 20th Founding Anniversary Celebration & 2014 International Congress and General Meeting NODAI Academia Centre, Tokyo University of Agriculture, Tokyo, Japan
- (30) H. Narioka, 1989, Study on the Physical Functions of Soil macropores and the Instrumentation for their Measurement, NODAI Research Institute, Tokyo University of Agriculture, Bulletin 1, pp. 4 – 7
- (31) H. Narioka, 1992, Study on Open Channel of the Entry Macropore in Volcanic Ash Subsoil, NODAI Research Institute, Tokyo University of Agriculture, Bulletin 3, pp.36 – 41
- (32) H. Narioka, M. Komamura, 2003, Soil structure and change of free groundwater in the Kanto Loam formation, *Groundwater Engineering – Recent Advances*, Kono, Nishigaki & Komatsu (eds). Swets & Zeitlinger, Lisse, ISBN 90 5809 385 9
- (33) Harris Georgoussis et al., 2009, Regional scale irrigation scheduling using a mathematical model and GIS, *ELSVIER - Science Direct, Desalination* 237, 108–116
- (34) Hedley, C.B., Yule, I.J., 2009. A method for spatial prediction of daily soil water status

- for precise irrigation scheduling. *Agricultural Water Management* 96, 1737–1745.
- (35) Henry D. Foth, 1990, *Fundamentals of soil science*, 8th edition, John Wiley & Sons, pp. 34-36
- (36) ICARDA, 2002, *Needs Assessment on Soil and Water in Afghanistan*, pp. 14-15
- (37) JIID (The Japanese Institute of Irrigation and Drainage), 1990, *Upland Irrigation*, pp. 48-78
- (38) Jianchu Shi, Sen Li, Qiang Zuo, Alon Ben-Gal, 2015, An index for plant water deficit based on root-weighted soil water content, *ELSVEIR, Journal of Hydrology*, 522, 285–294
- (39) Jury, W.A., Vaux, H.J., 2007. The emerging global water crisis: managing scarcity and conflict between water users, *ELSVEIR, Advances in Agronomy* 95, 1–76.
- (40) Keith Beven and Peter Germann, 1982, *Macropores and Water Flow in Soils*, *Water Resources Research*, Vol. 18, No. 5, pp. 1311-1325
- (41) Kruger, E., Schmidt, G., Bruckner, U., 1999. Scheduling strawberry irrigation based upon tensiometer measurement and a climatic water balance model, *ELSVEIR, Scientia Horticulturae* 81, 409–424.
- (42) Les Levidow et al., 2014, *Improving water-efficient irrigation: Prospects and difficulties of innovative practices*, *ELSVEIR, Agricultural Water Management* 146, 84-94
- (43) Lewis, D. T., 1977, *Subgroup Designation of Three Udolls in Southeastern Nebraska*, *Journal of Soil Science Society of America*, 41:940–945.
- (44) M. A. Ali, 2010, *Fundamental of Irrigation and On-farm water Management*, Springer, pp. 1 – 10
- (45) M. R. Carter and E. G. Gregorich, 2007, 2nd edition, *Soil sampling and method of analysis*, Canadian Society of Soil Science, pp 2
- (46) M.B. Khirkham, 2004, *Principles of Soil and plant water relationship*, *ELSEVEIR* pp. 55-107

- (47) Marc Pansu, 2006, Hand Book of Soil Analysis, Springer, pp 15-24
- (48) NASA online publications,
- (49) NRCS, 2012, version 3, Field Book for Describing and Sampling Soils, USDA NRCS
- (50) Neil Southorn, 1997, Farm Irrigation: Planning & Management, INKATA PRESS, pp. 23-70
- (51) Nestor M. Cid-Garcia, Angel G. Bravo-Lozano, Yasmin A. Rios-Solis, 2014, A crop planning and real-time irrigation method based on site-specific management zones and linear programming, ELSVEIR, Computers and Electronics in Agriculture 107, 20–28
- (52) Newman, J.P., Lieth, J.H., Faber, B., 1991. Evaluation of an irrigation system controlled by soil moisture tension for container-grown plants. In: Flower and Nursery Report for Commercial Growers, University of California, pp. 1–4.
- (53) Oki, L.R., Lieth, J.H., Tjosvold, S., 1996. Tensiometer-based irrigation of cutflower roses. Project Report to the California Cut-flower Commission
- (54) P. G. Home, R. K. Panda, S. Kar, 2002, Effect of method and scheduling of irrigation on water and nitrogen use efficiencies of Okra (*Abelmoschus esculentus*), ELSVIER, Agricultural Water Management 55, 159-170
- (55) P. Koorevaar, G. Menelik, and C. Dirksen, 1987, Element of soil Physics, ELSVIER, pp. 6 – 10, 60 – 70
- (56) R.J. Smith, S.R. Raine, J. Minkevich, 2006, Irrigation application efficiency and deep drainage potential under surface irrigated cotton, ELSVEIR, Agricultural Water Management 71, 117-130
- (57) Rattan Lal & Manoj K. Shukla, 2004, Principles of Soil Physics, Marcel Dekker, Inc. pp. 141- 145
- (58) Reeves M.J., 1980, Recharge of the English chalk, A possible mechanism, Geological Society, London, 14(4), 231-240
- (59) Robert E. White, 2005, Principles and Practice of Soil Science, The Soil as a Natural

Resource, Blackwell, pp. 75

- (60) SUGI Jiro, edited 1980, Planning for an Irrigation System, NODAI Research Institute, Tokyo University of Agriculture, pp. 22-33
- (61) Shinji Kawasaki et al., 2012, Current Situation and Issues on Agriculture of Afghanistan, Journal of Arid Land Studies, 22-1, 345-348
- (62) Songhao Shang and Xiaomin Mao, 2006, Application of a simulation based optimization model for winter wheat irrigation scheduling in North China, ELSVIER, Agricultural Water Management 85, 314 – 322
- (63) Terry A. Howell, 2001, Enhancing Water Use Efficiency in Irrigated Agriculture, Journal of American Society of Agronomy, 93:281–289
- (64) Thysen, I., Detlefsen, N.K., 2006, Online decision support for irrigation for farmers, ELSVIER, Agricultural Water Manage 86, 269–276
- (65) USAID, 2014, USIAD Projects on Agriculture sector of Afghanistan
- (66) USDA (United States Department of Agriculture) and NRCS (National Resources Conservation Services), 2003, 9th edition, Keys to Soil Taxonomy, USDA and NRCS
- (67) Ucdavis online publication teaching material
- (68) W. Warrick, 2002, Soil Physics Companion, CRS PRESS, pp. 49 – 80
- (69) World Bank, 2010, Regional Food Prices, Appendix 1, Afghanistan
- (70) Zengjiang Guo, Zhenwen Yu, Dong Wang, Yu Shi, Yongli Zhang, 2014, Photosynthesis and winter wheat yield responses to supplemental irrigation based on measurement of water content in various soil layers, ELSVIER, Field Crop Research 166, 102-111
- (71) Zhu, Q., Lin, H., 2011. Influence of soil, terrain, and crop growth on soil moisture variation from transect to farm scales. ELSEVIER - Geoderma 163, 45–54
- (72) Zuo, Q., Shi, J., Li, Y., Zhang, R., 2006. Root length density and water uptake distributions of winter wheat under sub-irrigation. Plant Soil 285, 45–55

Appendixes